DESIGN OF A BROADBAND DIRECTIVE YAGI BASED MIMO ANTENNA SYSTEM WITH LOOP EXCITER

BY

SYED SHAHAN JEHANGIR

A Thesis Presented to the

DEANSHIP OF GRADUATE STUDIES

KING FAHD UNIVERSITY OF PETROLEUM & MINERALS

DHAHRAN, SAUDI ARABIA

In Partial Fulfillment of the
Requirements for the Degree of

MASTER OF SCIENCE

In

ELECTRICAL ENGINEERING

FEBRUARY 2017

KING FAHD UNIVERSITY OF PETROLEUM & MINERALS
DHAHRAN 31261, SAUDI ARABIA

DEANSHIP OF GRADUATE STUDIES

This thesis, written by **SYED SHAHAN JEHANGIR** under the direction of his thesis adviser and approved by his thesis committee, has been presented to and accepted by the Dean of Graduate Studies, in partial fulfillment of the requirements for the degree of **MASTER OF SCIENCE IN ELECTRICAL ENGINEERING**.

Thesis Committee

Prof. Mohammad S. Sharawi
(Adviser)

H. Masoudi 14/3/2017

Prof. Husain M. Masoudi (Member)

Dr. Hussein Attia (Member)

Dr. Ali Ahmad Al-Shaikhi
Department Chairman

Prof. Salam A. Zummo
Dean of Graduate Studies

26/3/17

Date

To My Lovely Parents, Brother, and My Best Friend Tri Bagus Susilo.

ACKNOWLEDGMENTS

I would like to express my veracious gratitude towards the endless blessings of my creator. Apart from that, I owe my mother for the time that I have taken from her care to successfully complete my MS thesis, I really appreciate her for the patience and support.

Moreover, I Would like to thank my Supervisor, Prof. Mohammad S. Sharawi for his promptness, invaluable suggestions, and encouragement throughout this work. Working under his supervision and joining his research group- Antennas and Microwave Structure Design Lab (AMSDL) provided an excellent learning platform. This work would not have been possible without the resources of AMSDL.

I wholeheartedly thank Prof. Husain M. Masoudi and Dr. Hussein Attia for their discussions and comments. Their critics further culminated this work.

I am thankful to the senior members of the AMSDL- Dr. Umar Khan, Dr. Rifaqat Hussain, and Sagar Kumar Dhar who helped me in learning the fabrication process and using other lab facilities in the start. It would have been very difficult to master using new equipment without their time and cooperation.

I would like to thank King Fahd University of Petroleum an Minerals (KFUPM)

and the Deanship of Scientific Research (DSR) for providing funding opportunities that helped in completion of my MS research work.

Finally, and most importantly, I would like to thank my brother Syed Zeeshan Jehangir and my friend Tri Bagus Susilo for their continuous encouragement and motivation. I am very lucky to have such a nice brother and a sincere friend.

TABLE OF CONTENTS

LIST OF TABLES

LIST OF FIGURES

THESIS ABSTRACT

NAME: Syed Shahan Jehangir

TITLE OF STUDY: Design of a Broadband Directive Yagi Based MIMO Antenna System with Loop Exciter

MAJOR FIELD: Electrical Engineering

DATE OF DEGREE: February 2017

Printed multiple-input-multiple-output (MIMO) systems have become a hot area of research due to their promising features of providing high data rate, mitigating multi-path fading effects in wireless channels, providing better transmission quality, and coverage due to diversity and multiplexing gains. In this work, a 4-element circular Quasi-Yagi based MIMO antenna system with loop excitation is presented. This wide dual-band antenna system covers 1.45–2.55 GHz and 3.707–4.71 GHz bands supporting GPS, GSM/EDGE, UMTS/HSDPA, Bluetooth, Wi-Fi, and WiMAX standards. This antenna system has an end-fire directional radiation pattern with front-to-back ratio (FBR) of 13.8 dB, minimum measured gain of 5.8 dBi, and

directivity of 7 dB at 2 GHz using one director element. The minimum measured efficiency across the two covered bands was 65%. It had a minimum measured port isolation of 18 dB within its bands. The size of the MIMO antenna system is 263×263×0.8 mm^3 thus making it suitable for wireless access points and on vehicle applications.

After successful implementation of the first design, a novel 2-element single layer compact semi-ring slot based Yagi-like MIMO antenna system is presented. The center frequency of operation is 3.6 GHz targeting WiMAX applications. It has a measured bandwidth of 320 MHz which covers from 3.48–3.8 GHz. A very simple and compact reflector element having a size of 14×9.5 mm^2 is used to achieve a FBR of greater than 10 dB without using any complex back-lobe reduction technique or additional reflector layer which is usually used to get high FBR in slot antennas. A measured realized gain of 4.3 dBi, directivity of 6 dB, and a minimum measured total radiation efficiency of 73% across the entire band of operation were achieved. This MIMO antenna system has minimum measured isolation of 12 dB, maximum measured ECC of 0.0385, and diversity gain (DG) of 9.81 dB across the entire band of operation. The total board size of the MIMO antenna system is 80×40×0.8 mm^3 while the single antenna element has a size of 40×40×0.8 mm^3.

Finally, a highly miniaturized novel dual wide-bandwidth (BW) 2-element Quasi-Yagi MIMO antenna system is presented. A miniaturization of 68% is achieved using a semi-loop meandered driven element. The center frequency of operation is 2 GHz. The antenna system covers two bands: the Telemetry L-band with a minimum

measured BW (-6 dB) of 160 MHz, from 1.27–1.43 GHz, and the GSM/LTE band with a BW of 333 MHz from 1.8–2.133 GHz. It has a high measured FBR of around 15 dB at 1.35 GHz and 17 dB at 2 GHz. A gain of more than 5 dBi is measured for the single element with a total radiation efficiency of around 85% in both bands. The measured isolation of the proposed MIMO antenna is at least 15 dB with less than 0.0785 measured ECC values in both bands.

ملخص الرسالة

الاسم: سيد شاهان جيهانجر

عنوان الدراسة: تصميم نظام هوائيات MIMO مبني على هوائي Yagi واسع النطاق وموجه مع محفز دائري

مجال التخصص: الهندسة الكهربائية

تاريخ الدرجة: شباط 2017

أنظمة متعددة-المدخلات-متعددة-المخرجات (MIMO) المطبوعة أصبحت مجال هام للبحث بسبب مزاياها الواعدة في توفير معدل بيانات مرتفع، وتخفيف تأثيرات التلاشي في المسارات المتعددة في القنوات اللاسلكية، وتوفير جودة نقل وتغطية أفضل بسبب التنوع والكسب المضاعف. في هذا العمل، نظام هوائيات MIMO مبني على 4-عناصر Quasi-Yagi دائرية مع محفز دائري تم عرضه. نظام الهوائيات واسع وثنائي النطاق هذا يغطي النطاقات1.45-2.55 جيجاهيرتز و3.707-4.71 جيجاهيرتز الداعمة لمعاييرGPS,GSM/EDGE, UMTS/HSDPA, Bluetooth, WiFi, WiMAX. نظام الهوائيات هذا لديه نمط إشعاع باتجاه endfire مع نسبة الأمامي-إلى-الخلفي (FBR) تساوي 13.8 ديسبل، قيمة أقل كسب مُقاسة تساوي 5.8 ديسبل، واتجاهية تساوي 7 ديسبل على 2 جيجاهيرتز باستخدام عنصر موجّه. أقل كفاءة تمت قياسها ضمن النطاقين الذين تمت تغطيتهم كانت 65%. القيمة الصغرى المقاسة لانعزالية المنافذ تساوي 18 ديسبل ضمن نطاقات هذا النظام. حجم نظام هوائيات MIMO هو 263×263×0.8 ميلليمتر مكعب، وهذه يجعله مناسباً لنقاط الوسول اللاسلكية وعلى تطبيقات المركبات.

بعد التشغيل الناجح للتصميم الأول، تم عرض نظام هوائيات MIMO جديد شبيه Yagi مبني على شقة شبه حلقي مضغوط بطبقة واحدة بعنصرين. منتصف تردد التشغيل هو 3.6 جيجاهيرتز تهدف تطبيقات WiMAX. لديه نطاق عرضه المقاس 320 ميجاهيرتز والتي تغطي 3.48-3.8 جيجاهيرتز. تم استخدام عنصر عاكس مضغوط وبسيط جداً حجمه 14×9.5 ميلليمتر مربع لتحقيق FBR أكبر من 10 ديسبل بدون استخدام طريقة معقدة لتخفيض الإشعاع الخلفي أو طبقة عاكسة إضافية والتي بالعادة تستخدم لتحقيق FBR في الهوائيات الشقية. تم تحقيق 4.3 ديسبل كسب حقيقي مقاس، و6 ديسبل اتجاهية، و73% أقل كفاءة إشعاعية مقاسة على كامل نطاق التشغيل. نظام هوائيات MIMO هذا لديه 12 ديسبل كأقل انعزالية مقاسة، و0.0385 كأعلى قيمة ECC مقاسة، و9.81 ديسبل كسب التنوع على كامل نطاق التشغيل. الحجم الكامل لنظام هوائيات MIMO هو 80×40×0.8 ميلليمتر مكعب حيث أن حجم عنصر الهوائي الواحد هو 40×40×0.8 ميلليمتر مكعب.

أخيراً، تم عرض نظام هوائيات MIMO جديد مع نسبة تصغير عالية على نطاقي تشغيل واسعين مبني على عنصرين من Quasi-Yagi. تم تحقيق نسبة تصغير بقيمة 68% باستخدام عنصر مغذي شبه دائري ملتوي. مركز تردد التشغيل هو 2 جيجاهيرتز. نظام الهوائيات يغطي نطاقين: نطاق Telemetry L-band بعرض نطاق مقاس (6 ديسبل) يساوي 160 ميجاهيرتز، يغطي ترددات 1.27-1.43 جيجاهيرتز، ونطاق GSM/LTE بعرض نطاق يساوي 333 ميجاهيرتز يغطي ترددات 1.8-2.133 جيجاهيرتز. هذا النظام لديه FBR مقاسة عالية تقدر بحوالي 15 ديسبل على 1.35 جيجاهيرتز و17 ديسبل على 2 جيجاهيرتز. الكسب المقاس للعنصر الواحد يفوق 5 ديسبل مع كفاءة إشعاعية تقدر بحوالي 85% في كلا النطاقين. الانعزالية المقاسة لهوائيات MIMO المقترحة هي 15 ديسبل على الأقل مع أقل من 0.0785 لقيم ECC المقاسة في كلا النطاقين.

CHAPTER 1

INTRODUCTION

In the last few decades, wireless communication has evolved very rapidly. Nowadays small form factor devices are well equipped with multiple functionalities like making calls, browsing the internet, playing music, games, movies, and providing on road navigation. Wireless technology has now become an integral part of modern life and its features and applications are not only limited to the third or fourth generation $3G/4G$, but also will be extended to fifth generation 5G wireless devices. In this chapter, we briefly present an overview of wireless evolution and the need for multiple-input-multiple output (MIMO) technology.

1.1 Wireless communication Evolution

The initial first generation ($1G$) analog-based mobile phones had limited capabilities of data transfer. A few years later, the Global System Mobile (GSM) standard and second generation ($2G$) based mobile phones provided more voice and data capabilities and much more increase in the data rate (around 200 times) as

compared to $1G$. With the evolution of mobile phone technology and wireless local-area network (WLAN) standards, the cell phone industry moved to $3G$ and $4G$ in 2006 and 2011, respectively [1]. With the advent of this technology, portable devices are now equipped with video transferring and high-definition broadcasting applications. New WLAN standards such as 802.11ad can now provide high data rates in gigabits as compared to older standards.

The ingenuity of Radio Frequency (RF) engineers made it possible to reduce the size of mobile phones by introducing compact antenna designs and other microelectronic components. Fig. 1.1 shows the evolution of mobile phones from $1G$ to $4G$. It can be seen that, $1G$ mobile phones were bulky, heavy, and only supported voice calling features. Large size antennas were used in these mobile phones. Later on, $2G$ and $3G$ mobile phones were introduced with very small sizes having small antennas installed inside the casing of the mobile phones which can be seen in the middle of Fig. 1.1. With the advent of $3.5G$ and $4G$, the size of the phone started increasing again but with more features and multiple antennas to support high data rate applications as well as to provide a better visualization screen.

Fig. 1.1. The evolution of mobile phones [1].

1.2 MIMO Technology

Multiple antennas are required to cover different frequency bands covered by wireless standards. Many portable devices have now multiple functionalities as compared to early generations with the existence of multiple antennas. These multiple antennas cover different frequency bands of different standards and might support high data rates. New wireless standards use multiple-input-multiple output (MIMO) technology in order to increase the channel capacity as well as the reliability of a communication system. There are other enabling technologies which provides high data rates when integrated with MIMO like adaptive modulation and coding (AMC) and orthogonal frequency-division multiple access (OFDMA). The former two technologies are related to coding and modulation while MIMO is associated with the use of multiple antennas and multiple receivers. Multiple antennas can be easily installed at the base stations but it imposes a challenge when having multiple antennas placed in small form factor devices (i.e. access points)

due to the availability of limited space. It is usually required to place multiple antennas in such devices which do not affect the performance of neighboring antennas (i.e. highly isolated with low field correlation). According to Moores law as shown in Fig. 1.2, an exponential increase is found in both WLAN and cellular data and therefore most of the upcoming radio technology is expected to utilize MIMO technology [2]-[4].

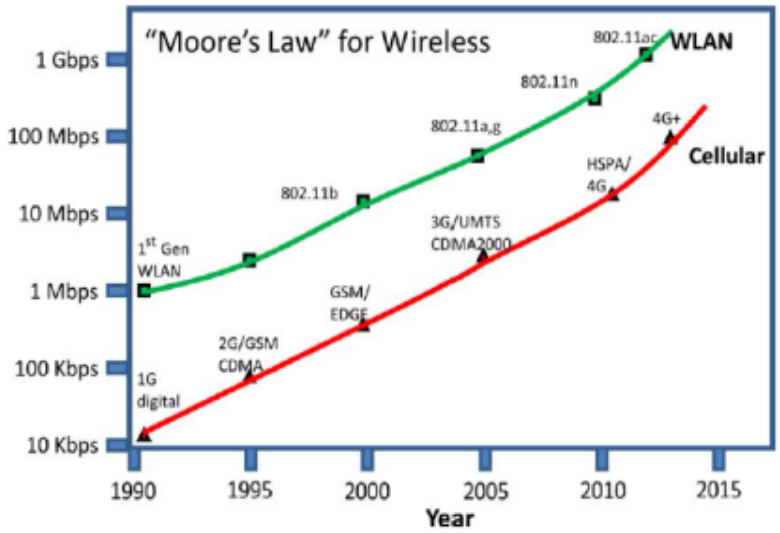

Fig. 1.2. WLAN and Cellular data speed trends [2].

In the presence of an ideal environment, channel capacity increases with an increase in the number of MIMO channels. For multiple antennas, Shannon equation is given by [5].

$$C = MB\ log_2(1+\frac{N}{M} \times SNR) \tag{1.1}$$

Where C is the channel capacity in bps, M is the number of antennas at the transmitter side, N is the number of antennas at the receiver side, B is the

bandwidth (in Hz) and SNR is the signal-to-noise ratio. From eq(4.1), it can be observed that the channel capacity can be increased by either increasing the bandwidth, SNR or the number of antenna elements at the transmitter and receiver side. However, to get wide bandwidth or increased power to get high SNR is limited by spectrum regulations [6]. The only feasible parameter is the number of antenna elements. Fig. 1.3 shows the increase in channel capacity by increasing the number of antenna elements.

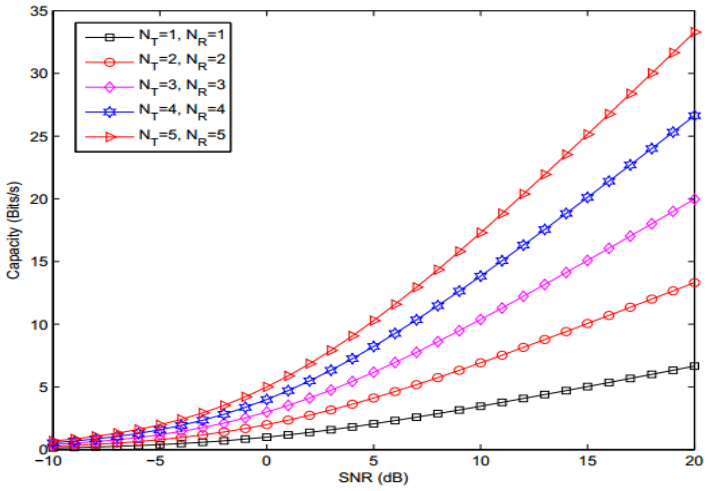

Fig. 1.3. Capacity increase in MIMO [7].

1.3 Work Motivation

In this research work, a new excitation technique (loop excitation) for Printed Yagi-Uda antennas is deeply investigated. We are targeting Yagi-Uda antennas because of their distinct features like: they are highly directive, have high gain, and high Front-to-Back Ratio (FBR). Printed Yagi antennas are robust, easy to fabricate, low in cost, and hence can be easily integrated with RF circuitry. They

have been used in antenna arrays, radars, weather forecasting, and other various wireless applications.

It is known that wideband characteristic is demanded in various wireless applications. But dipoles, loops and microstrip patch antennas are inherently narrowband radiators, although we can modify their geometries to obtain high bandwidths. Quasi-Yagi is the best example in this case. Yagi-Uda antennas are extensively used as end-fire antennas and are famous for their high gain and high FBR. Previously end-fire antennas like Vivaldi and linearly tapered slot antennas were commonly used as phased arrays and as millimeter wave imaging arrays [8]-[9]. The main advantage behind these antennas is the stacking of multiple arrays as layers and hence it allows extra space for RF circuitry like low noise amplifiers and mixers etc. But these tapered slot antennas generally require microstrip-to-slot or coplanar waveguide (CPW)-to slot-transition as a main part of its feeding network. Such feeding network has a great effect on having broad frequency bandwidth and also it increases the complexity of the design [10]. To combat these hurdles, Quasi-Yagi antennas came into existence with a feeding network consisting of a simple microstrip feed or a microstrip-to CPS (coplanar slot) transition. However, a major drawback of Quasi-Yagi antennas is their large size due to the presence of the large ground plane which acts as a reflector element.

Installing multiple antennas at the transmitter and receiver side increases channel capacity. However, such multiple antennas need to be very carefully designed for mobile terminals where limited space is available. Any coupling

between the antenna elements or radiation pattern correlation can significantly degrade the performance of a MIMO antenna system. Therefore such antennas need to be meticulously designed. In this work, we are focusing on designing a wideband Quasi-Yagi based MIMO antenna system with loop excitation. Since a loop antenna can be made as a dual band radiator, our goal is to design a Quasi-Yagi antenna having dual-band characteristics with wide bandwidth, high gain, high FBR, and high directivity using a simple feeding mechanism. In this work, a complete literature study related to passive Yagi, Quasi-Yagi and slot-like Yagi antennas is presented. We have observed that various excitation elements were used in literature based on different geometry configurations like: Quasi-Yagi antennas, Microstrip-Yagi antennas, Yagi antennas with Monopole excitation and Yagi antennas with Folded and Meandered Dipole excitation but none of the designs had used loop antenna as an active element (the one which is excited). Only Two Yagi based MIMO antenna designs operating at 5.2 GHz with dipole excitation are present in literature. However none of the designs targeted the GSM/WLAN/ISM bands.

The proposed Yagi based MIMO antenna with loop excitation will cover GPS, GSM/EDGE, UMTS/HSDPA, Bluetooth, Wi-Fi, and WiMAX bands. A second MIMO design based on a semi-ring slot as an active element will be investigated. It will use a very simple and compact slot reflector (CSR) element (which is the dual of conventional truncated ground plane acting as a reflector) having size of only $14 \times 9.5\ mm^2$ to achieve high FBR ratio of more than 10 dB without using

any complex back-lobe reduction techniques, multiple reflectors or any additional reflector layers as found in literature. This compact semi-ring slot based Yagi-like MIMO antenna system can be used inside wireless hand held devices. Finally, to achieve reduction in overall size of the initially presented Quasi-Yagi design, a miniaturization technique based on loop excitation will be investigated that will make its size compact enough to be used in small wireless terminals.

1.4 Thesis objectives

There are several objectives to be accomplished by the end of this work:

1. To design a dual wideband single Quasi-Yagi antenna element targeting the standard bands of GPS, GSM/EDGE, UMTS/HSDPA, Bluetooth, Wi-Fi, and WiMAX, with loop excitation using a simple feeding mechanism. The antenna will operate at the center frequency of 2 GHz with a single element size of around 120×80 mm^2. A minimum measured bandwidth of 400 MHz, gain of 5 dBi, and FBR of 10 dB will be achieved with a minimum measured efficiency of 60%. A 4-element circular Yagi based MIMO antenna system with loop excitation will implemented based on the single element design with an overall size of less than 300×300 mm^2. This MIMO antenna system will have high port isolation of more than 15 dB.

2. To design a compact (40×40 mm^2) single element slot based Yagi-like antenna having FBR of more than 10 dB. The desired frequency of operation for this design is 3.6 GHz targeting the WiMAX standard. This Yagi-like

design will have a minimum bandwidth of 200 MHz, efficiency of more than 70%, and directivity of around 4 dB without using any director element. A very simple and compact complementary slot reflector (CSR) element having size of 14×9.5 mm^2 will be used for reducing the back-lobe radiation unlike complex back-lobe reduction techniques presented in literature. A 2-element Yagi-like slot based MIMO antenna system will be designed based on the single element one having high isolation of more than 10 dB and field correlation value of less than 0.5 between the elements. The desired size of this antenna system is 80×40 mm^2.

3. To introduce a novel loop miniaturization technique for Quasi-Yagi antennas and to achieve a miniaturization of more than 60% targeting the lower frequencies as compared to the initial loop based Quasi-Yagi design (objective-2). The single antenna miniaturized model will have a size of not more than 60×50 mm^2 at 2 GHz, with a ground plane width of less than 20 mm. It will cover the Telemetry L-band and the GSM/LTE band with a minimum measured bandwidth of 150 MHz. The targeted gain, efficiency, and FBR values are 5 dBi, 75%, and 15 dB, respectively. A 2-element MIMO configuration will be implemented as well. The overall size of the antenna system will be 120×50 mm^2. A novel defected ground structure (DGS) will be introduced to achieve a high FBR of more than 15 dB in both bands.

CHAPTER 2

THEORITICAL BACKGROUND

In this chapter, we briefly discuss some of the important parameters of performance of a single antenna like radiation pattern, resonance, directivity, efficiency, gain, and bandwidth. Then we present another set of important parameters to be considered for MIMO antenna systems like total active reflection coefficient, isolation, correlation coefficient, mean effective gain, and diversity gain. The definition of each parameter along with relevant mathematical equations are presented in this chapter. Finally, we introduce Yagi-Uda and Quasi-Yagi antennas, its distinct features, performance parameters, operating principles, and its applications.

2.1 Basic Antenna Performance Metrics

An antenna can be simply defined as a metallic device (wire or rod) meant for transmitting and receiving radio waves. A wide variety of antennas can be found

in literature but microstrip antennas are found to be of the most interest due to their distinct features like light weight, low profile, low volume, and its easy integration with RF circuitries. Here, we present some of the important features of a single antenna element.

2.1.1 Radiation Pattern

Radiation pattern of an antenna provides the spatial distribution of its radiated electromagnetic energy. The coverage of an antenna can be well analyzed by considering the radiation pattern of an antenna. In most of the cases, radiation patterns are calculated in the far-field (Fraunhofer) region. Fig. 2.1 shows the 3-D radiation pattern of an antenna at two GSM bands i.e. 900 and 1800 MHz.

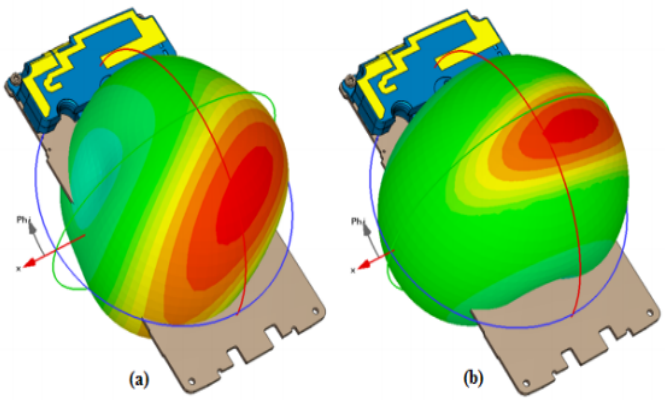

Fig. 2.1. Illustration of the 3D-radiation pattern of an antenna [11].

2.1.2 Resonance

The resonance condition of an antenna is defined as a point where the input impedance of an antenna becomes real. Every antenna has at least one resonance

frequency which is defined by its material and structure [12].

2.1.3 Directivity

Directivity is one of the important parameters of an antenna which describes the concentration of energy radiated by an antenna towards a specific direction. Directivity of an antenna is the ratio between radiation intensity in the given direction averaged over the radiation intensity over all directions. According to [12], average radiation intensity is the total power radiated by an antenna divided by 4π as shown in eq.(2.1) where D is the directivity, U is the radiation intensity (Watts/unit solid angle), U_0 is the radiation intensity of an isotropic source, and Prad is the total radiated power (watts).

$$D(\theta, \phi) = \frac{4\pi U(\theta, \phi)}{P_{rad}} \tag{2.1}$$

2.1.4 Efficiency

The efficiency of an antenna is defined as the ratio of amount of power radiated by an antenna to the amount of power supplied to the antenna. It is a measure of the mismatch losses at the antenna input terminals as well as losses in the antenna structure like conductive or dielectric losses [12]. Mathematically, the overall efficiency (η_0) can be expressed as eq.(2.2) where (η_0) is the total radiation efficiency, (η_{cd}) factor accounts for conductive and dielectric losses while (η_r) factor

is due to the any impedance mismatches and Γ is the reflection coefficient.

$$\eta_0 = \eta_{cd} \times \eta_r = \eta_c \times \eta_d \times (1 - |\Gamma|^2) \tag{2.2}$$

2.1.5 Gain

Gain of an antenna is a relative quantity and is defined with respect to a certain reference antenna. Gain of an antenna is the ratio between the power gain in a certain direction and the power gain of the reference antenna [12]. According to eq.(2.3), gain of an antenna can be related to the efficiency and directivity as

$$Gain = \eta_0 \times Directivity \tag{2.3}$$

2.1.6 Bandwidth

The bandwidth of an antenna is the range of frequencies within which the performance of an antenna is analyzed referring to certain standards of -10 dB bandwidth or -6 dB bandwidth (for electrically small antennas -ESA). For narrowband antennas, bandwidth is usually expressed as the difference between the upper and lower frequencies while for wideband antennas, bandwidth is expressed in terms of fractional bandwidth i.e percentage difference of the frequencies over the center frequency [1].

2.2 MIMO Antenna Metrics

2.2.1 Total Active Reflection Coefficient (TARC)

In case of MIMO antenna system, scattering parameters are not enough to properly characterize the efficiency and bandwidth [13], and therefore for a better realization , TARC is used which is defined as the ratio of square root of the total reflected power to the square root of the total incident power [14]. For N-element MIMO antenna, TARC is given by eq.(2.4) where a_i and b_i represents the incident and reflected signals, respectively. For a two element MIMO antenna system, TARC can be computed using the scattering parameters [15] as given by eq.(2.5) where S_{11} represents the reflection coefficient while S_{12} represents the transmission coefficient. TARC accounts for random signal combination as well as coupling between the ports. It has a value between 1 and 0, whereas 0 means that all the incident power is radiated while a 1 means that all the power is reflected back [1].

$$\Gamma_a^t = \frac{\sqrt{\sum_{i=1}^{N}|b_i|}}{\sqrt{\sum_{i=1}^{N}|a_i|}} \tag{2.4}$$

$$\Gamma_a^t = \frac{\sqrt{|S_{11} + S_{12}e^{j\theta}|^2 + |S_{21} + S_{22}e^{j\theta}|^2}}{\sqrt{2}} \tag{2.5}$$

2.2.2 Isolation

Isolation in MIMO antenna systems is a measure of power coupled between the adjacent antenna elements through substrate, ground plane and ports. Isolation is measured using S-parameters. It should be noted that isolation doesnt account for the energy coupled due to radiation patterns in air. For a good MIMO performance, a minimum isolation of at least 10 dB should be obtained between the adjacent ports. A variety of isolation enhancement techniques are present in literature, mainly defected ground structures (DGS), using parasitic elements, neutralization lines, and using metamaterials [16].

2.2.3 Correlation Coefficient(ρ)

Correlation coefficient is a measure of how much the channels are correlated or isolated from each other and it also accounts for the effects of the environment. In a MIMO antenna system, low correlation is desired between the communication channels in order to achieve better diversity performance. The square of the correlation coefficient is known as envelop correlation coefficient (ECC). ECC can be calculated using eq.(2.6) where $\vec{F_i}(\theta, \phi)$ is the $3D$ field radiation pattern of the antenna when the i-th port is excited and Ω is the solid angle. Eq. 2.6 is valid when the channel is assumed to be isotropic. Calculation of $3D$ radiation patterns measurements is a difficult task as it involves numerical integration. An alternate method of calculating the correlation coefficient is derived in [17] as given by eq.(2.7) which is based on S-parameters and is only valid for high efficient

antennas.

$$\rho_e = \frac{|\iint_0^{4\pi}[\vec{F}_1(\theta,\phi) \times \vec{F}_2(\theta,\phi)]d\Omega|^2}{\iint_0^{4\pi}|\vec{F}_1(\theta,\phi)|^2 d\Omega \iint_0^{4\pi}|\vec{F}_2(\theta,\phi)|^2 d\Omega} \tag{2.6}$$

$$\rho_{eij} = \left| \frac{|S_{ii}^* S_{ij} + S_{ji}^* S_{jj}|}{\sqrt{(1-|S_{ii}^2| - |S_{ji}^2|)(1-|S_{jj}^2| - |S_{ij}^2|)}} \right|^2 \tag{2.7}$$

2.2.4 Mean Effective Gain (MEG)

The gain of a MIMO antenna system is usually measured in an anechoic chamber which doesnt account for the effects of the environment on the gain performance of a MIMO antenna system. MEG is the measure of gain performance of a MIMO antenna system when the effects of the environment are considered. A mathematical expression as given by eq.(2.8) and eq.(2.9) is presented in [17] where XPD is cross-polarization power ratio (which is the ratio of vertical mean incident power to the horizontal mean incident power), $P_\theta(\theta,\phi)$ and $P_\phi(\theta,\phi)$ represents the power distribution and $G_\theta(\theta,\phi)$ and $G_\phi(\theta,\phi)$ represents the antenna gain components. A number of channel models can be found in literature. In [17], a general uniform distribution channel model which represents a regular Rayleigh fading channel is presented as shown by eq.(2.10). The average XPD values for this model are 0 and 6 dB for indoor and urban environments respectively [18]. Similarly in [19], MEG was analyzed using a Ricean channel model.

$$MEG = \int_0^{2\pi}\int_0^{\pi}\left[\frac{XPD}{1+XPD}G_\theta(\theta,\phi)P_\theta(\theta,\phi) + \frac{1}{1+XPD}G_\phi(\theta,\phi)P_\phi(\theta,\phi)\right] \tag{2.8}$$

$$\int_0^{2\pi}\int_0^{\pi}\Big[G_\theta(\theta,\phi)+G_\phi(\theta,\phi)\Big]\sin\theta d\theta d\phi = 4\pi$$

$$\int_0^{2\pi}\int_0^{\pi}[P_\theta(\theta,\phi)]\sin\theta d\theta d\phi = \int_0^{2\pi}\int_0^{\pi}[P_\phi(\theta,\phi)]\sin\theta d\theta d\phi \tag{2.9}$$

$$XPD = \frac{P_V}{P_H}$$

$$P_\theta(\theta,\phi) = A_\theta\ exp\Big[-\frac{[\theta-(\frac{\pi}{2}-m_V)]^2}{2\sigma_V^2}\Big], (0\le\theta\le\pi) \tag{2.10}$$

$$P_\phi(\theta,\phi) = A_\phi\ exp\Big[-\frac{[\theta-(\frac{\pi}{2}-m_H)]^2}{2\sigma_H^2}\Big], (0\le\theta\le\pi)$$

2.2.5 Diversity Gain (DG)

Diversity is usually achieved when multiple versions of transmitted signal are received through different channels. In case of uncorrelated channel, the combined signal at the receiver will provide higher SNR levels and better signal reception. DG is the measure of the difference between the SNR of the combined signals to that of a single antenna system. The diversity gain can be calculated from correlation coefficient [20] as given by eq.(2.11)

$$DG = 10\times\sqrt{1-\rho_e} \tag{2.11}$$

2.3 Introduction to Yagi-Uda Antennas

This section covers the fundamental concepts related to classic Yagi-Uda antennas as well as Quasi-Yagi antennas. It also covers the operating principles, distinct features, main parameters of performance, and applications of Yagi-Uda antennas.

2.3.1 Classic Yagi-Uda Antennas

The operating principle and original design of Yagi-Uda antenna was first described in Japanese in an article which was published in the Journal of I.E.E of Japan by S.Uda [21]. In later article, Uda's colleague H.Yagi described the operation of the same antenna in English [22].

This antenna can operate in the HF (3–30MHz), VHF (30–300MHz), and UHF (300–3000MHz) ranges [12]. As shown in Fig. 2.2, this antenna consists of linear dipole elements. The number of these elements varies from application to application keeping in view the desired output and complexities. These elements can be linear dipoles, loops or rectangular patch antennas depending upon the application. Among these elements, the one which is energized directly is called a Driven element and the rest of the elements are called Parasitic elements. Among the parasitic elements, those who have natural frequencies equal to or lower than that of the incident wave, are called Wave Reflectors, and the element which has a natural frequency higher than that of the incident wave, are called Wave Directors [23] . So, playing with this wave reflecting and directing properties of Yagi-Uda

antennas, a sharp beam and high gain can be obtained. A Folded dipole antenna is the most common feeding element for Yagi-Uda antennas.

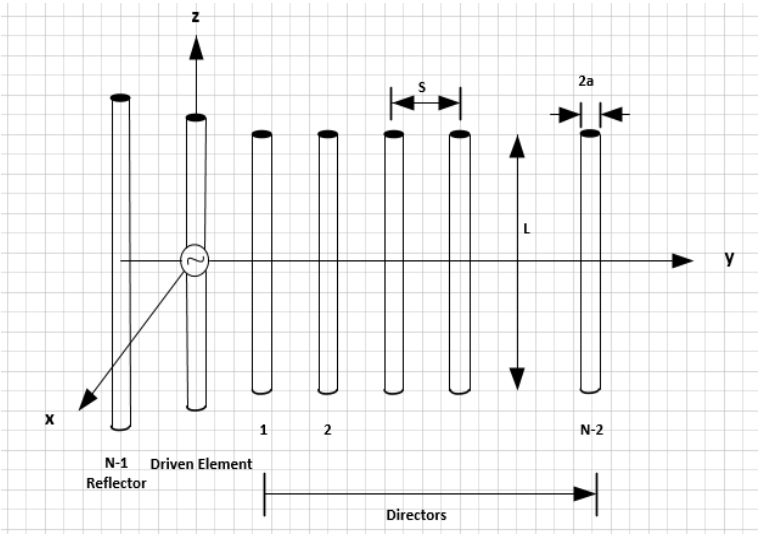

Fig. 2.2. Basic Yagi-Uda antenna configuration.

2.3.1.1 Operating Principles

The Yagi-Uda antenna works on the principle of energy coupling. The electromagnetic energy is coupled from the driven element through space into the parasitic dipoles and then re-radiated to form a sharp beam. Since, a dipole radiates power equally around its axis, so it can couple strong power to its neighbors. The director element directs the beam in the end-fire direction and the reflector reflects the waves in end-fire direction and a sharp beam is obtained. This radiator antenna has been widely used as an end-fire antenna and that is why the length of director elements is kept smaller than the driven element to make the entire beam more directive.

The sharpness of the beam and gain of a Yagi-Uda antenna is highly dependent

on the spacing between directors and the number of director elements. But this spacing and the number of directors to be used is optimized to get a certain limit, going beyond this limit decreases gain. It has been experimentally shown for a Yagi-Uda antenna having total length of 6λ, that increasing the spacing beyond 0.3λ has reduced the gain to $5-7$ dB [12]. It is not necessary to have uniform spacing and uniform diameter of these elements. It depends on the desired output which we want to achieve. Typically, the length of the driven element is kept slightly less than $\lambda/2$ (*usually* $0.45-0.49\lambda$), whereas the lengths of directors are about $(0.4-0.45\lambda)$. The length of the reflector is kept slightly greater than the driven element. The separation between the directors is generally kept between 0.3 to 0.4λ. The spacing between the driven element and the reflector is kept smaller than the spacing between the driven element and the first director whose optimum value is 0.25λ [12].

Practically, very little effect has been found by increasing the number of reflectors to two, thats why usually only one reflector is used. However increasing the number of directors affects the gain significantly [22]. There is a maximum limit, after which increasing the number of directors has no significant impact on gain. The reason for this is the reduction of the magnitude of induced current on the more extreme elements. There is no exact numeric figure of how many directors should be used. The maximum number of directors to be used is found through optimization. Some antennas have number of directors ranging from 6 to 12 but with a large size [12].

2.3.1.2 Unique features of Yagi-Uda Antennas

Yagi-Uda antennas have some distinct features like:

- It is highly directional.
- It has an end-fire radiation pattern.
- It has a high Front-to-Back (FBR) ratio (usually greater than 15 dB).
- It has Low cross-polarization (usually less than -15 dB)
- It has a high Gain (greater than 3 dB)
- Inherently it has a bandwidth of 2%, but it can be increased to 48%.
- It has a low input impedance but can increased through spacing between driven and reflector element or using step-up elements)
- The antenna configuration is simple to build.
- These antennas are robust and are highly compatible with printed circuitry.
- They are easy to fabricate.
- Simple feeding networks can be employed.
- Its design is less costly.
- It is a light weight radiator.
- It has a low profile (small height).

2.3.1.3 Challenges

Although its geometry is simple to build, its optimization is difficult, because parasitic elements (reflectors and directors) are coupled electromagnetically and they are interdependent with each other. Any changes in parameters of one element will change the current distribution on other elements. Hence, the mutual optimization of different parameters is an intriguing task.

2.3.1.4 Main Parameters of Performance

The main parameters of performance in Yagi-Uda antenna are; number of directors, feeding network and spacing between elements. The main characteristics of interest in Yagi-Uda antenna are: bandwidth, front-to-back ratio, forward and backward gain, polarization, input impedance, length, and diameters of the elements along with their corresponding spacing. With the advent of modern high processing computers, best results are achieved using numerical techniques.

It has been shown both numerically and experimentally that:

- The driven element size and diameter has negligible effects on the forward gain but has a large effect on the backward gain, return loss, and input impedance [12]. It has been reported in [24] that by changing the length of the driver element, return loss, center frequency, and bandwidth (is increased) are affected.

- The directors are considered to be the most important elements in Yagi-Uda antenna configuration. Their length, number, and spacing has significant

effect on the radiation pattern and directivity; while it has a small effect on the backward gain and input impedance of the antenna [12].

1. **Length of director elements:**

   Increasing the length of the director element, decreases the radiation beamwidth. But if the director element length becomes equal or greater than the driven element, it acts as a reflector and the back-lobe starts increasing [25]. Also, increasing length of the director, decreases the impedance bandwidth as reported in [26].

2. **Number of directors:**

   It has been reported in [25] that increasing the number of directors from 1 to 6 has the following affects:

   - F/B ratio has been increased by about 15%.
   - Gain has been increased from 2 dBi to 5.5 dBi.

   The design implemented in [27] also states that increasing directors from 1 to 6, increases the gain about 45%. Similarly, it has been reported in [28] that increasing the number of directors from 5 to 12, gain has been increased by 18%.

3. **Spacing of directors:**

   The spacing between the driven element and the first director and between directors is an important parameter to be considered during the design optimization. Increasing the spacing between the driven element and the first director significantly decreases the bandwidth

of antenna and improves the reflection coefficient [29]. Increasing the separation between directors themselves to a certain limit; improves the directivity and return loss as the mutual coupling decreases between the directors [25].

- Reflector size and spacing has negligible effect on the forward gain but has significant effect on the backward gain (front-to-back ratio) and input impedance. As mentioned above, we can increase the input impedance without compromising any parameters performance by introducing a step up element or we can also modify the reflector element size and spacing [12]. The truncated ground plane used in Quasi-Yagi antennas and spacing between the driven element and the truncated ground plane has significant effects on operating frequency range and bandwidth, while it has small effects on the directivity. Moreover, truncation of the ground plane increases the FBR, reduces the overall size, and increases the radiation efficiency [24].

2.3.2 Quasi-Yagi Antennas

The concept of Quasi-Yagi antenna was first introduced in [30]. These antennas have similar characteristics as compared to the classic Yagi antennas except for the truncated ground plane on the bottom layer which serves as a reflector element instead of using additional reflectors. By using such a reflector element, an end-fire radiation pattern is obtained with a comparatively small overall size.

We know that wideband characteristic is the demand for various wireless

applications. But dipoles, loops and microstrip patch antennas are inherently narrowband radiators, although we can modify their geometries to acquire high bandwidths. Quasi-Yagi is the best example in this case. Yagi-Uda antennas are extensively used as end-fire antennas [23]. Previously end-fire antennas like Vivaldi and linearly tapered slot antennas were commonly used as phased arrays and as millimeter wave imaging arrays [31]-[32]. The main advantage behind these antennas is the stacking of multiple arrays as layers and hence it all allows space for RF circuitry like low noise amplifiers and mixers etc. But these tapered slot antennas generally requires microstrip-to-slot or coplanar waveguide (CPW)-to slot-transition as a main part of its feeding network. Such feeding network has a great effect on broad frequency bandwidth and also it increases the complexity of the design [33]. To combat these hurdles, Quasi-Yagi antennas came in its existence whose feeding network consists of a simple microstrip feed or a microstrip-to CPS (coplanar slot) transition.

2.3.3 Applications of Yagi-Uda Antennas

Yagi antennas can find a wide range of applications like radars, local positioning systems (LPS), and wireless sensor networks where high gain, high directivity, and high FBR is required [34]. Other major areas of applications of Yagi-Uda antennas are :

- Millimeter wave imaging arrays
- Phased arrays

- Biomedical applications
- Remote sensing
- Weather forecasting
- Radars
- Local Positioning Systems (LPS)
- Wireless Sensor Networks

2.4 Summary

In this chapter, we have discussed some of the basic parameters of an antenna like its radiation pattern, resonance, gain, directivity, efficiency, and bandwidth. We have also covered the important parameters of a MIMO antenna system such as TARC, correlation coefficient, isolation, MEG, and diversity gain. All the mathematical expressions of each parameter and physical interpretations were discussed.

We have also introduced classic Yagi and Quasi-Yagi antennas and covered their fundamentals in detail. We have also studied the basic operating principles, unique features, main parameters of performance, and some of the applications of the Yagi-Uda antennas. Such antennas have low profiles, low costs, and are highly compatible with printed RF circuitry because they are robust and can be easily fabricated.

CHAPTER 3

LITERATURE REVIEW

This chapter presents a comprehensive study of the literature related to printed Yagi antennas. Based on their geometry and driven elements, Yagi antennas can be broadly categorized as:

1. Quasi-Yagi Antennas
2. Microstrip-Yagi Antennas
3. Yagi Antennas with Monopole Excitation
4. Yagi Antennas with Loop Excitation
5. Yagi Antennas with Folded and Meandered Dipole Excitation
6. Yagi Antennas with Multiple Reflectors
7. Yagi-MIMO Antennas
8. Slot Yagi-like Antennas

9. Others

Printed Quasi-Yagi antennas which cover the major portion of literature review are discussed in detail in section 3.1. These antennas are categorized on the basis of their compact planar structure where the ground plane acts as a reflector element, and there is no need of additional reflectors. Section 3.2 discusses Yagi antennas based on Microstrip Patch elements. Yagi antennas where a Monopole is used as a driven element are discussed in section 3.3. Very few designs are reported regarding Yagi antennas with Loop excitation and are discussed in section 3.4. Section 3.5 presents Yagi antennas where Folded dipole or Meandered dipole are used as the driven elements followed by section 3.6 where Yagi antennas with multiple reflectors are discussed.

MIMO antennas which are already a very hot research area in wireless communication but few works appeared so far using Yagi antennas. In fact only two MIMO designs based on Yagi antenna are found which will be discussed in section 3.7. Yagi-like slot based antennas and different back-lobe reduction techniques are discussed in section 3.8. Other application based different Yagi designs are discussed in Section 3.9.

3.1 Quasi-Yagi Antennas

This section discusses designs based on planar Quasi-Yagi antennas. The design and operating principle of these antennas is based on the classic Yagi-Uda antenna as discussed in the introductory chapter. However, some modifications like truncated

ground plane which acts as a reflector gives good results in terms of mutual coupling, gain, bandwidth, front-to-back ratio, and efficiency.

The design presented in [33] gives a very good insight of how the truncated ground plane acting as a reflector element affects the results. The use of a truncated element instead of a conventional reflector provides a better FBR and also make this antenna compact in size. It also provides a space for RF circuitry like amplifiers, etc., and results in a very compact design which is fully compatible with microstrip-based MMIC (Monolithic Microwave Integrated Circuit) circuitry. This antenna consists of a printed dipole director and a driver element as shown in Fig. 3.1. The driven element is fed by a broadband microstrip-to-coplanar strips (CPS) transition which is usually used for bandwidth enhancement. The antennas total size including the feed transition is $0.50 \times 0.60\lambda_0$. The antenna is built on a Duroid substrate with dielectric constant of 10.2. This antenna covers the X band (8-12 GHz). It is found that this design is at least two times smaller than the standard horn antenna which covers the same frequency band. It is shown that this antenna has a gain of 6.5 dB, 18 dB FBR, and 15 dB cross polarization, and 17% bandwidth. The same design as the one shown in Fig. 3.1 is presented in [30] with increased bandwidth of 48%. This work was basically aimed for getting improved bandwidth and low mutual coupling. This higher bandwidth is achieved by optimizing the parameters of the microstrip-to-CPS feed. It is shown that this antenna has a gain of 6.5 dB, 18 dB FBR, 12 dB cross polarization, and a very low mutual coupling of less than 22 dB when implemented in array configuration.

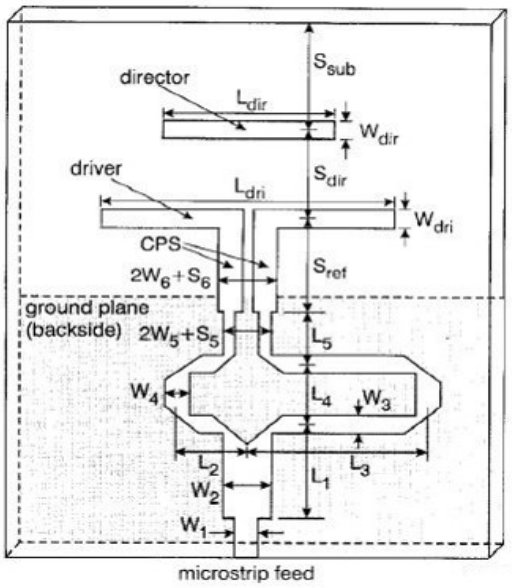

Fig. 3.1. Quasi-Yagi antenna with microstrip-to-CPS transition [33].

A slightly different version of the antenna discussed in [33] is presented in [35]. Here instead of using a microstrip-to CPS transition, a microstrip-to waveguide transition is used. A Waveguide transition is used because of its low loss characteristics. This design is compatible with MMIC and RF photonics technology. This antenna covers the X-band: 8.2 to 12.4 GHz, and have a bandwidth of about 40% with return loss better than 12 dB.

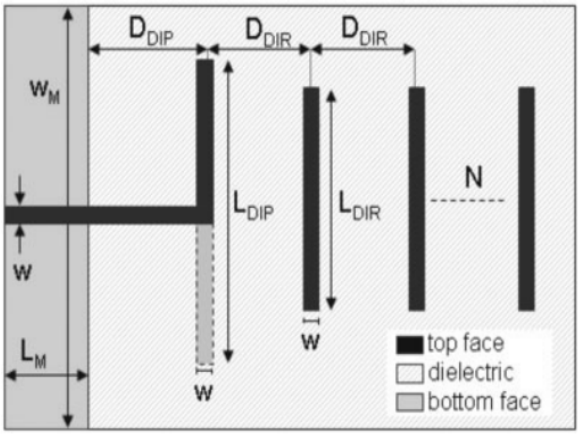

Fig. 3.2. Yagi-Like Printed Antenna with Simplified Feeding [39].

A Coplanar strip (CPS) is found to be a very important part of the feeding network in Quasi-Yagi antennas. CPS is a uniplanar transmission line structure which is widely used in opto-electronic devices [36]. A balun between microstrip and the CPS is usually required to integrate velocity-matched distributed photodetector (VMPD) with RF circuitry. In [36], an efficient 2 back to-back microstrip-to-CPS transitions are designed. The microstrip-to-CPS transition is used by many designs in the literature. The crux behind using a transition is to introduce 180 degree phase delay in the two branches of a microstrip line by changing their lengths. By doing this, we can get an odd dominant propagation mode in coupled microstrip which can then be converted into CPS mode when the ground is truncated. In [37], the same design of [33] is modified further which operates in the C-band. It has a bandwidth of 50%, gain of 6.5 dB, FBR of greater than 20 dB, and cross polarization level less than -18 dB.

Designs in [38] and [39] show very simple feeding technique where a microstrip

line is used for feeding. One arm of the dipole is fabricated on one the top side and other on the bottom side as shown in Fig. 3.2. The frequency of operation is 2.5 GHz. It has a bandwidth of 10% and gain of 7 dBi. The width of the geometry WM is 64 mm and the length is about 95 mm considering only 1 director element. It has a bandwidth of 10% and gain of 4 dBi (with one director) and 7 dBi (5 directors). This complementary feeding design does not require any additional transitions (microstrip-to CPS or microstrip-to-slot line). Using this feeding technique, the radiation losses are reduced and the length of the driven dipole is reduced by 32% as compared to other uniplanar designs [39].

The design presented in [40] represents a Yagi antenna with multi-band characteristics. The overall size of the antenna is 50×60 mm^2. It is designed for 700 MHz band, DCS1800, GPS, GSM900, and Bluetooth/WLAN applications as shown in Fig. 3.3. This design consists of CPW-to-CPS transition which is able to transform the even-mode CPW electric field to odd-mode electric field of CPS line. The overall efficiency of antenna is greater than 80% for all bands and directivity is on average of 4 dBi for the three bands. Designs from [41]-[44] represents multi-band Quasi-Yagi antennas. The targeted bands of these antennas are mostly WLAN around 2 GHz, 3 GHz, and 5 GHz. Among these designs, [41] and [42] displays quite simple feeding techniques and [43] uses a concave parabolic reflector.

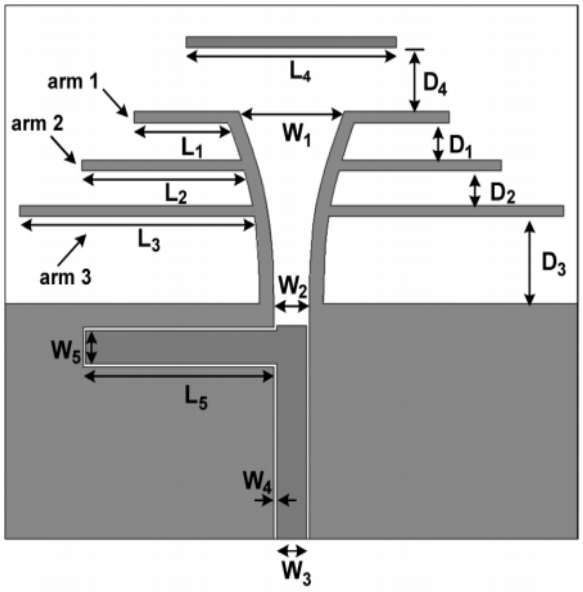

Fig. 3.3. Multi-band Quasi-Yagi antenna with CPW-CPS Transition [40].

Furthermore, designs [45]-[50] represents co-planar waveguide-fed Quasi-Yagi antennas as used in [40] hence appeasing the difficulties faced in using balun structure for microstrip-to-CPS transition. These antennas are fabricated on a single layer and does not require etching of copper on both sides unlike [38]-[39]. This type of feeding helps in reducing the overall size of the antenna and such antennas are easily integrated with microwave circuitry and solid-state devices. Among these designs, the one presented in [45] is shown in Fig. 3.4 which is reported as the simplest uniplanar quasi-Yagi antenna ever reported. This antenna is realized on substrate Rogers RT 6010 (0.64 mm thick with a dielectric constant of $\epsilon_r = 10.2$). This design is found to be very compact ($0.67\lambda_0 \times \lambda_0$) and it operates in X-band from 8-12 GHz. It consists of two director elements and one driven element. The truncated ground plane acts as a reflector. The antenna is fed by a

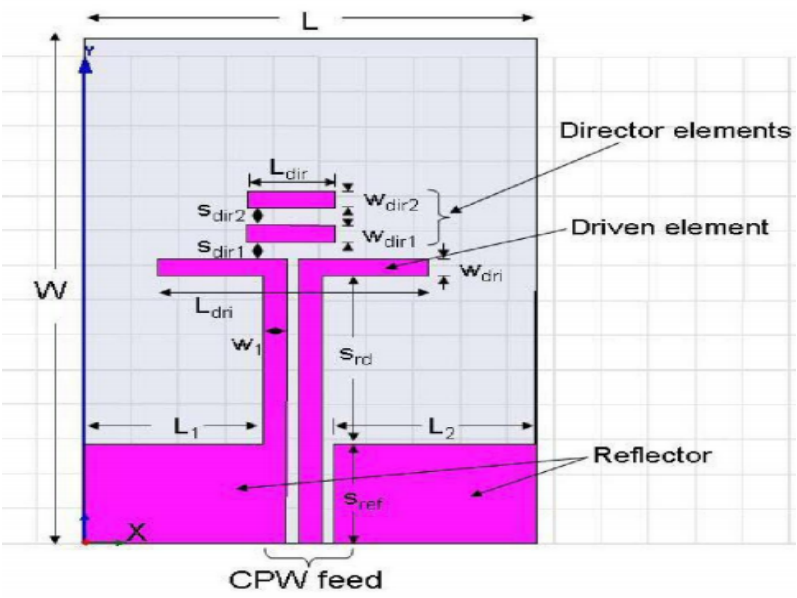

Fig. 3.4. CPW-fed quasi-Yagi antenna [45].

CPW transmission line as shown. This antenna has a bandwidth of 40%, gain of 8.8 dBi, and FBR of 13 dB. In [46], for the first time additional backed conductor feeding called as CB-CPW feeding is presented. This type of feeding helps in providing mechanical support and heat sinking ability as compared to other CPW feeding structures. This additional structure also improves the effectiveness of reflector and gain is increased from 3.84 to 4.2 dB.

Quasi-Yagi antennas which are based on ultra-wideband transition are presented by [51]-[55]. Such designs used a dipole as the driven element and a single director with a truncated ground plane which acting as a reflector element. These designs used microstrip-to-CPS transition as shown in Fig. 3.5 which excites the odd mode by providing 180^0 phase delay due to path difference of two legs of 3 dB power splitter [51], as discussed in [36]-[37]. A Quarter-wave transformer is used for impedance matching of the power splitter. In [55], along with CPS transition,

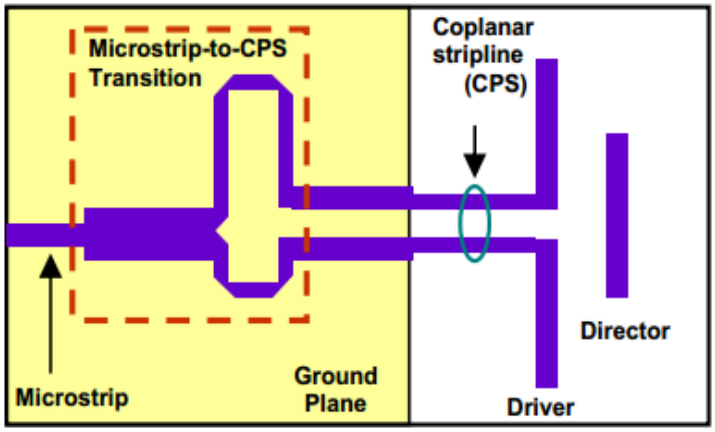

Fig. 3.5. Microstrip-to-CPS Transition [51].

a radial stub is employed for improving the matching [56].

Quasi-Yagi antennas with slot-line feeding are presented in [57]-[59]. One of the designs is shown in Fig. 3.6. The antenna is fabricated and etched on both sides of RT/Duroid substrate (0.635 mm thickness with dielectric constant of $\epsilon_r = 10.2$). The overall size of the antenna is 50×60 mm^2. The antenna consists of a driven element, a director, and slot-line feeding with microstrip line and slot-line stubs which are at 90^0 and have different radii and are used to achieve wideband impedance matching. The microstrip with a stub is designed below the substrate. The microstrip line has a characteristic impedance of 50Ω while the slot-line has approximately 80Ω. This antenna has a bandwidth of 46% operating in frequency band from 4.64-7.42 GHz. It has a gain of around 6 dBi with a FBR of better than 17 dB. The cross-polarization is recorded to be less than -15 dB across the entire bandwidth.

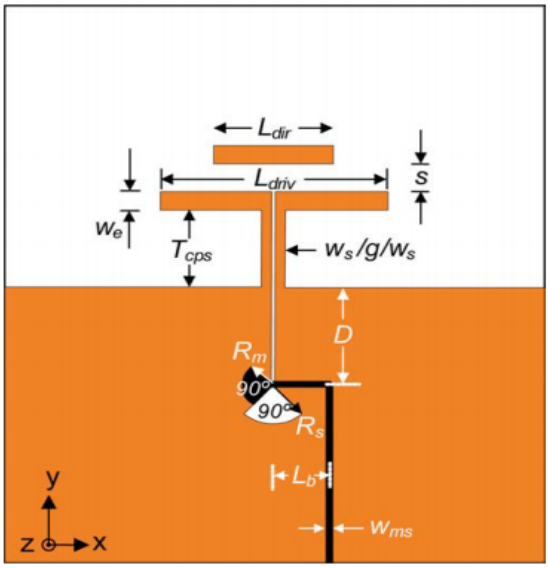

Fig. 3.6. Slot-line-fed Quasi-Yagi antenna [57].

Broadband Quasi-Yagi antennas with new driver element which looks like a Bow-tie antenna configuration is presented for wireless applications in [60]-[62]. The design shown in Fig. 3.7 is presented in [60]. Bow-tie antennas are widely employed due to their broadband characteristics. It is fabricated on fiberglass substrate with ϵ_r of 4.4 and thickness of 1.58 mm. The overall size of the antenna is approximately 89 mm×66 mm. This antenna operates at 1.9 GHz and 2.4 GHz and covers Bluetooth and WLAN bands. It has a bandwidth of around 47% with very return loss of around 30 dB.

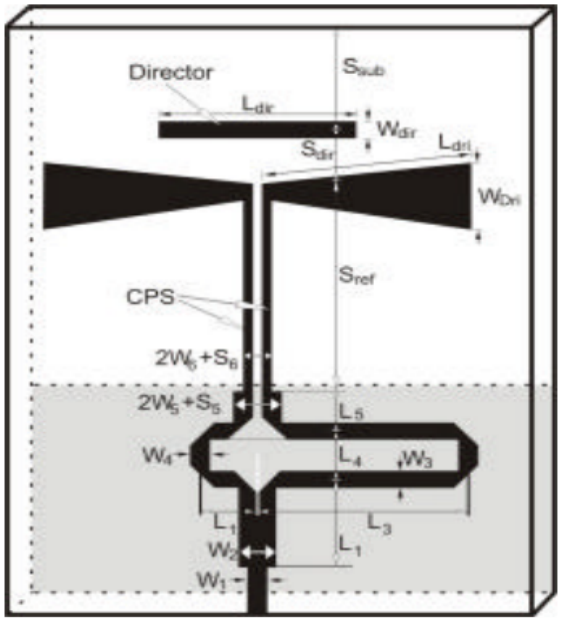

Fig. 3.7. Layout of Quasi-Yagi Bowtie antenna [60].

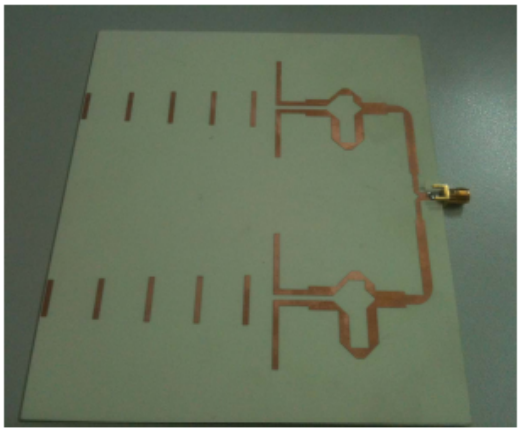

Fig. 3.8. 1×2 Quasi-Yagi antenna array [63].

Quasi-Yagi arrays are presented in [63]-[82] which are based on the same design of [33] to get high gain with compact structures. One such design is presented in [63] and shown in Fig. 3.8. The antenna is fabricated and etched with copper metallization on both sides. The substrate thickness is 1.52 mm, metallization

thickness is 0.07 mm, and the dielectric constant is $\epsilon_r = 3.48$. The total area is reported as 70 mm×140 mm. This antenna operates from 4 GHz to 5 GHz and has a gain of 11.5 dB with a bandwidth of 15%. Another design implemented using the same technique but for a 2×2 structure and is reported to have a gain of more than 13 dB [63]. In [79], a novel Yagi-Uda dipole array fed by a Microstrip-to-CPS transition is presented. To obtain a balanced signal for CPS, a wideband microstrip-to-CPS transition is used with Yagi-Uda dipole antenna. The antenna is fabricated on Duroid substrate with a dielectric constant of 10.2 and thickness of 25 mm. To get better FBR, a 90^0 bent is introduced at the input of microstrip line. This antenna has a gain of 9.1 dB and a bandwidth of 10.3%. It has a better FBR of 15 dB. This design is found as a best alternative to tapered slot antennas and other high profile planar antennas.

Several other Quasi-Yagi designs are presented in [83]-[106] with certain modifications to achieve specific results targeting different applications, e.g. in [83], patch elements are used as the driven element instead of dipoles for power combining and phased array applications. The rest of the geometry structures remain the same as of [33], though with different sizes. As patch elements are more broadside so more isotropic radiation patterns are obtained as compared to classical Quasi-Yagi antennas where dipoles are used as the driven element. Also, good cross polarization levels and FBR are obtained. In [84], a tilted dipole is used as the driven element which can be used in future wireless communications systems. This tilted dipole further improved the bandwidth of antenna. In [85],

an E-shaped driven element with patch directors is presented. Good results are obtained in terms of bandwidth which is 57% at the center frequency of 2.5 GHz, high FBR of 28.5 dBi, cross polarization level of less than -16 dB and, directivity of 5.4 dBi. In the designs presented in [86] and [87], a simple feeding technique is used while in [74] one director element is placed very close to the driven element to obtain better and stable gain throughout the entire band along with greater bandwidth (20% increase in bandwidth as compared to traditional Quasi-Yagi antenna). The design of [88] presents a Quasi-yagi antenna which is backed by a metallic reflector element used to get off-side radiation pattern instead of end-fire. This design can be used in beam steering applications.

A novel printed antenna with circular polarization (CP) is discussed in [89] which is based on the Quasi-yagi design of [33]. The design is very useful in terms of very wide bandwidth (60.4%) which is reported as twice as compared to a typical printed CP antenna. This CP is achieved by feeding two Quasi-antennas with proper feeding where 90^0 phase difference is obtained. For this purpose T-Junctions and delay lines are used. The design presented in [90] discusses bandwidth enhancement and size reduction. It has been reported that this antenna has 16.6% reduction in size as compared to other printed Quasi-Yagi antennas. A Quasi-Yagi antenna integrated with a horn antenna is presented in [91] which is best suitable for applications in milli-meter wave frequencies. Furthermore, the Quasi-Yagi antenna designs presented in [92] and [93] are fabricated using silicon technology. The design in [92] is best suitable for 100-GHz metal oxide

semiconductor radio-front designs. Another interesting modification which is made to the basic Quasi-Yagi design is presented in [94]. This design has a low Radar Cross Section (RCS) by using arrow-shaped Koch dipoles as the driven and director element. These Koch dipoles has the ability to miniaturize the design in a traditional way to reduce the RCS.

The design in [95] presents another impressive variation of the basic Quasi-yagi antenna which uses a folded dipole as the driven element. A folded dipole has good bandwidth characteristics as compared to typical half-wave dipole [96], therefore this design was meant to achieve wide bandwidth. Also, the input impedance of a folded dipole is in the range of approximately 70–280Ω which further makes this design very interesting and demanding, as it has more flexibility of feeding networks to be incorporated with, as compared to half-wave dipole.

The design presented in [97] is targeted for power combing using stacked/trays of Quasi-Yagi antennas where each tray consists of two back-to-back Quasi-Yagi antennas. While the design in [98] which is fabricated on Teflon substrate is meant for millimeter wave applications. In spite of the large number of applications and designs discussed in this section targeting the areas of wireless communication, phased array structures, power combining, and millimeter wave applications; Quasi-Yagi antennas are also used for medical diagnosis as presented in [99]. The design discusses Magnetic Resonance (MR)-Compatible printed Yagi antenna for phased array Hyperthermia applications used in cancer treatment. Another variation of the basic Quasi-Yagi antenna is presented in [100] where arrow-shaped dipoles are

used for digital TV band applications.

An ultra-wideband printed quasi-Yagi antenna is presented in [101] for water detection in the Egyptian desert. This design utilizes another variant which is a meandered line driven dipole element. Another printed Quasi-Yagi antenna design is presented in [102] to achieve wide bandwidth and high gain. Broadband microstrip-fed Quasi-Yagi antenna with simple unique feeding is presented in [103]. Its targeted band of operation is X-band and has an impedance bandwidth of 50%. A high performance 94 GHz Quasi-Yagi antenna which is fabricated on GaAs substrate is presented in [104]. This antenna is found to be easily compatible with active semiconductor devices using GaAs technology.

This section covered literature study of almost all the Quasi-Yagi antennas except the active and reconfigurable designs. These designs were discussed based on their feeding variations, driver element variations, bandwidth variations, substrate variations along with the targeted applications. From this comprehensive study, it can be concluded that Yagi antennas are very important and are widely used based on their unique features. The coming sections further discusses printed Yagi antennas with different variations of using monopoles, microstrip patch, folded dipoles, and loop antennas as the driven element.

3.2 Microstrip Yagi Antennas

Classic Yagi arrays have been widely used in Mobile Satellite Vehicle (MSAT) applications. In [105], a Yagi-Uda array is used as a microstrip Yagi array. This

configuration is developed for the MSAT system. Prior to this work, two medium gain designs were developed in the U.S. One was called electronically steered planar phased arrays [106] and the other was called mechanically steered arrays [107]. These antennas were found to be very expensive along with high profiles. However, the design discussed in [105] combat these disadvantages and it is found that this mechanically steered planar microstrip Yagi array is having low cost with a low profile antenna. The antenna is designed at 1.6 GHz. In this design, microstrip patch elements are used instead of dipoles. All the elements are located on the same horizontal plane supported by a dielectric substrate as shown in Fig. 3.9. The main beam of the array is tilted by the effect of mutual coupling between the patches by optimizing the distance between them. It should be noted that this design consists of only 4 patch elements: one driven element, one reflector, and two metallic director patch elements. Hence, it has reduced the complexity of the design compared to other planar arrays.

This antenna works on the principle of conventional Yagi-Uda dipole. We discussed previously that in case of a classic Yagi-Uda dipole antenna; electromagnetic energy is coupled from the driven dipole to the parasitic dipoles through space. However, in this case energy is coupled from driven patch towards parasitic patches not only through space but also through the surface waves in the substrate. Distance between these patches is an important parameter which is optimized to get the required coupled energy and beam is tilted from broadside to end-fire direction (not perfectly end-fire). Here in [105], the distance between the driven

element and the reflector patch is optimized (0.35λ) to get the required gain of 10 dbic (with respect to isotropic circularly polarized radiation). While the spacing between the driven and the director patch element is optimized to 0.3λ. The size of the board used is 10×17 inches^2. It has been concluded through simulation and measurement that the antenna has a gain of 9.5 dbic.

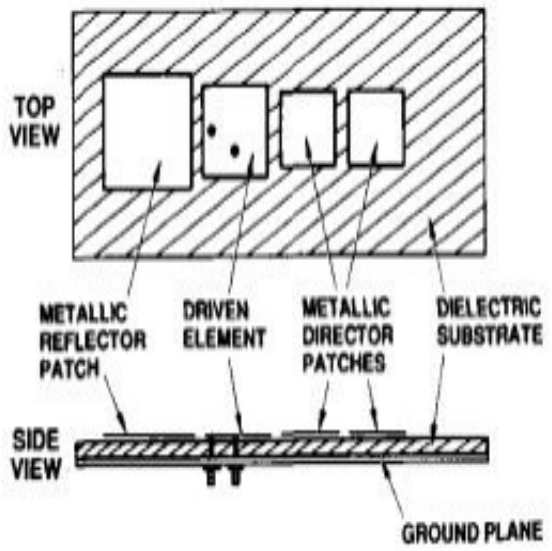

Fig. 3.9. Microstrip Yagi configuration [105].

Yagi-Uda antenna arrays have been widely used as Lens Coupled Imaging Arrays for the Millimeter and Submillimeter-wave regions [108]. In this design, radiator elements are photolitho-graphically fabricated using half wave dipoles on a glass substrate. On the other side of the substrate, directors are used along with hemispherical lens to increase the radiation patterns. That is why it is called lens coupled Yagi array. The measured gain of this antenna is 8 dB and it works at 50 GHz band. These antennas are widely used in remote sensing and in environmental measurements. An interesting implementation of a microstrip

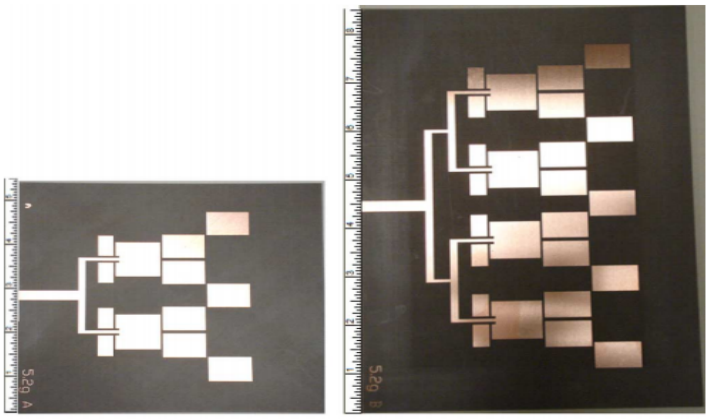

Fig. 3.10. Illustration of Microstrip Bi-Yagi and Quad-Yagi antennas [109].

yagi array is presented in [109] in the form of Bi-Yagi and Quad-Yagi antennas arrays. Fig. 3.10 shows the structure of these antennas. The designs shown in Fig. 3.10 are derived from the original microstrip Yagi array presented in [110]. The main benefit of this structure as compared to [110] is the enhancement in gain around (3-6 dB). Both these designs are fabricated on double copper clad board of RT/Duroid with dielectric constant of 2.2. The operating frequency was 5.2 GHz. The substrate thickness was 62 mm. The substrate size of microstrip bi-Yagi was 4560×5400 mm^2 while for the quad-Yagi was 4940×8496 mm^2. The main beam of this structure is tilted between angles from 33^0-44^0. However steering of the main beam can be controlled by the adjusting the spacing between the driven elements and the first column of directors. The gain for these two structures was reported as 13.0 and 15.6 dBi, respectively with efficiencies above 89%. The level of cross-polarization was below -18 dB and the F/B ratio was approximately 10 dB. Both these structures are best suitable to be integrated with active components for applications in wireless local-area networks. In [111], the same design of Bi-yagi

antenna array of [109] was modified to increase the F/B ratio to 15 dB and a high gain of 10.7 dBi was achieved. According to the author, it is the first ever reported high gain microstrip Yagi array antenna.

Another microstrip printed Yagi antennas is presented in [112] for Wi-Fi applications. Here two microstrip Yagi arrays are connected using corporate feed network as shown in Fig. 3.11. This antenna covers 5 GHz Wi-Fi band. It was fabricated on FR-4 substrate with thickness of 1.6 mm and dielectric constant of 4.7. The size of the substrate was 65×80 mm^2. A higher gain of 9.5 dB was achieved with a better FBR of 17 dB.

The designs given in [113] and [114] present a low cost and highly efficient 60 GHz printed Yagi antenna array as shown in Fig. 3.12. The size of the substrate is $8015\mu m \times 10687\mu m$. It has 2 layers containing patch radiators. Both layers contain driven element and parasitic elements. The driven element of lower layers excites the upper array. The substrate for layer 1 is 254 μm thick and has a low dielectric constant of 2.2, while the substrate of layer 2 is 635 μm thick having a dielectric constant of 2.2. This antenna has a high gain of 10.3 dB achieved at 60 GHz, a bandwidth of 19.4%, and a radiation efficiency of 96%. This design is found suitable for imaging and mining applications.

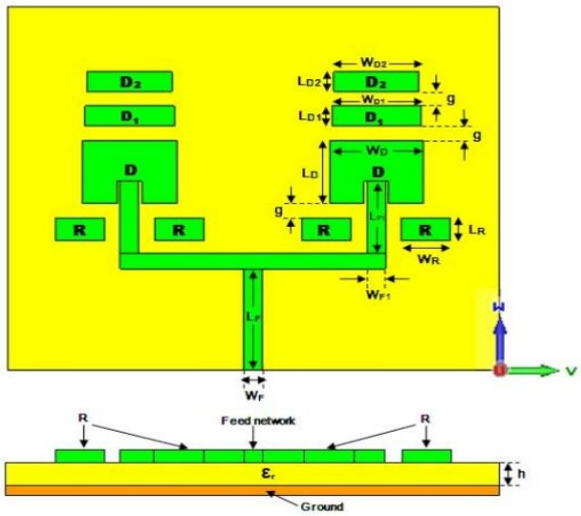

Fig. 3.11. Geometry of microstrip Yagi antenna [112].

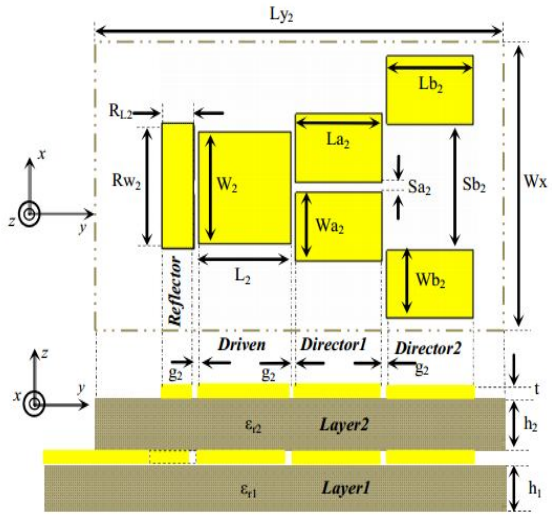

Fig. 3.12. Configuration of antenna design [113].

In addition, some other variations in design of microstrip Yagi antennas can be found in [115]-[120] depending upon the targeted frequency bands and applications. Among these designs, [115] is based on double printed microstrip Yagi for millimeter wave applications around 30 GHz. [116] presents a microstrip Yagi design using dipoles for wireless communication in 5 GHz band. The design presented in [118]

(circularly polarized microstrip antenna) and [119] are based on stacked layers of rectangle patches and circular patch elements, respectively. Their frequencies of operation are 862 MHz and 60 GHz, respectively. [120] discusses printed microstrip Yagi antenna designed for monitoring of physiological parameters at 2.4 GHz. Fig. 3.13 shows a microstrip Quasi-Yagi Array with annular sector directors [121] which is realized on a substrate having thickness of h=1.5 mm and dielectric constant of 2.55. The operating frequency is 5.8 GHz. The proposed antenna is very compact having size of $1.2\lambda_0 \times 1.2\lambda_0$. It has been shown both by simulation and measurement results that by using dual directors, gain is improved from 8.2 dBi to 10 dBi and bandwidth is increased from 13.6% to 17.6%.

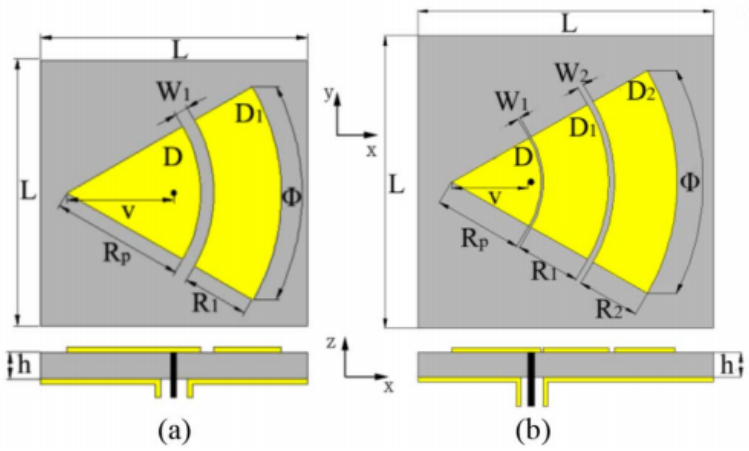

Fig. 3.13. Geometry of the antenna. (a) Single director (b) Dual director [121]

Upcoming section 3.3 presents common Yagi-Uda designs based on Monopoles as their driven element.

3.3 Yagi Antennas with Monopole Excitation

Previously in section 3.1, Quasi-Yagi designs have been discussed with variation of driver elements, e.g, dipole, tilted dipoles, and patch elements etc. Also, designs with different feedings were discussed. In section 3.2, printed microstrip Yagi antennas were discussed. This section, briefly presents printed Yagi antenna designs where the driven element is a monopole antenna.

The design presented in [122] is a low cost and compact efficient radiator based on printed monopoles for GPRS (General Packet Radio Services) applications and is shown in Fig. 3.14 and Fig. 3.15. The antenna consists of five elements, the driven element, two directors, one reflector, and one parasitic element which is usually placed very near to the driven element in order to increase the bandwidth. These monopoles are printed on both sides of the substrates. It should be noted that the driven element is fed by a connector directly without any other feeding network or a balun and it reduces the complexity of the design. The antenna is fabricated on FR-4 substrate with dielectric constant $\epsilon_r = 4.4$. The size of the antenna is 180 $mm \times 90$ $mm \times 50$ mm. The antenna operates in GPRS frequency range (Tx- 1.710-to-1.785 GHz) and (Rx-1.805-to-1.885 GHz). This antenna has a gain of 5.7 dBi.

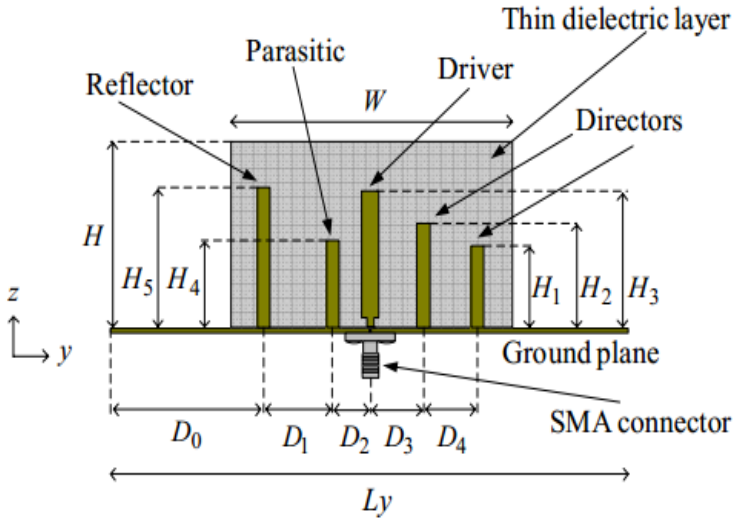

Fig. 3.14. Yagi-Uda antenna composed of printed monopoles [122].

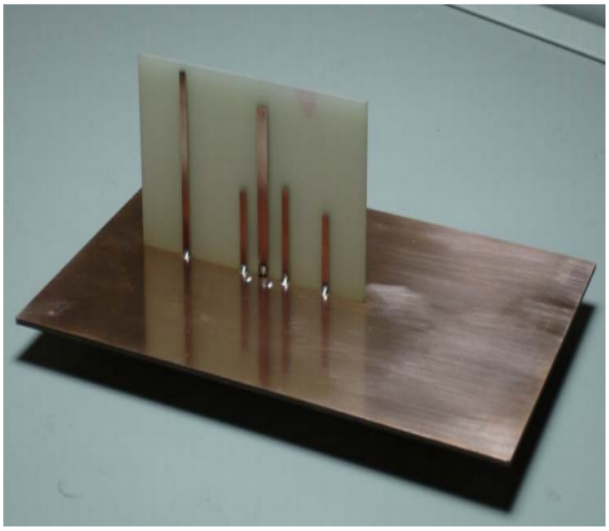

Fig. 3.15. Fabricated Yagi-Uda antenna composed of printed monopoles [122].

A vertical W-band monopole Yagi antenna is proposed in [123] as shown in Fig. 3.16. The monopoles stands on a ground metallic plane above a high-k soda lime substrate. The driven monopole is fed by using coplanar waveguide. The antenna is fabricated using surface-micromachining fabrication technology. It has a high performance as compared to other printed antennas of W-band as the

substrate has very less radiation losses. The signal energy is coupled from driven element towards the parasitic elements in the air and has less interaction with substrate. The driven monopole is fed by a CPW and therefore requires no baluns or other feeding networks. Therefore, the complexity of the design is reduced as compared to other printed Yagi antennas specifically Quasi-Yagi antennas where microstrip-to-CPS transition or CPW-to-CPS transitions are usually used. This antenna operates at 100 GHz, has a bandwidth of 12%, and directivity of 8.2 dBi. This antenna is CMOS compatible and can be easily integrated with RF circuitry.

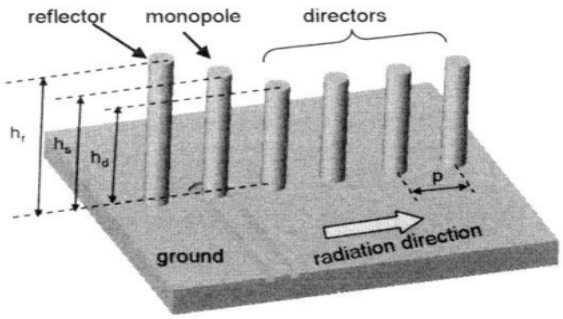

Fig. 3.16. Vertical Monopole W-band Yagi Uda structure [123].

Further implementation of monopole based Yagi antennas can be found in [124]-[128]. A multi-band fractal sierpinski monopole element is designed in [124] which is incorporated in the design of dual-band Yagi antenna which operates in S and C-bands. A very compact ($0.5\lambda_0 \times 0.5\lambda_0$) 2.4 GHz WLAN band antenna with monopole as a driven element is presented in [125]. This antenna has a gain of more than 5 dBi. In [127], closely spaced planar monopole Yagi antenna is presented which operates at 1 GHz. It has a gain of 8.1 dBi and F/B ratio of 11

dB. [128] presents a small multi-sector monopole Yagi-uda array (MS-MPYA) on a circular ground plane. This antenna is found smaller than a typical horn antenna. The center frequency of antenna is 19.5GHz. It has a gain of 15 dB and FBR of 20 dB. The antenna has 12 sectors of 30^0 HPBW and covers all directions.

3.4 Yagi Antennas with Loop Excitation

This section deals with Yagi antennas having loop antenna as the driven element. Very few works are reported in literature based on Yagi-uda configuration with loop excitation.

The design presented in [129] discusses a Quasi-Yagi loop antenna with high gain targeted for imaging applications. The design geometry is shown in Fig. 3.17.The antenna is fabricated on Silicon dioxide layer (SiO2) with $\epsilon_r = 4.84$ above the silicon substrate of $\epsilon_r = 11.7$. The size of the substrate is $5002\mu m \times 3502\mu m$. Both layers of substrate are coated with SiO_2 for the purpose of electrical isolation. This antenna consists of elliptical loop shaped driven and two director elements with a ground plane. The antenna is fed using CPW feeding. To improve impedance matching, a matching section has been designed between CPW and the driven element. The center frequency of operation is 94 GHz. This antenna has FBR of 12.1 dB and gain of 6.5 dBi.

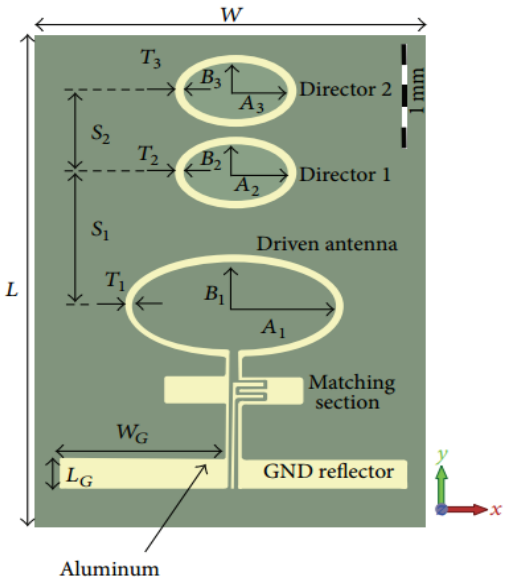

Fig. 3.17. Quasi-Yagi antenna with loop excitation [129].

The design presented in [130] is a slot loop antenna having several directors targeted for LTE applications. This antenna consists of five elements: three director arrays, one driven slot loop antenna, and a planar reflector element as shown in Fig. 3.18. Each director array has nine rectangular loop elements which increases the antenna gain. The driven slot loop antenna is selected because it has a wide impedance bandwidth. The substrate used is FR4 with $\epsilon_r = 4.4$ and thickness of 1 mm. The overall size is around 150 $mm \times 165$ mm. As slot antenna has a high input impedance, so a balun is used on the back side of the slot antenna. The antenna has a gain of 11 dBi and FBR of 18 dB.

Furthermore, designs presented in [131]-[132] present circularly polarized Yagi loop antennas. The design of [131] presents one point fed wire Yagi loop antenna where the driven element has a single gap in the driven element. By changing

the position of the gap, polarization is easily changed. It has a gain of 8 dBi and FBR of 15 dB. The design presented in [132] discusses a circularly polarized mixed Loop-Dipole Yagi antenna. The driven element is a dipole, while reflector and directors are loop elements. This antenna has a gain of around 10 dBi.

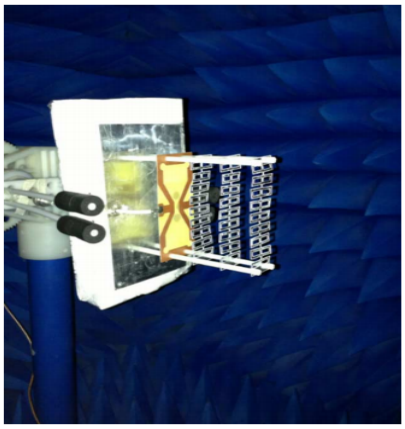

Fig. 3.18. Slot Loop Yagi Antenna [130].

3.5 Yagi Antennas with Folded and Meandered-Dipole Excitation

The unique characteristic of a folded dipole antenna is its high input impedance. Due to its high input impedance, these antennas are practically easy to feed with high impedance microstrip lines commercially available. This section briefly discusses few designs because very little work has been done on Yagi antennas having driver element as a folded or a meandered dipole. A differentially fed millimeter-wave Yagi antenna with a folded dipole as the driven element is presented in [133]. The antenna is built on Rogers RT/Duroid substrate with thickness of 0.381 mm

and $\epsilon_r = 2.2$. The five directors, driving folded dipole, and the CPS-feed are on the top of the substrate while the reflector is on the bottom side as shown in Fig. 3.19. The antenna is approximately 15×15 mm^2. It is also connected directly to an RFIC differential chip. The input impedance of this antenna is high around 153Ω because of the folded dipole. The CPS lines are found to have impedance ranging from 100–200Ω, that's why the folded dipole was selected for the millimeter wave structure. It has a gain of 8-10 dBi with a cross-polarization level of -22 dB. The operating frequency band is from 22-26 GHz and it has a very high radiation efficiency of more than 90%.

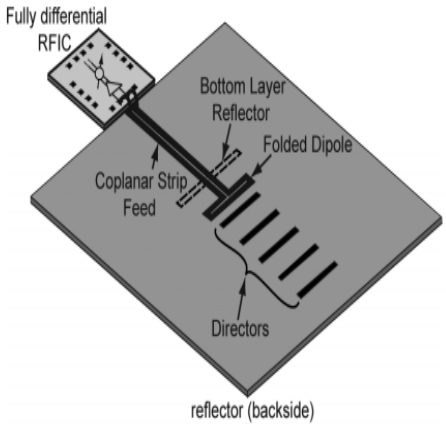

Fig. 3.19. CPS-fed Yagi Antenna with a Folded Dipole [133].

In [134], a compact closely spaced folded dipole based Yagi antenna is presented for achieving high gain. The antenna operates at 1 GHz. The spacing between the elements is only 0.02λ. It has a gain of 6.7 dBi. Likewise, another W-band Yagi antenna with folded dipole can be found in [135]. It has a gain of 14 dBi at 78 GHz and its efficiency is more than 90%.

A novel compact printed Yagi antenna for GPS application is presented in

[136] where meandered dipole is used as the driven element as shown in Fig. 3.20. The antenna is fabricated on FR4 substrate with $\epsilon_r = 4.4$ and thickness of 0.8 mm. The antenna is operating at 1.575 GHz. Half of the meandered dipole is on the top side while other half is on the bottom side of the substrate. The parabolic reflectors are on the both side of the substrate. It has efficiency of 92%, gain of 7.31 dBi, and FBR of 11.6 dBi. It has a very low cross polarization of about -33.5 dB. Another small and slim printed Yagi antenna for mobile application can be found in [137]. Using the meandered structure, the length of this antenna is reduced by almost 43% as compared to a typical dipole antenna.

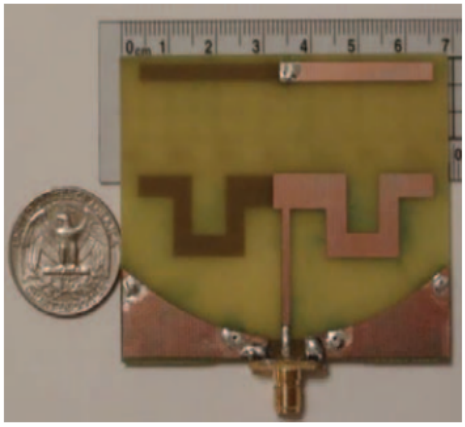

Fig. 3.20. Fabricated compact printed Yagi antenna structure [136].

3.6 Yagi Antennas with Multiple Reflectors

This section briefly discusses printed Yagi antennas where multiple reflectors are used.

The design presented in [138] is a wideband double dipole Yagi antenna which

is fed using a microstrip-slot CPS transition. The traditional dipole is replaced by two parallel dipoles to achieve multi-resonances as shown in Fig. 3.21. It has two stubs for wideband impedance matching [139]: one is microstrip radial stub and other is a slot radial stub. Both have different radii and are at 90^0 to each other. It has a pair of reflectors. These two reflectors are used to further increase the gain. This antenna is fabricated on FR4 substrate with dielectric constant of $\epsilon_r = 10.2$ and thickness of 0.635 mm. The size of the substrate is 60 $mm \times 80$ mm. The antenna has a gain of around 7.4 dBi.

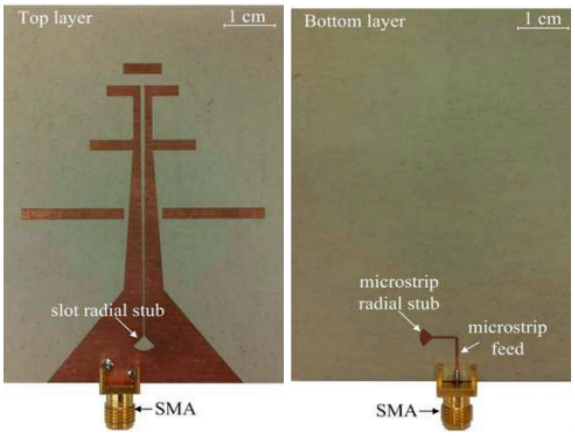

Fig. 3.21. Wide-band double-dipole planar Yagi antenna [138].

Another broad-band CPS-fed Yagi antenna is presented in [140] with a pair of reflectors. The operating frequency was 4.9 GHz and it has a gain of 7.1 dBi. Similarly,

truncated ground plane as reflector, multiple dipoles are used as reflectors and the length of the antenna is reduced. Due to multiple reflectors, the FBR is significantly increased without affecting the forward gain. Firstly the truncated ground plane is used as a reflector. The gain and FBR are 8.5 dB and 13.4 dB,

respectively. Then the truncated ground plane was reduced to four dipoles acting as reflectors. Significant improvement is noticed in FBR and the new value of FBR is 19.4 dB.

3.7 Yagi-MIMO Antennas

As stated earlier, very few works are found related to Yagi based MIMO antennas in literature. In fact only two designs are present [142]-[143]. The design presented in [142] is shown in Fig. 3.22. This antenna is operating at 5.2 GHz. The antenna is fabricated on Rogers RT/Duroid substrate with a dielectric constant of $\epsilon_r = 10$ and thickness of 1.28 mm. The size of each antenna is 22 $mm \times 22$ mm large while the overall size of the structure is 55 $mm \times 48$ mm. Reflector, director, and the driven element is on the same side of the substrate. The ground is shaped in a way which will not affect other grounds of two elements and will reduce metallization in these areas. The antenna is fed by proximity coupling by using microstrip-to-CPS transition above the hole in the ground plane. A triangular structure is selected to cover each sector of 120^0 and to have low mutual coupling. It is reported to have a gain of 6 dBi. The design presented in [143] is shown in Fig. 3.23. It is consisting of 4-elements with an overall size of 154×154 mm^2 and gain of 9.5 dBi using three director elements.

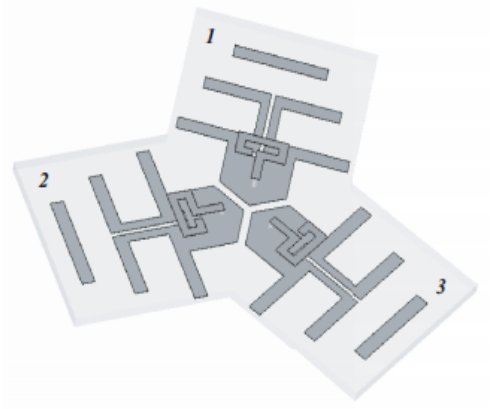

Fig. 3.22. Yagi based MIMO array structure [142].

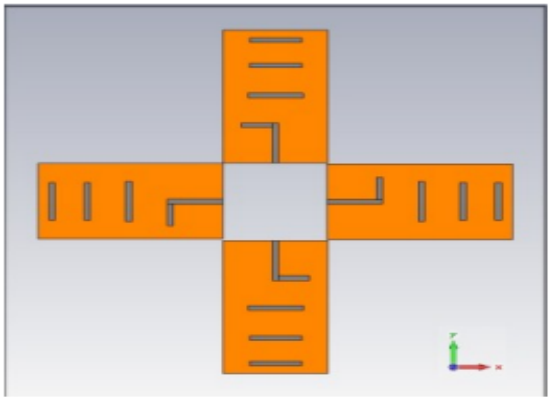

Fig. 3.23. Printed Yagi-Uda array for MIMO systems [143].

3.8 Slot Yagi-Like Antennas

Yagi antennas are famous for high directional end-fire radiation patterns. As slot antenna has an omni-directional pattern, several back-lobe reduction techniques have been used in literature to achieve directional radiation patterns with high FBR.

The design presented in [144] and [145] used resistor and inductor loading

while [146] employed coplanar waveguide (CPW)-fed rectangular microstrip ring antenna to suppress the back-lobe radiation pattern. The designs presented in [147] and [148] shaped the ground plane and used isolated soft surfaces, respectively to achieve high FBR. In [149], multiple reflector elements were used to achieve a FBR of around 13.4 dB. In [150] and [151], additional metallic sheets were used to get a directional radiation pattern. The design presented in [150] is shown in Fig. 3.24. It was realized on a substrate with dielectric constant $\epsilon_r = 2.65$ and substrate thickness of 1.52mm. Its operating frequency was 4.2 GHz. A gain of 12 dB (with 2 directors) and bandwidth of 27.8% was achieved. The reflector element size was 80×90 mm^2 while the overall Size was $80\ mm \times 90\ mm \times 50\ mm$. The design presented in [151] is shown in Fig. 3.25. Its operating frequency was 880 MHz. It had a gain of 5 dB and bandwidth of 83 MHz with a reflector size of $150\ mm \times 65\ mm$.

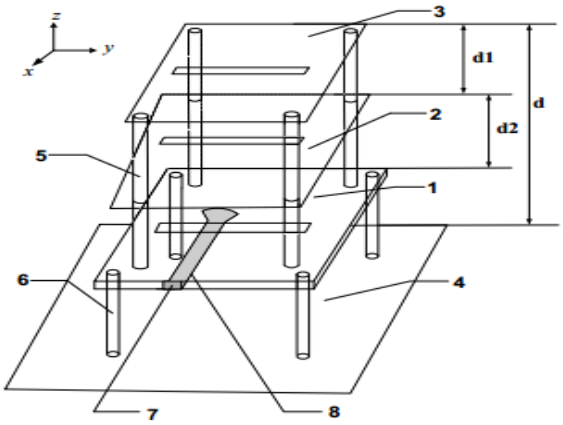

Fig. 3.24. Multi-Layer Slot Yagi antenna [150].

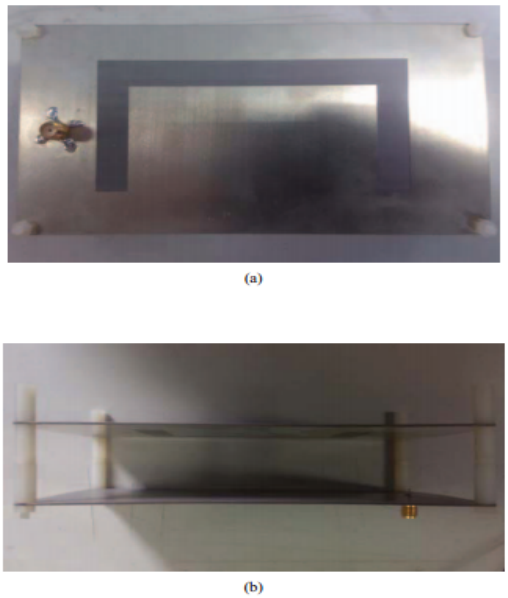

Fig. 3.25. Slot Yagi-Like antenna (a) top View (b) side view [151].

3.9 Other Yagi Antennas

This section is comprised of Yagi designs with different structures which are not categorized in the previously mentioned sections.

A novel design of printed Yagi-Uda antenna is presented in [152]. This design consists of five elements. To get good radiation performance, driven element has been modified as shown in Fig. 3.26. This Yagi antenna is placed on a substrate having thickness of 1.0 mm and permittivity of 4.4. The size of the substrate is approximately 54×60 mm^2. It has a center frequency of 2.4 GHz. This design achieves a high absolute gain of 8.3 dBi and a bandwidth of 10% for VSWR<2. It also has a better FBR of greater than 11.9 dB.

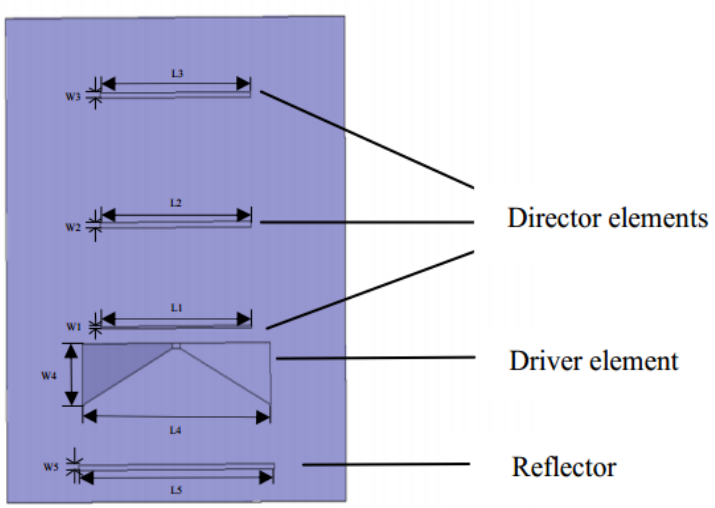

Fig. 3.26. A novel Yagi-Uda dipole antenna [152].

The design presented in [153] is CPW-to-CPS fed antenna with an inverse triangular director as shown in Fig. 3.27. The substrate thickness is 1.52 mm with dielectric constant of $\epsilon_r = 4.2$. This antenna covers WLAN band from 5.38 to 8.48 GHZ. It has a bandwidth of greater than 40%. The total size of the antenna is $42 \times 50 \times 1.52\ mm^3$.

Fig. 3.27. Yagi antenna with inverse triangular director [153].

Similarly other Yagi antennas can be found in [154]-[164]. Among these, [154]

and [155] are not printed antennas which are designed for TV applications and satellite signal reception, respectively. A two element tunable beam antenna is presented in [156]. Designs presented in [157], [158] and [159] are silicon based antennas for CMOS applications. The design in [160] is a wire bond on-chip Yagi-Uda array antenna for radio applications. Furthermore, design discussed in [161] is a compact Yagi antenna for handheld UHF RFID reader. A 60 GHz on-body Yagi-Uda array is presented in [162]. Similarly, a single and dual polarized vertically stacked Yagi antenna is discussed in [163] for microwave and millimeter wave integrated systems. [164] discusses Substrate Integrated Waveguide (SIW) fed Yagi antenna which is operating at 10 GHz.

To summarize, a tree of Yagi-Uda antennas under different categories is shown in Fig. 3.28. It is concluded from the study that a lot of work has been done on Quasi-Yagi antenna and very few studies are present in our band of interest (1.8-2 GHz). Only one loop based antenna is found in our band of interest which is a multi-layer design. It should also be noted that only two MIMO antenna designs are present in literature, but not a single design is present in our interest band with loop antenna as the driven element. Hence our motivation behind this work is to implement Yagi-Loop based MIMO antennas because of its attractive feature: wide dual bandwidth, high FBR, and also because no study till now is reported to have Yagi loop MIMO configuration.

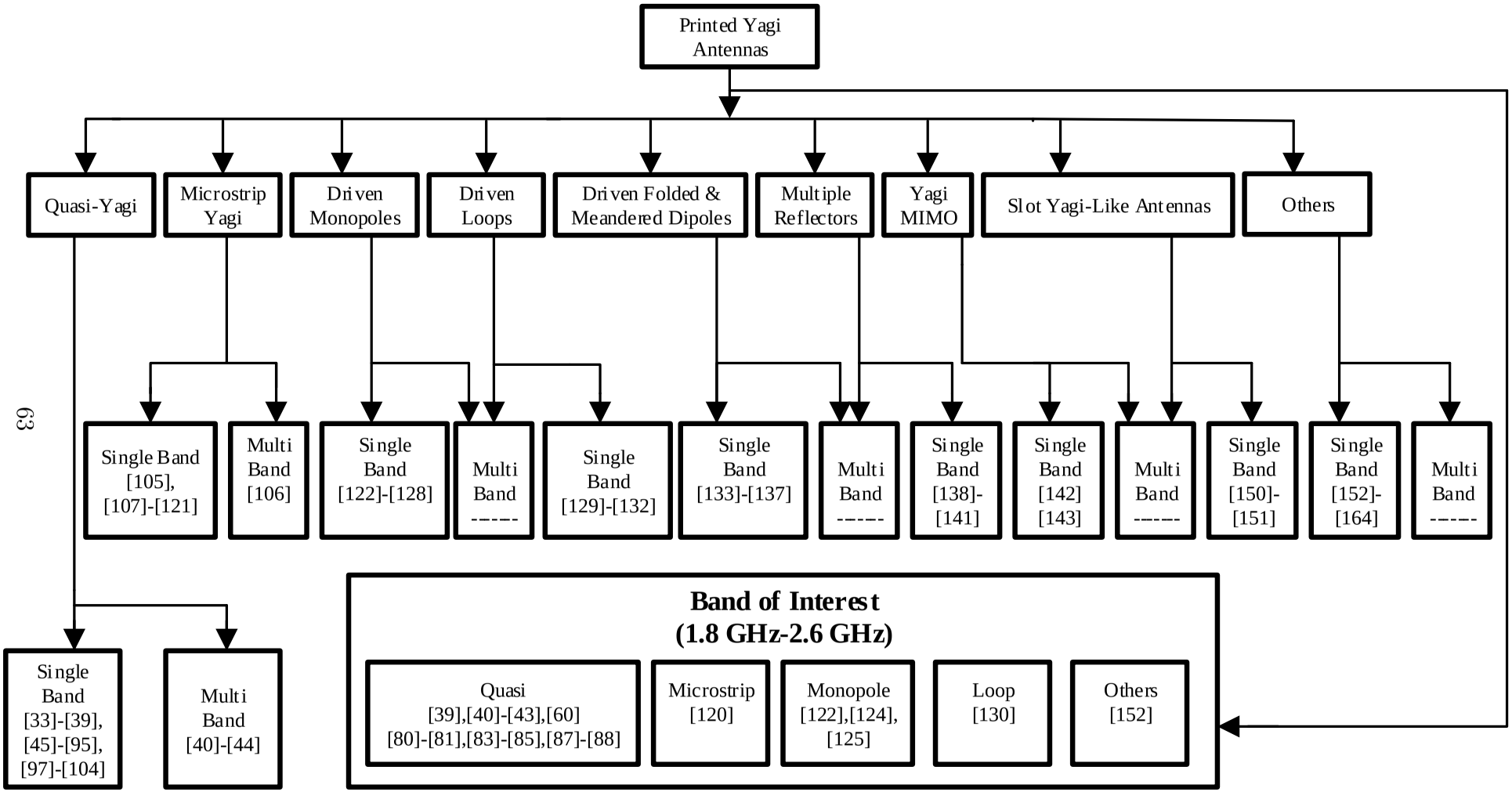

Fig. 3.28. Tree of Yagi-Uda antennas under different criteria.

CHAPTER 4

RESULTS AND DISCUSSION

In this chapter, we present three loop excited Yagi MIMO designs with their simulated and fabricated models as well as simulated and measured results. Firstly, we will start with a single element i.e. Quasi-Yagi based antenna with loop excitation and then we will present 4-element Quasi-Yagi MIMO antenna system. Then we will discuss slot based single as well as MIMO Yagi-Like antenna system in detail followed by the miniaturized Yagi design towards the end of the chapter.

4.1 A 4-Element Dual Wideband Circular Quasi-Yagi MIMO Antenna System with Loop Excitation

In this section, a 4-element circular Quasi-Yagi based MIMO antenna system with loop excitation is presented. This wide dual-band antenna system covers 1.45-2.55 GHz and 3.707-4.71 GHz bands covering GPS, GSM/EDGE, UMTS/HSDPA,

Bluetooth, Wi-Fi, and WiMAX bands. This antenna has an end-fire directional radiation pattern with FBR of 13.8 dB, minimum measured gain of 5.8 dBi, and directivity of 7 dB at 2 GHz using one director element. The minimum measured efficiency across the two bands was 65%. The proposed antenna ensured good MIMO performance in terms of isolation and correlation. It has a minimum measured isolation of 18 dB across both bands. Due to its geometry configuration, pattern orthogonality is obtained which gives very low envelope correlation coefficient values not exceeding 0.1589 in both bands. The size of the MIMO antenna system is 263×263 mm^2 thus making it suitable for wireless access points and on vehicle applications.

4.1.1 Proposed Single Element and MIMO Antenna Geometry

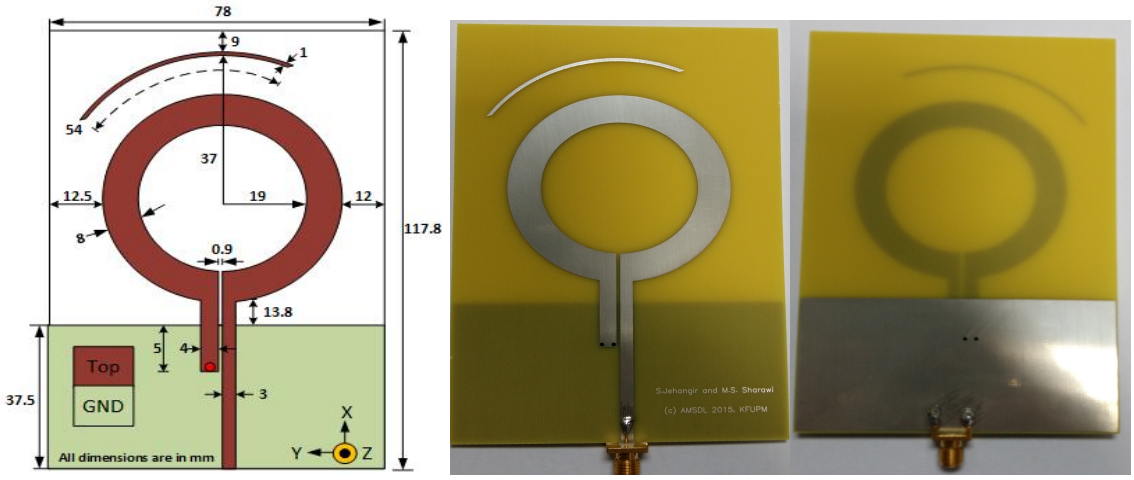

(a) (b) (c)

Fig. 4.1. Single antenna geometry (a) proposed model (b) fabricated prototype-top view (c) fabricated prototype-bottom view - All dimensions are in millimeter (mm).

Fig. 4.1 shows both the proposed geometry model and fabricated prototype of the single antenna element. The overall size is 117 $mm \times 78$ mm. This antenna is realized on a commercially available FR-4 substrate having thickness of 0.8 mm, dielectric constant of $\epsilon_r = 4$, and loss tangent of 0.02. The driven loop and the director element are on the top layer of the substrate while the truncated ground plane (acting as a reflector element) having length of 37.5 mm is on the bottom layer of the substrate. The thickness of the loop is tuned to 8 mm and the spacing between the ground and the loop is optimized to 13.8 mm. The thickness of the shorted leg is 4 mm and its length is set to 5 mm. The spacing between the two legs of the loop is 0.9 mm. The rest of the detailed dimensions are shown in Fig. 4.1(a).

Fig. 4.2 shows the proposed model and fabricated prototype of the 4-element MIMO antenna system. The size of the ground plane is 103×103 mm^2. A square hole of 28×28 mm^2 was made to attach SMA connectors with the fabricated design. The rest of the design dimensions are shown in Fig. 4.2(a). All dimensions are in mm.

4.1.2 Results and Discussion

4.1.2.1 Single Yagi Element

A single Yagi antenna element with loop excitation was first modeled in $HFSS^{TM}$ and then fabricated. The fabricated model can be seen in Fig. 4.1(b). Fig. 4.3

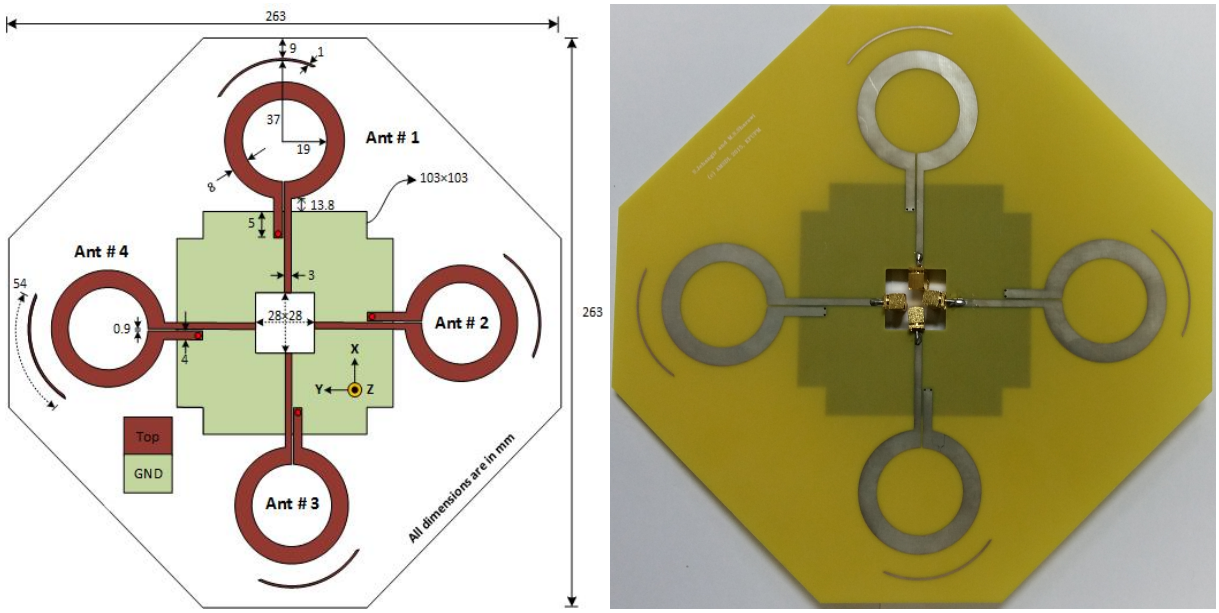

(a) (b)

Fig. 4.2. MIMO antenna geometry: (a) proposed model (b) fabricated prototype

shows the effect of considering the director element on s-parameters. It also shows simulated and measured s-parameters curves of a single Yagi antenna with one director element. A good agreement is found between the simulated and measured results. It can be observed that the impedance bandwidth in the first band is increased from 610 MHz to 970 MHz by using a single director element. However the bandwidth is reduced when a second director element is employed. Using a director element also affects the return loss in the first band and its value is reduced from 28 dB to 23 dB. No significant effect on the bandwidth by using the director element has been found in the second band.

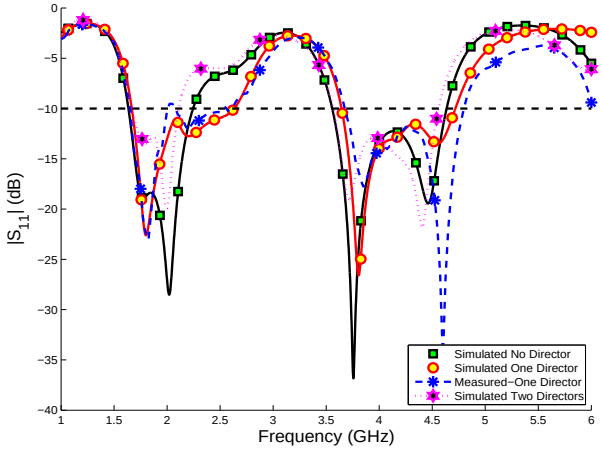

Fig. 4.3. Effect of director element on reflection coefficient of a single Yagi element.

Fig. 4.4 shows the effect of the director element on gain, FBR, and directivity. It can be seen that when a single director element is considered, gain and FBR is increased by around 4 dB. The FBR and directivity is not significantly increased when a second director element is considered. Fig. 4.5 shows the current distribution with and without using the director element. We can see the current nulls and maxima which ensures the end-fire directional radiation pattern for a Yagi antenna. It can be seen that by using the director element, the current density in the end-fire direction is significantly increased which eventually increases the gain and directivity. In our case, we have observed that the resonating mode for our design is close to 1.5 λ_g at 2 GHz.

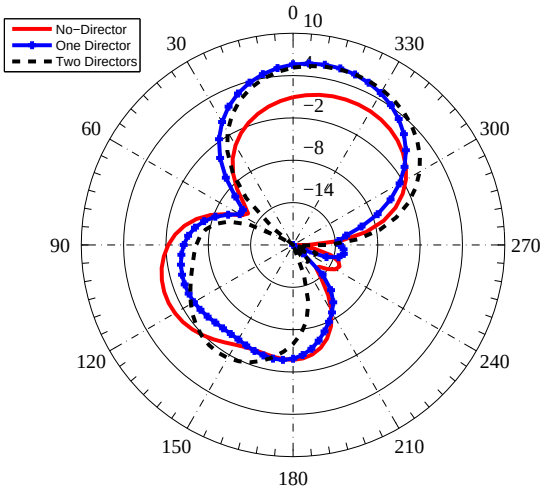

Fig. 4.4. Effect of the director element on gain, FBR, and directivity.

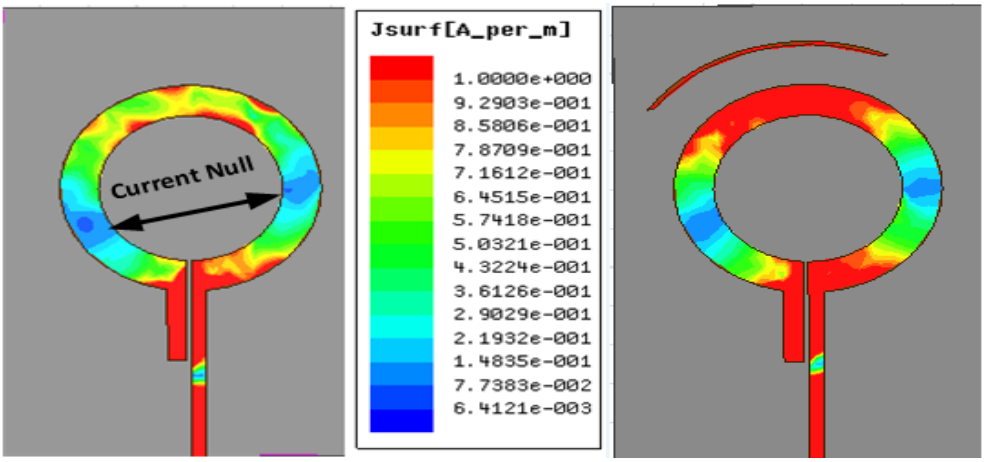

(a) (b)

Fig. 4.5. Current distribution (a) without and (b) With director element.

A parametric analysis was conducted on the various parameters of the design. During this study, it was observed that increasing the width of the driven element and shorted leg increases the impedance bandwidth up to a certain limit and hence these values were tuned to 8 mm and 4 mm, respectively. The Spacing

between the ground plane and the driven element affects the FBR and its value was set to 13.8 mm. The width and length of the director element also affects the bandwidth, FBR, and return loss and their values were tuned to 1 mm and 54 mm, respectively. The spacing between the driven element and the first director is one of the important parameters of performance of Yagi-Uda antennas. Table 1 summarizes the effect of this spacing on the gain and FBR. It can be observed that gain and FBR increases with increase in the spacing until 10 mm. Beyond this value, both gain and FBR ratio decreases and at a spacing of 13 mm, the FBR becomes 1 dB which represents an omnidirectional pattern. Therefore, a spacing of 10 mm is chosen between the driven element and the first director.

The ground plane which acts as a reflector element in Quasi-Yagi antennas is another important parameter that affects the performance in terms of FBR. By using large ground planes, the back-lobe is significantly reduced and eventually high FBR is obtained. Table 2 summarizes the effect of the length of the ground plane on FBR. It can be seen that increasing the length of the ground plane till 37.5 mm increases the FBR significantly and beyond this value, FBR starts decreasing. Therefore, the length of the ground plane was chosen to be 37.5 mm to get the desired results. After the optimization of these parameters, a gain of 5.94 dBi, directivity of 6.21 dB, bandwidth of 970 MHz, and FBR of 9.5 dB were obtained for a single Yagi antenna with one director element only.

Table 4.1. Effect of spacing between the first director and the driven loop element

Spacing(mm)	Gain(dB)	FBR(dB)
3	2.36	2.9
5	4.34	3.1
7	4.76	3.55
9	5.19	7.56
10	5.94	8.6
11	3	4.59
13	2.63	1

Table 4.2. Effect of length of the ground plane on FBR

Length of GND (mm)	FBR(dB)
29	2.12
31	2.14
33	6.34
35	6.38
37.5	9.5
38	4.59
40	4.5

4.1.2.2 4-Element Yagi based MIMO Antenna System

Fig. 4.6 and Fig. 4.7 shows both the simulated and measured reflection coefficient and isolation curves of the proposed 4-element MIMO antenna system. It can be seen that this MIMO antenna system shows a wide impedance bandwidth of 55% and 24% in both bands respectively, and it has a minimum return loss of 23 dB in both bands. The minimum measured isolation within both bands is 18 dB which ensures good port efficiency performance.

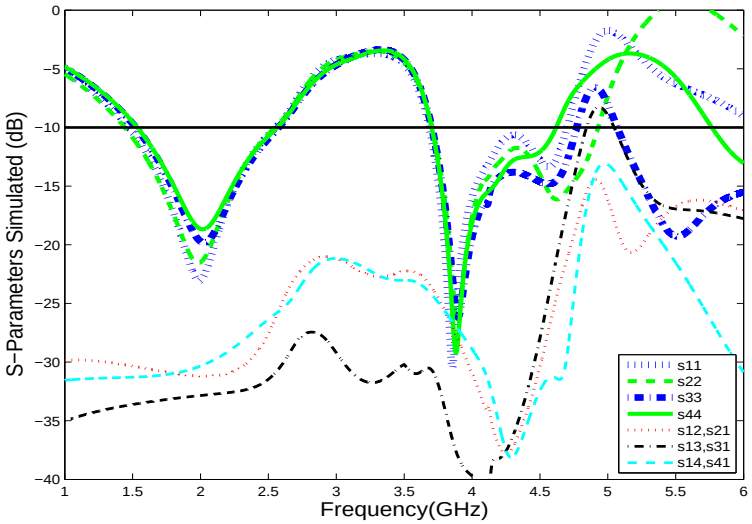

Fig. 4.6. Simulated Reflection Coefficient and Isolation curves

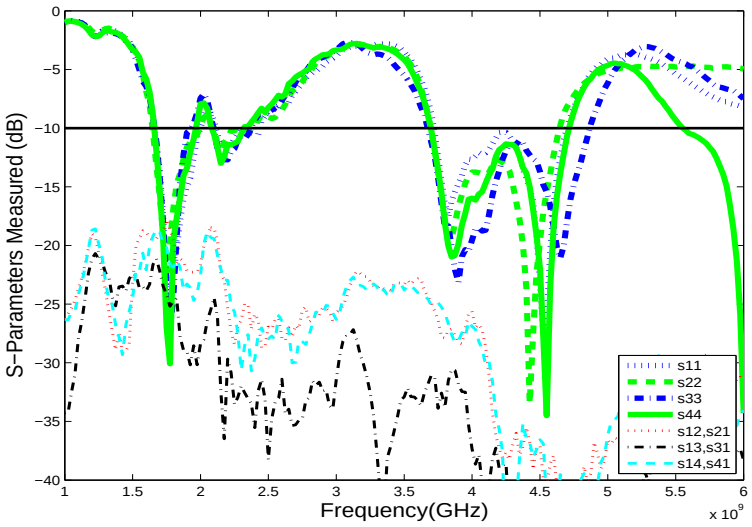

Fig. 4.7. Measured Reflection Coefficient and Isolation curves

To evaluate the radiation characteristics of the MIMO antenna system, it was measured in a Satimo STARLAB anechoic chamber at MVG Italy as shown in Fig. 4.8. Fig. 4.9 shows the measured maximum gain and efficiency of the 4-element MIMO antennas. The minimum measured gain is 5.8 dBi at 2 GHz and 5 dBi at 4.2 GHz which is close to the simulated gain values of 6.6 dBi at 2 GHz and 5.2

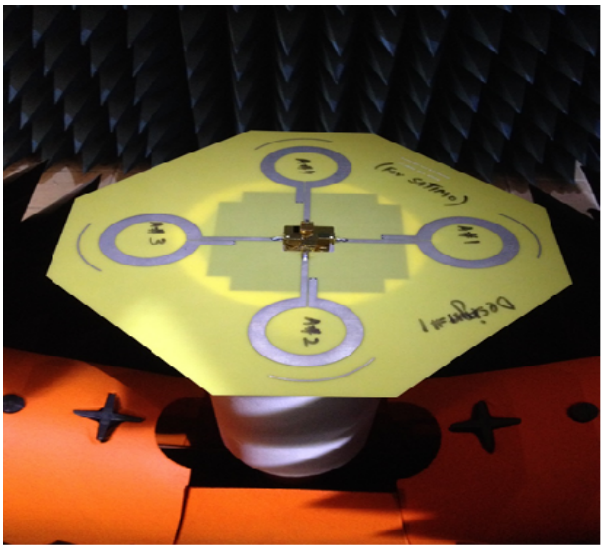

Fig. 4.8. Measurement setup inside anechoic chamber.

dBi at 4.2 GHz. The minimum measured efficiency is greater than 65% which is also close to the simulated efficiency of 70% across both bands. A good agreement is found between the simulated and measured results.

Fig. 4.10 shows the normalized measured and simulated radiation patterns of the four elements in terms of E_{Total} at 2 GHz*. Due to geometry configuration, the radiation patterns of elements 1 and 3 and elements 2 and 4 are 180^0 apart while patterns of adjacent elements are orthogonal to each other as shown in both ϕ and θ planes. Fig. 4.10 (a) shows the measured and simulated $\phi - max = 12^0$ and 16^0 (theta cuts) for elements 1 and 3 respectively, while Fig. 4.10 (b) shows the $\phi - max = 106^0$ and 104^0 cuts for elements 2 and 4 respectively, Fig. 4.10 (c) and (d) shows the measured and simulated patterns obtained at $\theta = 90^0$ (phi cuts)

* The 2D normalized patterns were also computed at 4.2 GHz. The FBR was slightly reduced by 1.2 dB. However rest of the dimension as well as tilting angles almost remained the same and therefore, the figure was not included here to avoid redundancy.

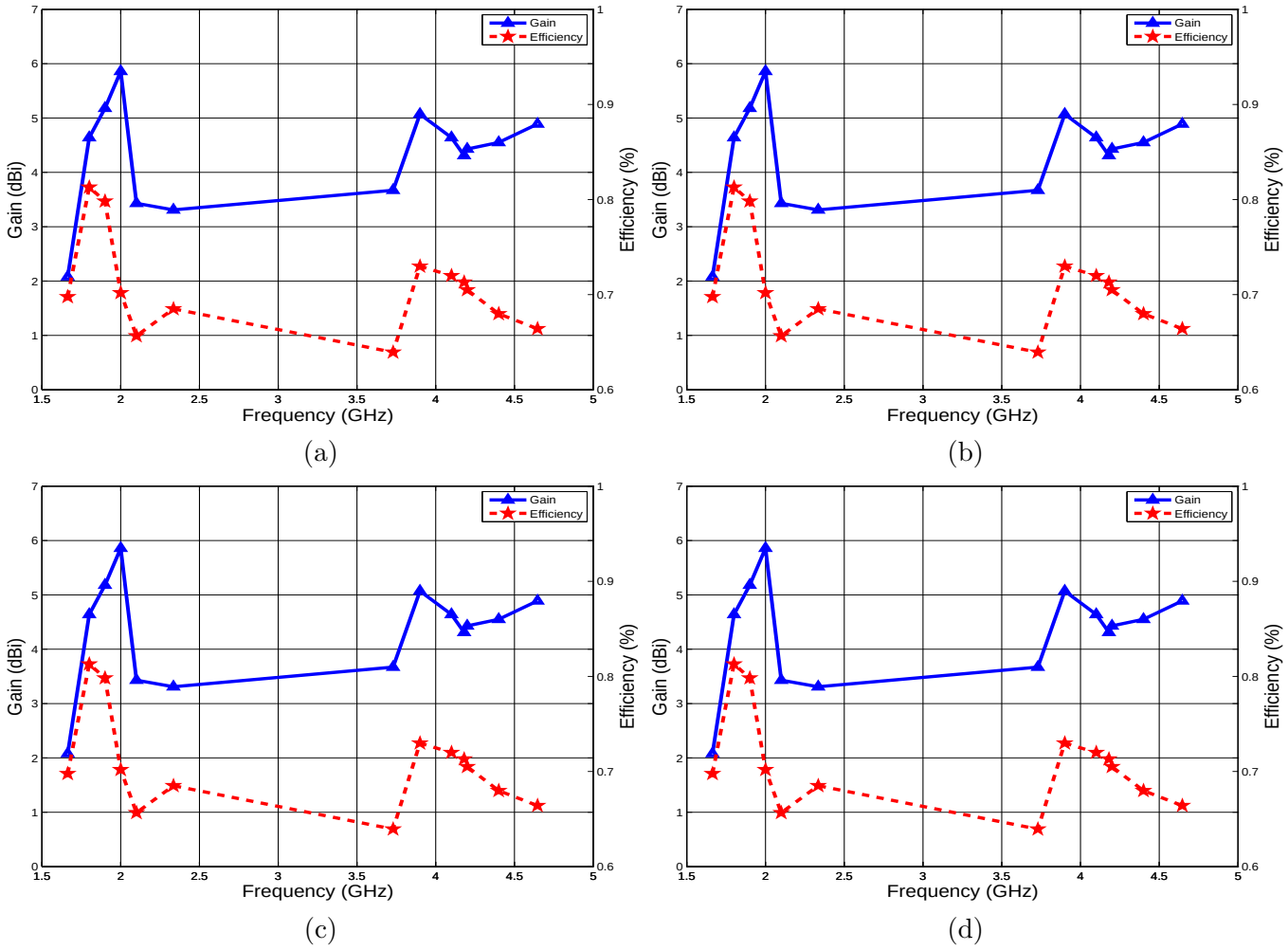

Fig. 4.9. Measured gain and efficiency of the MIMO antenna System (a) Antenna-1 (b) Antenna-2 (c) Antenna-3 (d) Antenna-4

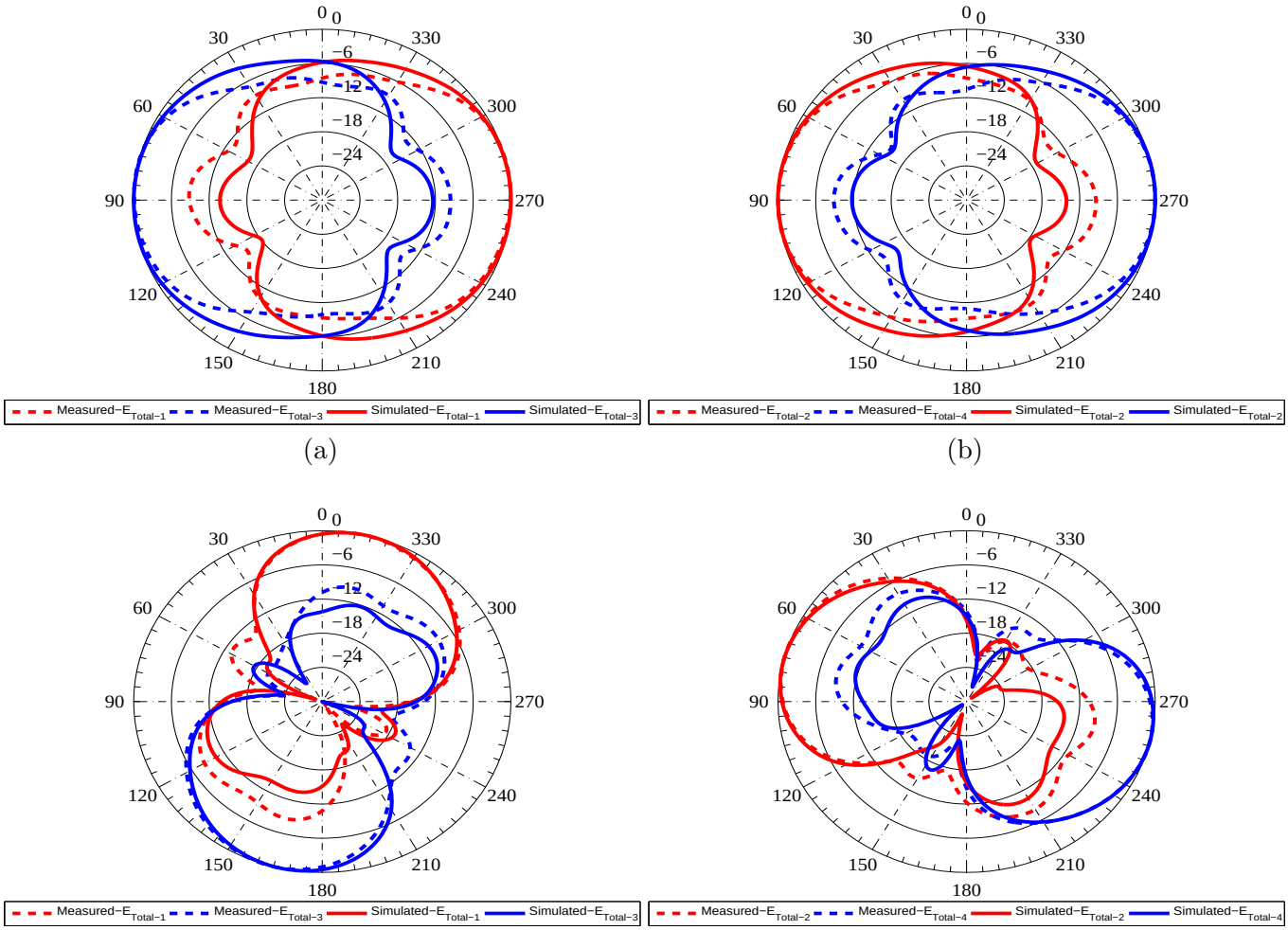

Fig. 4.10. Normalized measured and simulated radiation patterns E_{Total} at 2 GHz. (a)$\phi = 12^0$ -element 1, $\phi = 16^0$ -element 3 (b) $\phi = 106^0$ -element 2, $\phi = 104^0$ -element 4 (c) $\theta = 90^0$, element 1 and 3 (d) $\theta = 90^0$, element 2 and 4.

for elements 1, 3 and 2, 4 respectively, and it can be seen that the patterns are highly directional. It can also be observed that in both of these planes, radiation patterns are completely tilted and hence it ensures very low correlation between the MIMO channels. Both simulated and measured results in both planes shows very good agreement. The calculated ECC values from the measured 3D patterns did not exceed 0.1589 within all covered bands.

4.2 A Single Layer Semi-Ring Slot Yagi-Like MIMO Antenna System with High Front-to-Back Ratio

In this section we discuss the second design based on a novel 2-element single layer semi-ring slot Yagi-like MIMO antenna system with a compact complementary slot reflector. This antenna system covers the 3.5 GHz band for WiMAX applications. It has a minimum measured bandwidth of 320 MHz covering from 3.48-3.8 GHz. A simple and compact slot reflector element having the size of $14 \times 9.5\ mm^2$ is used to achieve a minimum measured front-to-back ratio (FBR) of 10 dB without using additional metallic layers, reflector elements or any complex back-lobe reduction technique. The total board size of the MIMO antenna system is $80 \times 40 \times 0.8\ mm^3$ while the single antenna element has a size of $40 \times 40 \times 0.8\ mm^3$. The antenna system is fabricated and tested. Good agreement is found between simulated and measured results. A measured realized gain of 4.3 dBi, directivity of 6 dB and a minimum measured total radiation efficiency of 73% across the entire band of operation were achieved. This MIMO antenna system has minimum measured isolation of 12 dB, maximum measured envelope correlation value of 0.0385 and diversity gain of 9.81 dB across the entire band of operation.

To use a slot antenna as the driven element (the one which is excited) in a Yagi-Uda structure, is a challenging problem because the radiation pattern of a

slot antenna is omnidirectional (FBR is 1 dB). To achieve a directional radiation pattern and high FBR, several techniques have been used in literature as discussed previously in section 3.8 of chapter 3.

FBR and gain are directly proportional to the length of the ground plane. The main problem usually faced in designing Yagi antennas is their large size due to the presence of the large ground plane or reflector element (to achieve high FBR) and large number of director elements (to achieve high gain and directivity) which eventually increases the size of the antenna. Due to this reason, Yagi based MIMO antennas, usually cannot be placed closely inside small devices due to the limited space available. Therefore, only two designs [142] and [143] based on Yagi MIMO configuration are found in literature (that are large in size) and no work based on slot Yagi-like MIMO antenna systems can be found so far.

The proposed single layer design is based on the half wavelength slot ($\lambda_g/2$) which is known as an equivalent magnetic dipole. Since magnetic dipoles have the same radiation properties as electric dipoles but with different polarization [12], they can be employed as driving elements in Yagi antennas. The proposed Yagi-like MIMO antenna system is compact with an overall size $80 \times 40 \times 0.8\ mm^3$. As slot antennas are etched out of the ground plane and there is no extra ground or reflector layer to reduce the back-lobe radiation, we introduce a very simple and compact complementary slot reflector (CSR) element having the size of $14 \times 9.5\ mm^2$.

The proposed reflector element can be considered as the dual of the conventional metallic reflector element. It increases the current distribution and pulls

the beams in the end-fire direction and hence a minimum measured FBR of 10 dB is achieved without using any complex back-lobe reduction techniques, multiple reflectors or any additional reflector layers as used in literature.

4.2.1 Antenna Design Details

The antenna is designed on a commercially available FR-4 substrate with $\epsilon_r = 4$, thickness $t = 0.8\ mm$ and loss tangent of 0.02. The proposed single element geometry and its fabricated prototype for Model-A are shown in Fig. 4.11 and Fig. 4.12, respectively. The length of the semi-ring slot is half guided wavelength ($\lambda_g/2$) around 22.6 mm at the center frequency of 3.6 GHz. The width of the slot is tuned to 3.3 mm. The slot and the reflector element are etched out of the ground plane (bottom layer). The slot is fed using a transmission line on the top layer. The width and length of the transmission line are tuned to 3 mm and 14.2 mm respectively, to match to 50Ω at the SMA connector location. Note that the width of the transmission line used will yield lower than 50Ω impedance, but the effect of the length, feeding point location at the slot edge as well as the line extension beyond it, will all affect the impedance seen at the input. The optimization of all, will yield the matching required at the SMA input point. Using a 50Ω line width will require another set of optimized parameters for the 3-other dimensions, but will yield similar results at the input port. To avoid any confusions, we present both models A and B for both single as well as MIMO antenna systems. Model-A has a transmission line (T-Line) width of 3 mm (33.5Ω) while Model-B has a T-line

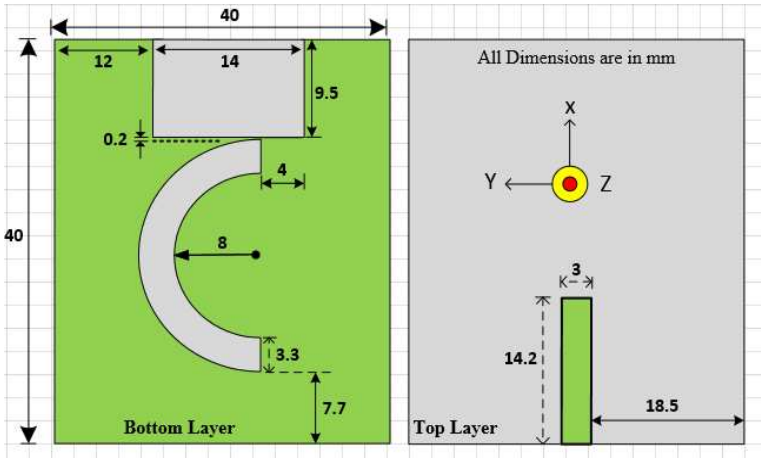

Fig. 4.11. Model-A: Proposed antenna geometry model (a) bottom layer (b) top layer.

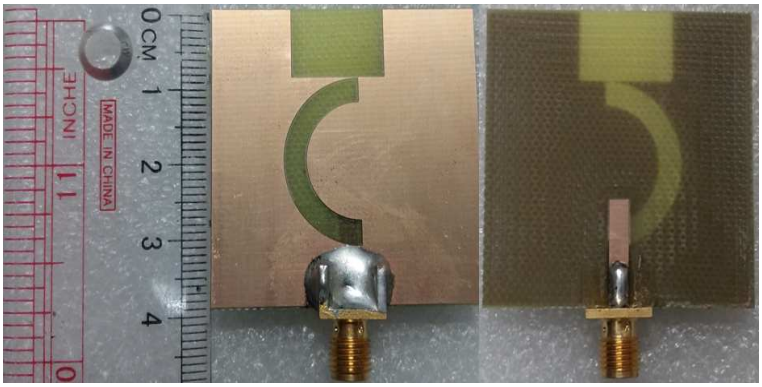

Fig. 4.12. Model-A: Fabricated prototype (a) bottom layer (b) top layer.

width of 1.64 mm (50Ω).

Fig. 4.13 shows the proposed MIMO antenna geometry for Model-A. The separation between the two elements is tuned to 28 mm. The rest of the design dimensions are shown on the same figure.

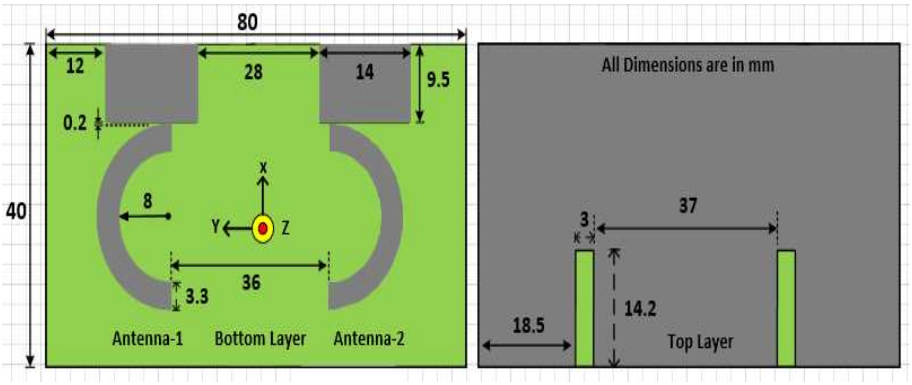

Fig. 4.13. Model-A: Proposed MIMO antenna geometry model (a) bottom layer (b) top layer (All dimensions are in mm).

4.2.2 Results and Discussion

4.2.2.1 Complete Loop Slot Analysis

Fig. 4.14 shows the current distribution of a complete loop slot obtained at the center frequency of 3.6 GHz. The slot was fed using a transmission line above the substrate as shown in Fig. 4.11. It can be seen that the current density is maximum at both sides of the loop while it is minimum in the end-fire direction which ensures a broadside omnidirectional radiation pattern in the y-z plane. The length, width and position of the CSR were optimized in order to obtain maximum current density in the end-fire direction only. But, it can be observed that the current distribution is not significantly affected by using a CSR. Fig. 4.15 shows the 2D radiation patterns of a complete slot without CSR and at three different positions with CSR element. It can be seen that the radiation pattern is omnidirectional and is not affected by the CSR. This section provides detailed explanation to the reader on why we used a semi-ring slot as our driven element

instead of using a complete ring slot.

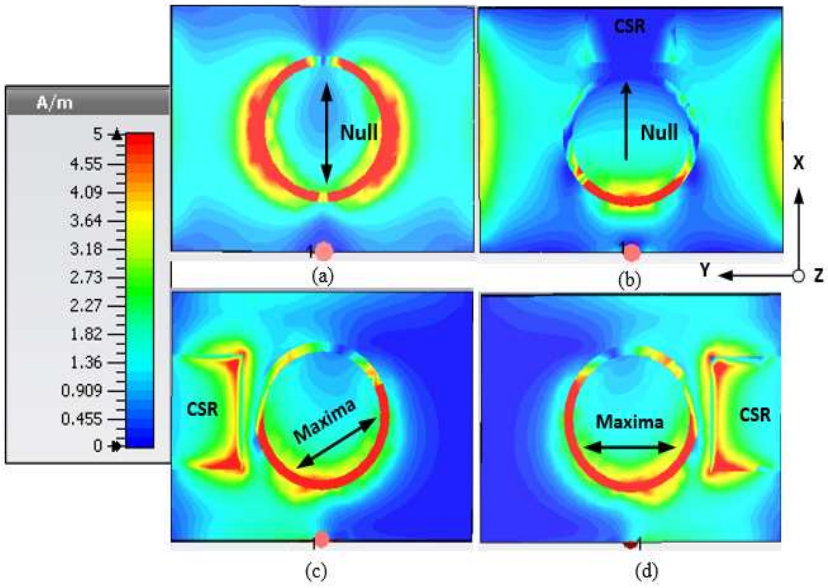

Fig. 4.14. Current distribution of complete loop slot at 3.6 GHz (a) without CSR (b) with CSR-position 1 (c) with CSR-position 2 (d) with CSR-position 3.

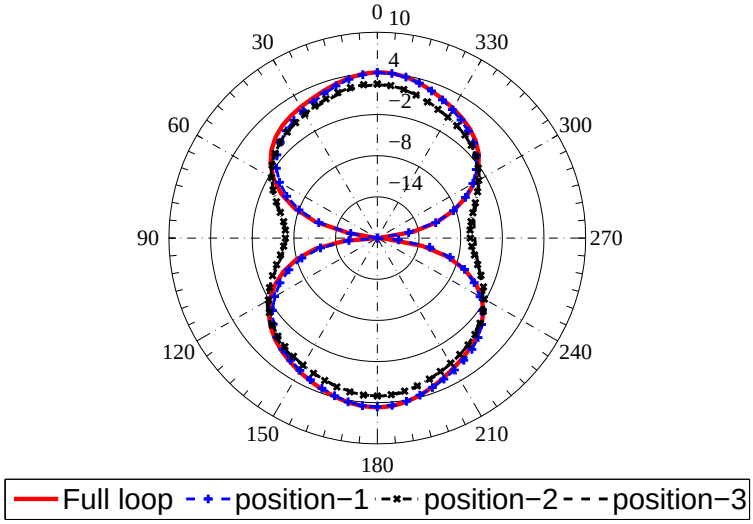

Fig. 4.15. 2D radiation pattern without and with CSR at positions 1, 2 and 3 (y-z plane).

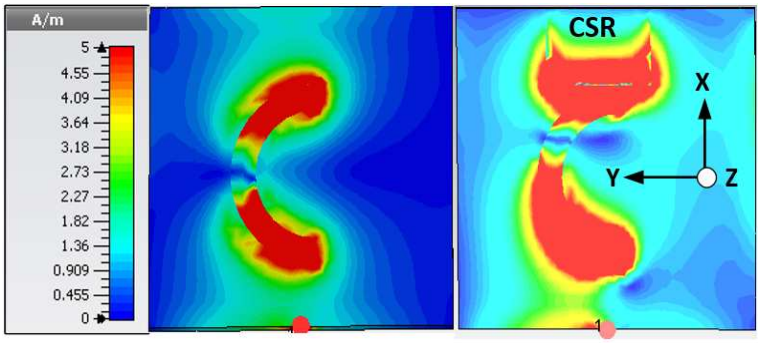

Fig. 4.16. Current distribution of semi-ring slot at 3.6 GHz (a) without CSR (b) with CSR.

4.2.2.2 Half-Loop (semi-ring) Slot Analysis

Fig. 4.16 shows the current distribution with and without considering the CSR element for a half-loop (semi-ring) radiating slot. It can be seen that in case of the semi-ring slot, the current maxima is shifted to the +/- *X-directions* (the feeding position remains the same) and therefore, an omnidirectional pattern is obtained in *x-z* plane as shown by both *azimuth* and *elevation* cuts in Fig. 4.17 (without CSR case). Unlike a conventional reflector in Yagi antennas, this CSR element acts as the dual of the conventional metallic reflector element. It increases the current distribution area and pulls the beam in the end-fire direction (*along x-axis)* and hence a high simulated FBR of 12.6 dB is achieved as shown in both planes in Fig. 4.17 (with CSR case).

4.2.2.3 Single Element Half Loop Slot Results

The proposed single element was modeled in *CST* along with a complete SMA connector model and then fabricated. In both models, copper was modeled as

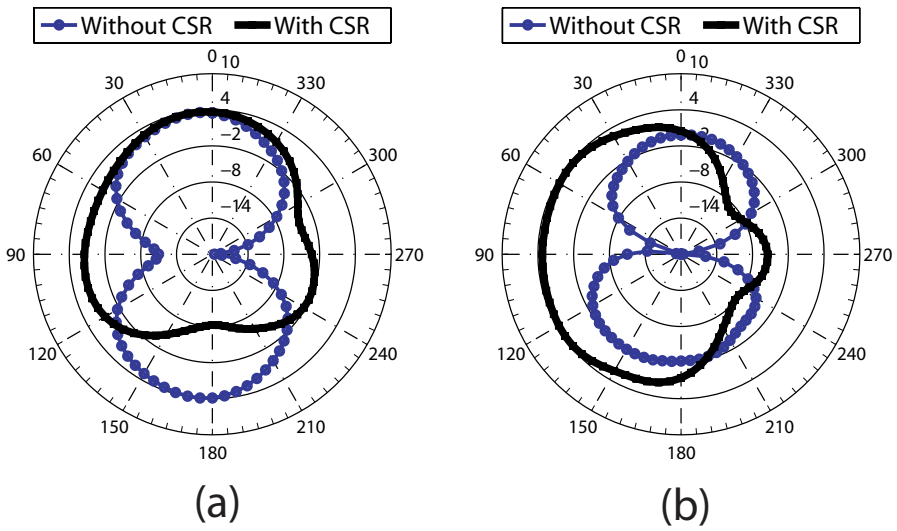

Fig. 4.17. 2D radiation patterns of a semi-ring slot without and with CSR (a) *azimuth cut (at* $\theta = 90^0$*)* (b) *elevation cut (at* $\phi = 5^0$*).*

lossy metal and not PEC to have better comparison with the measured results. The antenna was fabricated in house (at KFUPM) using an LPKF (S103) milling machine. The S-parameters were measured using an Agilent N9918A vector network analyzer.

A parametric study was conducted on different parameters of the design and it was observed that increasing the width of the radiating slot, increases the bandwidth, gain and efficiency while reducing the return loss and hence its value was fixed to 3 *mm*. Decreasing the width of the slot reflector element slightly affected the gain and return loss and its value was fixed to 14 *mm*. The spacing between the slot element and the reflector was found to directly affect the FBR, gain and return loss. Table 4.3 summarizes the effect of this spacing on FBR, gain and return loss. It can be observed that at a spacing of 2 *mm*, the FBR is 1.2 dB which represents an omnidirectional pattern. Decreasing the spacing between the

Table 4.3. Effect of spacing between slot and reflector element on FBR, gain and return loss

Spacing (mm)	FBR (dB)	Gain (dBi)	Return loss (dB)
2	1.2	4.81	28.42
1.8	4.38	4.73	26.61
1.6	6.2	4.71	26.62
1.4	7.7	4.62	26.40
1.2	8.40	4.562	25.8
1	8.41	4.551	25.76
0.8	8.45	4.42	25.45
0.6	8.61	4.42	25.41
0.4	11.48	4.212	24.8
0.2	12.6	4.1	24.73

slot and the CSR element or ultimately increasing the length of the CSR element, increases the FBR but decreases the gain and return loss and its value was set to 0.2 mm.

Fig. 4.18 shows the simulated and measured reflection coefficient curves for both models. The fabricated prototype of Model-B can be seen in the inset of the figure along with the T-line dimensions. For Model-A, the simulated and measured -10 dB bandwidths were 370 and 374 MHz, respectively, thus good agreement was obtained. It can be seen that in case of Model-B, there is a small shift of 9 MHz, and the bandwidth is slightly reduced. It should be noted that in case of Model-B, in order to get 50Ω impedance at the SMA location using 50Ω T-line, different parameters like T-Line width (optimized to 1.64 mm), T-Line length (optimized

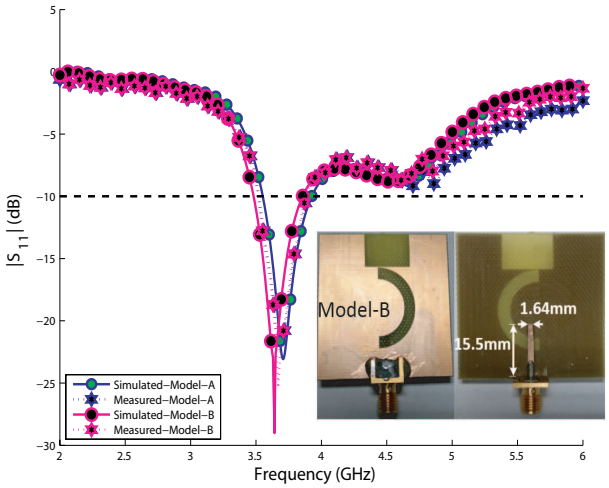

Fig. 4.18. Simulated and measured single element reflection coefficient curves.

to 15.5 mm), extension of the T-Line (optimized to 1.3 mm), and relative location (optimized to 0.9 mm to the left of the location of model-A feed) of T-Line with respect to that of model-A, were optimized. A good agreement between the results of both models was obtained.

To evaluate the radiation characteristics of the antenna, it was measured in a Satimo STARLAB anechoic chamber at MVG-Italy. Fig. 4.19 shows both the simulated and measured gain and efficiency curves. It can be observed that that the minimum measured and simulated realized gains were around 2.36 dBi and 3 dBi, respectively, across the entire band, while the minimum measured and simulated total radiation efficiency were 75% and 79% respectively, across the band. The measured results are in good agreement with the simulations. Small differences in the results are due to the non-idealities of material properties, equipment calibration and connector and cable losses.

A summary of the proposed antenna metrics compared to other slot-based

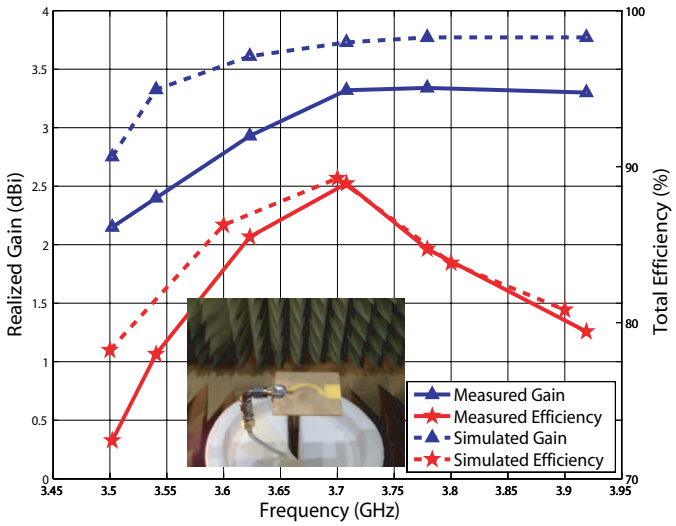

Fig. 4.19. Measured and simulated gain and efficiency of a single element (inset shows the measurement setup).

Yagi designs present in literature is shown in Table 4.4. It can be seen that the proposed design is based on a single layer as compared to the designs present in literature. The size of the CSR element as well as the overall size of the proposed design is very compact as compared to others in literature. The gain of the proposed design is comparatively low as compared to others, as our goal is to achieve high FBR, and we have not employed any director element. Also, it can be seen that the proposed design has the widest operating bandwidth.

4.2.2.4 MIMO Antenna System Results

A parametric study was conducted on the spacing between the antenna elements. Table 4.5 summarizes the effect of this spacing on FBR, isolation, and gain. It can be observed that by increasing the spacing between the antennas, isolation increases continuously while FBR and gain increases until a spacing of 28 mm and

Table 4.4. Comparison of Antenna Parameters to Slot based Single Element Yagi-Like Designs

Parameters	[150]	[151]	This work
Technique used	Multi-layer	Multi-layer	Single layer CSR
Reflector size (mm^2)	80×90	150×65	14×9.5
Overall size (mm^3)	$80 \times 90 \times 50$	——	$40 \times 40 \times 0.8$
FBR (dB)-Simulated	——	——	12.6
Gain (dBi)-Simulated	12 (2-directors)	5	3.55
Center frequency (GHz)	4.2	0.880	3.6
Bandwidth (MHz)-Simulated	——	83	378

starts decreasing beyond this value. Therefore, a spacing of 28 mm was chosen to get the desired high FBR. The spacing between MIMO elements is not usually half a wavelength and it varies from application to application [1],[165]-[169].

Table 4.5. Effect of spacing between the two antenna elements on FBR, isolation and gain

Spacing (mm)	FBR (dB)	Isolation (dB)	Gain (dBi)
18	4	6.51	3.61
20	4.92	6.514	4.38
23	9	12.63	4.51
25	10.3	12.41	4.57
28	11	12	4.61
30	8.41	13.43	4.28
32	8.19	13.96	4.11

Fig. 4.20 and Fig. 4.21 show the simulated and measured S-parameters for Models A and B respectively, including the effects of the SMA connector. The fabricated MIMO antenna prototypes can be seen in the insets of the figures. Good agreement between the results of both models is obtained. The minimum measured isolation within the entire band is 12 dB which ensures good port efficiency performance. Our goal is to achieve a compact size MIMO antenna system. In MIMO literature, there is no standard isolation limit defined. However, isolation between 10 dB to 15 dB is considered acceptable for practical applications [165]-[169]. Isolation can be improved via various methods if needed as shown in [1].

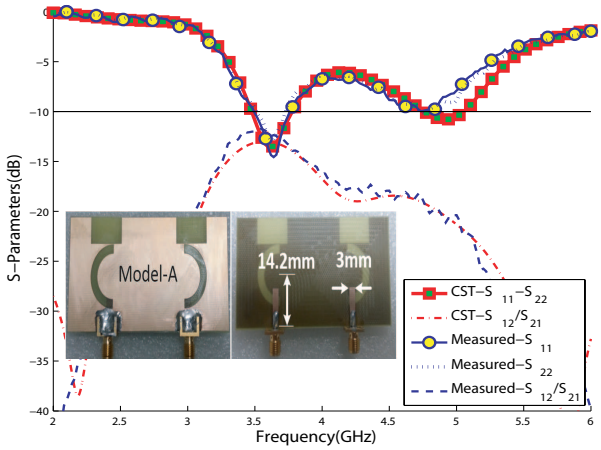

Fig. 4.20. Measured and simulated MIMO s-parameters for Model-A.

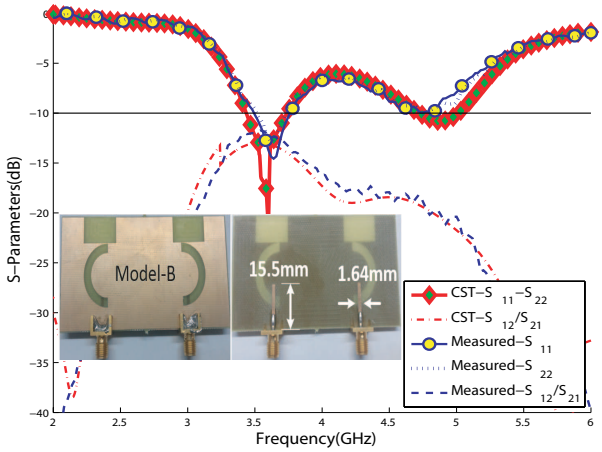

Fig. 4.21. Measured and simulated MIMO s-parameters for Model-B.

Fig. 4.22 shows the simulated and measured gain and efficiency of the 2-element MIMO antenna system. It can be seen that the minimum measured and simulated realized gain are 4.3 dBi and 4.1 dBi respectively, while the minimum measured and simulated total radiation efficiency are 73% and 78% respectively, across the band. The MIMO antenna setup inside the chamber can be seen in the figure inset. The measured results are in good agreement with the simulations. The difference between the measured and simulated maximum gain values does

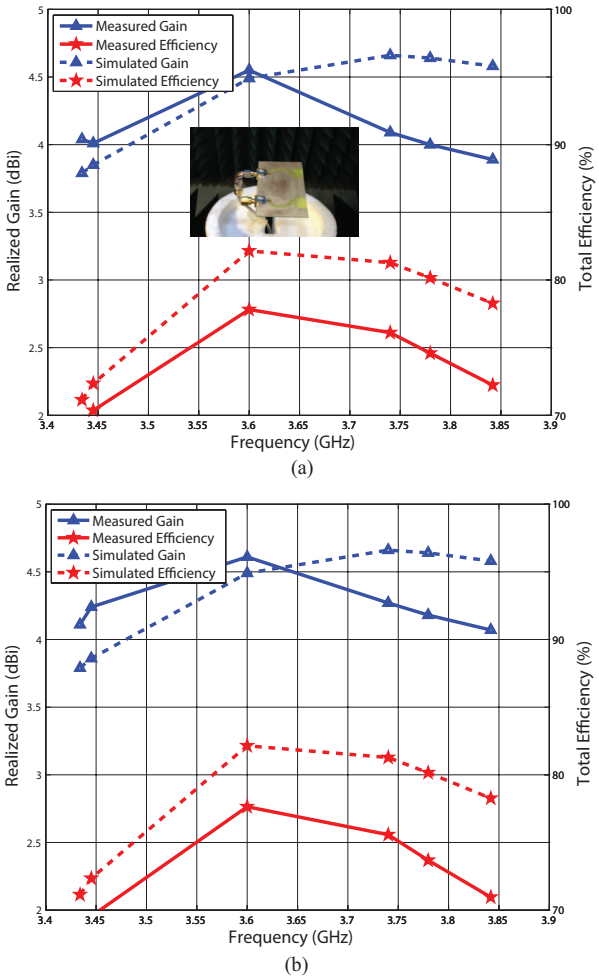

Fig. 4.22. Measured and simulated gain and efficiency of the MIMO antenna system (a) antenna-1 (b) antenna-2 (inset of (a) shows the measurement setup).

not exceed 0.7 dBi in all measurements, which is considered very good compared to other works in literature. According to the data sheet of the anechoic chamber used (SATIMO star lab), the gain accuracy is within +/- 0.8dB [170]. The lower efficiency for the MIMO case comes from the fact that port coupling can degrade the efficiency more compared to the single element case.

Fig. 4.23 shows the normalized measured and simulated radiation patterns of the two elements of model-A in terms of E_{Total} at 3.6 GHz in both θ and

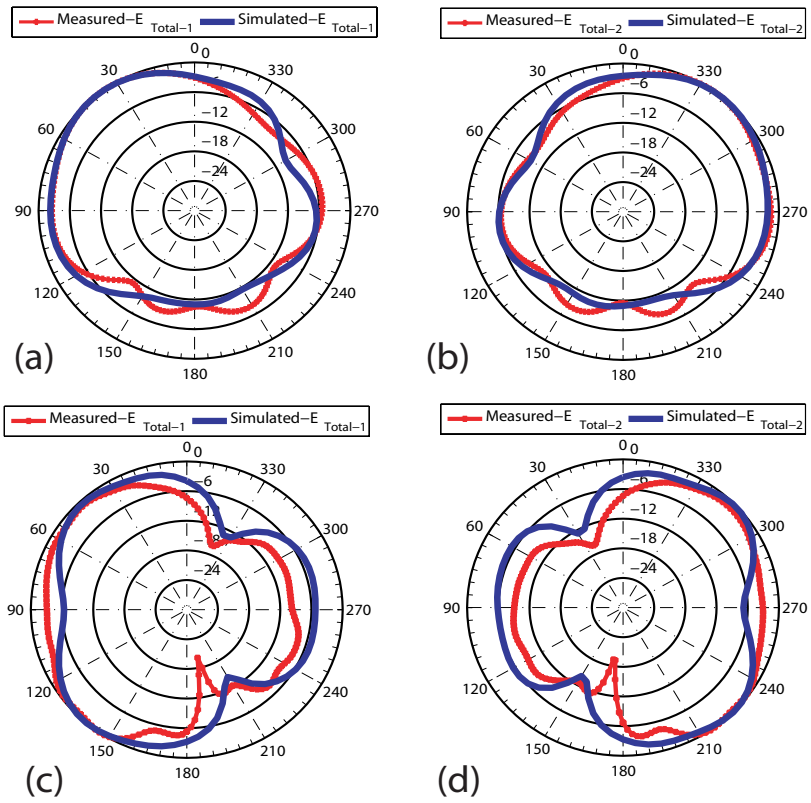

Fig. 4.23. Normalized measured and simulated radiation patterns E_{Total} (in dB) at 3.6 GHz. (a) azimuth cut at $\theta = 90^0$, element 1 (b) azimuth cut at $\theta = 90^0$, element 2 (c) elevation cut at $\phi_{max} = 112^0$, element 1, (d) elevation cut at $\phi_{max} = 68^0$, element 2.

ϕ planes. Fig. 4.23 (a) and Fig. 4.23 (b) shows the measured and simulated patterns obtained at $\theta = 90^0$ (phi cuts) for element 1 and 2, respectively. It can be observed that the field for element 1 and 2 are maximum at $\phi = 40^0$ and $\phi = 320^0$ respectively, and are apart from each other by 80^0. Fig. 4.23 (c) and Fig. 4.23 (d) shows these patterns obtained at $\phi_{max} = 112^0$ (theta cuts) and $\phi_{max} = 68^0$ for element 1 and 2, respectively. It can be seen that fields for element 1 and 2 are maximum at $\theta = 140^0$ and $\theta = 220^0$ respectively, and are also apart from each other by 80^0. As evident from the figure, the radiation patterns are almost

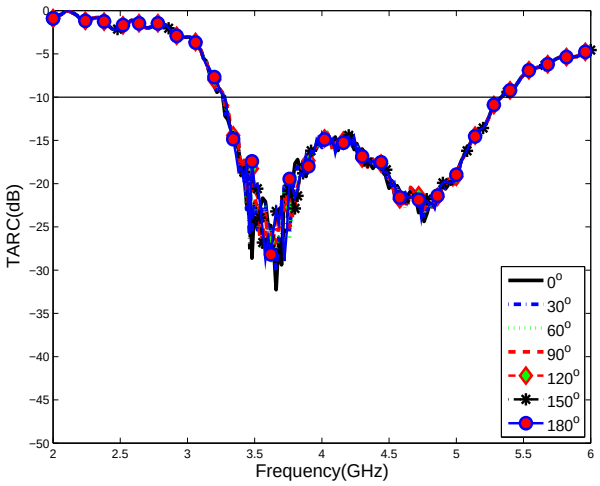

Fig. 4.24. TARC curves for MIMO antenna system.

orthogonal in both θ and ϕ planes and hence ensures very low correlation between the MIMO channels. Both simulated and measured results in both planes shows good agreement. The measured FBR[1] shown by both azimuthal and elevation planes of Fig. 4.23 is around 10 dB and 12 dB, respectively, which is close to the simulated FBR of 11 dB and 9 dB in both azimuthal and elevation planes, respectively.

Total Active Reflection Coefficient (TARC) provides better characterization of a MIMO antenna system in terms of efficiency and bandwidth. For specified phase excitation between the ports, a single TARC curve can be used to find the resonant frequency and impedance bandwidth of the whole antenna system [1]. Fig. 4.24 shows the measured TARC curves calculated from measured s-parameters of model-A according to the expression presented in [1]. It can be seen that the MIMO antenna system has a very stable response in terms of resonance and

[1] The FBR is calculated from the difference between the point where the E_{Total} is maximum and the point 180^0 apart from the maximum.

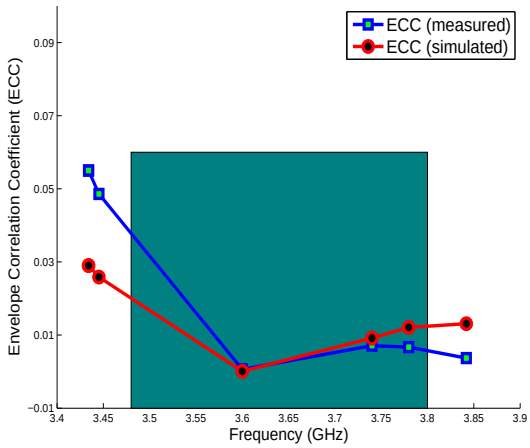

Fig. 4.25. Measured and simulated ECC curves for the proposed MIMO antenna system.

impedance bandwidth irrespective of the phase variation.

To evaluate the diversity performance of the MIMO antenna system, the ECC was calculated from the measured 3D radiation patterns using (4.1). Fig. 4.25 shows the measured and simulated ECC curves for the MIMO antenna system. It can be observed that the maximum measured envelope correlation value is 0.0385 over the entire band 3.48-3.80 GHz while it reaches to 0.00598 at the center frequency of 3.6 GHz which ensures that the radiation patterns are highly uncorrelated in the far field[2]. At lower frequencies, the spatial separation in terms of lambda gets smaller which increases the ECC. The difference between the measured and simulated ECC values is only 0.017, which is very small and shows good agreement. The diversity gain (DG) is computed from ECC using (4.2) as presented in [20]. The average DG of the MIMO antenna system is found to be 9.81 dB within our band of interest which is very close to the maximum value of 10 dB, and hence

[2] The maximum value of ECC set for the 4G standards is 0.5

this MIMO antenna system ensures good diversity performance. Multiplexing Efficiency also depends on the ECC and efficiencies of the antennas inside the MIMO antenna system. The multiplexing efficiency of the MIMO antenna system is found to be around 72.97%, which is calculated from the measured ECC value and measured efficiencies according to the expression presented in [171]. Hence, the MIMO antenna system ensures good MIMO performance in terms of isolation, ECC, TARC, DG, and Multiplexing efficiency.

$$\rho_e = \frac{|\iint_0^{4\pi}[\vec{F}_1(\theta,\phi) \times \vec{F}_2(\theta,\phi)]d\Omega|^2}{\iint_0^{4\pi}|\vec{F}_1(\theta,\phi)|^2 d\Omega \iint_0^{4\pi}|\vec{F}_2(\theta,\phi)|^2 d\Omega} \tag{4.1}$$

$$DG = 10 \times \sqrt{1-\rho_e} \tag{4.2}$$

4.3 A Highly Miniaturized Semi-Loop Meandered Dual Wideband Quasi-Yagi MIMO Antenna System

In this section a novel dual wide-bandwidth (BW) 2-element Quasi-Yagi MIMO antenna system is presented with 68% miniaturization, which is achieved using a semi-loop meandered driven element. The center frequency of operation is 2 GHz. The antenna system covers two bands: the Telemetry L-band with a minimum measured BW (-6 dB) of 160 MHz, from 1.27-1.43 GHz, and the GSM/LTE band with a BW of 333 MHz from 1.8-2.133 GHz. The simulation and

measurement results are in agreement. The proposed antenna system ensures good Yagi performance in terms of FBR, directivity, and gain. It has a high measured FBR of around 15 dB at 1.35 GHz and 17 dB at 2 GHz, which is achieved without using a large ground plane or extra metallic structures, multiple reflector elements or any complex technique for back-radiation minimization. A gain of more than 5 dBi is measured for the single element with a total radiation efficiency of around 85% in both bands. The measured isolation of the proposed MIMO antenna is at least 15 dB with less than 0.0785 measured envelope correlation coefficient (ECC) values in both bands.

Many antenna miniaturization techniques can be found in literature like shorting posts or shorting walls [172], introducing slots [173], using metamaterials [174], material loading [175], and defected ground structures (DGS) [176]. However, most of these techniques are implemented on microstrip patch antennas or their derivations and only two Yagi-miniaturized designs [177]-[178] can be found in literature. The design presented in [177] has a gain of 4 dBi and FBR of greater than 6 dB covering the band from 2.3-2.69 GHz. It has a size of $65 \times 120 \times 130$ mm^3. The design presented in [178] is based on Koch-fractal Yagi geometry at 431 MHz, where 24% miniaturization is achieved. It has a gain of around 5.7 dBi, FBR of 16.7 dB, and bandwidth of 9 MHz. The size of the antenna is around $214 \times 380 \times 203$ mm^3. Both designs suffer from huge sizes, use large reflectors, and cover single narrow bands.

Quasi-Yagi antennas based on loop excitation with a small GND plane give

omnidirectional patterns that are not of interest (FBR $\simeq$ 1 dB). The back-lobe reduction techniques discussed earlier are complex, occupy large size, and are targeted for either microstrip or slot antennas and no such technique can be found for Quasi-Yagi antennas.

Here, we present a highly miniaturized 2-element Yagi MIMO antenna system that is based on loop excitation. A miniaturization[3] factor of 68% is achieved using simple loop meandering and a small GND plane having the width of only 19.1 mm which is almost half of the width of the GND plane used in the first design. To achieve highly directional end-fire radiation pattern with high FBR, a novel simple DGS structure with multiple slits is presented which switches the main beam by 90^0 making it end-fire directional and further suppresses its back-lobe radiation to achieve high FBR of around 17 dB. The proposed antenna system is compact with single element size of $60 \times 50 \times 0.76$ mm^3 and total board size of $120 \times 50 \times 0.76$ mm^3 for the 2-element MIMO configuration.

4.3.1 Antenna Design Details

The antenna is designed using an $FR-4$ substrate with dielectric constant (ϵ_r) of 4, thickness of 0.76 mm, and loss tangent of 0.02. The proposed antenna model is shown in Fig. 4.26. The length of the semi-loop meandered element is twice the guided wavelength ($2\lambda_g$) which is around 140 mm at the center frequency of 2 GHz. The diameter of the loop is 39 mm and its width is tuned to 1 mm. The

[3] The miniaturization ratio is calculated from the difference between the area of the proposed model and the area of first design.

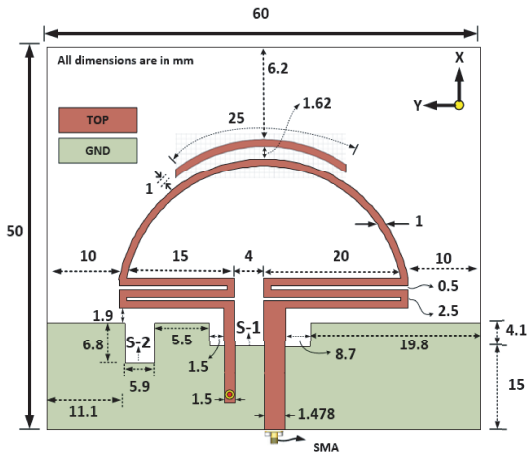

Fig. 4.26. Proposed antenna geometry model.

overall size of the geometry is 60×50 mm^2, while the size of the GND plane is 60×19.1 mm^2. The driven semi-loop element is excited using simple microstrip line feeding below the substrate. The length of the transmission line is tuned to 15 mm while its width is set to 1.478 mm (50Ω) to get minimum reflection loss and match to 50Ω of the SMA connector. The rest of the detailed dimensions are shown in Fig. 4.26. All dimensions are in mm.

Fig. 4.27 shows the proposed MIMO antenna model. The distance between the two MIMO antennas is set to $0.133\lambda_0$ which corresponds to 20 mm at 2 GHz. The rest of the design dimensions are shown in Fig. 4.27.

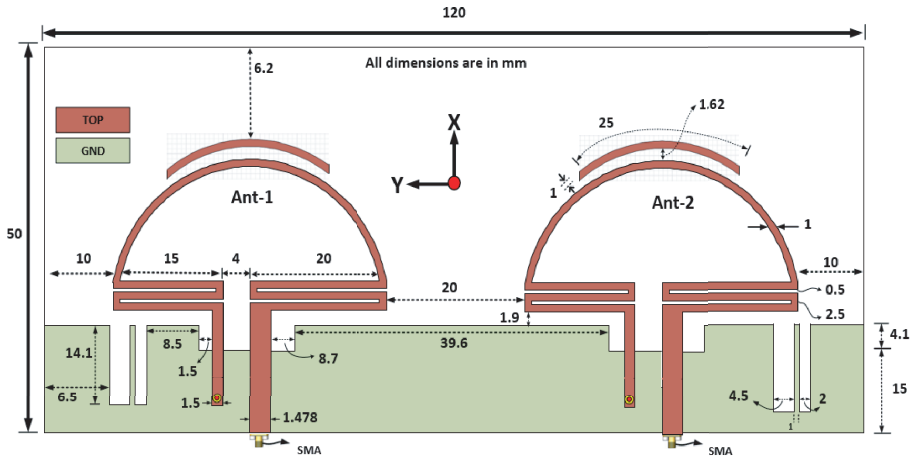

Fig. 4.27. Proposed MIMO antenna geometry.

4.3.2 Results and Discussion

4.3.2.1 Design Principles and Truncated GND Plane or Reflector Analysis

Loop antennas have several resonating modes like $0.5\lambda_g$, $1\lambda_g$, $1.5\lambda_g$, and $2\lambda_g$ [12]. Therefore, the length of the loop element is tuned accordingly to get resonance in the desired bands of operation. In our case, we have observed that the resonating mode for the semi-loop meandered driven element is close to $2\lambda_g$ at 2 GHz which corresponds to a length of 140 mm. The length of the reflector element is 60 mm while the length of the director element is tuned to 25 mm in accordance to [12]. This principle of designing printed Quasi-Yagi antennas is followed by the majority of works present in literature, e.g. [105]. The same principle can be applied to similar antenna geometries targeting other frequencies.

The size of the reflector and its spacing from the driven element has negligible

effect on the forward gain but has significant effect on the FBR [12]. Therefore, to suppress the back-lobe radiation and to achieve high FBR, the truncated GND plane which acts as a reflector for Quasi-Yagi antennas need to be carefully designed. Moreover, the size of the GND plane is also directly related to the overall size of the antenna system.

We start our analysis from the width of the GND plane. Initially, in order to achieve small overall size, we tuned the design with the width of the GND plane set to 7 mm. We then further carried our analysis on the GND plane and also observed its sensitivity on s-parameters as shown in Fig. 4.28. It can be observed that for the GND width of 7 mm, the antenna is multi-band with a minimum measured -6 dB bandwidth of 249 MHz (0.780-1.029 GHz) in the lower band and 286 MHz (1.932-2.218 GHz) in the upper band covering several LTE bands. However, when the width of the GND plane is increased by only 3 mm, the behavior is significantly changed and becomes stable afterwards. For this reason, throughout this work, a GND plane width of 19 mm was selected to allow enough GND plane for stable operation.

4.3.2.2 Defected GND Structure Analysis–Radiation Pattern Switching by 90^0

To avoid using complex back-lobe suppression techniques discussed before [144]-[151], one simple solution is to use a large GND plane as discussed in the first, where the width of the GND plane was tuned to 38 mm. But using large GND planes will eventually increase the overall size of the antenna system. On the

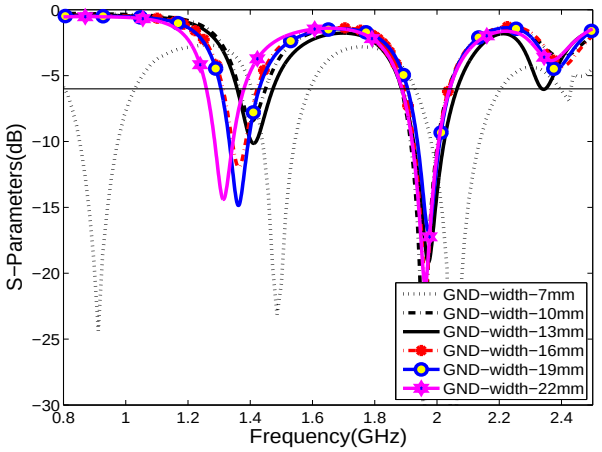

Fig. 4.28. S-parameter curves for different GND plane widths.

other hand, in case of a smaller GND plane without DGS, the current density is maximum in a non-desired direction, i.e. the Y-Z plane which is orthogonal to the desired end-fire direction as shown in Fig. 4.29(a). However, by using the slit (S-1) in the GND plane exactly below the transmission line, the maxima of the current density is shifted to the X-Z plane as shown in Fig. 4.29(b).

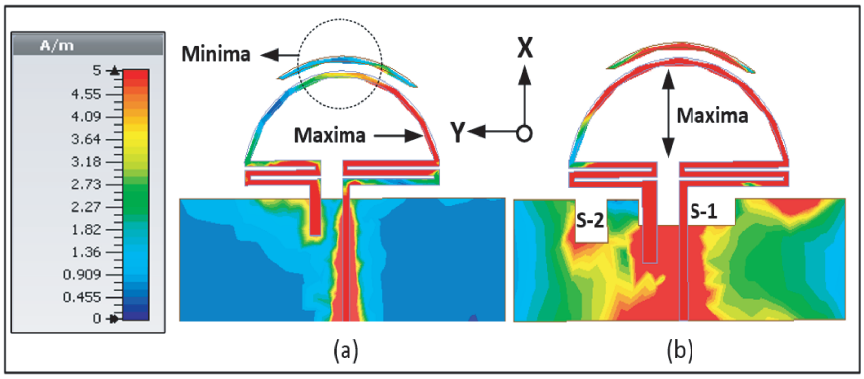

Fig. 4.29. Current distribution at 2 GHz (a) without DGS (b) with DGS.

The above phenomenon is also verified by observing the $2D$ radiation patterns in both azimuth and elevation planes for three different cases: GND plane width of 38 mm without DGS, GND plane width of 19.1 mm without DGS, and GND

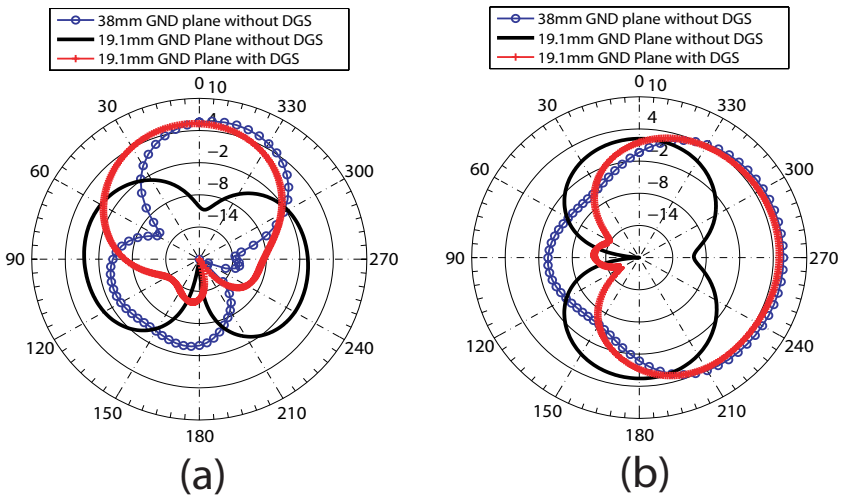

Fig. 4.30. 2D radiation patterns for GND plane width of 38mm without DGS, GND plane width of 19.1mm without DGS, and GND plane width of 19.1mm with DGS (a) *azimuth cut (at* $\theta = 90^0$*)* (b) *elevation cut (at* $\phi = 0^0$*).*

plane width of 19.1 mm with DGS as shown in Fig. 4.30. It can be noticed that for a small GND plane having a width of 19.1 mm without DGS case, the radiation pattern is omnidirectional along *Y-Z* plane as shown in both azimuth and elevation planes. However, the radiation pattern is shifted by 90^0 and the desired directional end-fire radiation pattern is obtained by either using a large GND plane having a width of 38 mm or by using half a GND plane having a width of 19.1 mm with DGS. Also it can be observed that the proposed DGS shows even better performance (8 dB greater FBR) over the large GND plane in terms of FBR.

4.3.2.3 Single Antenna Element Results

The single antenna element shown in Fig. 4.31 was modeled and simulated in CST^{TM} including the SMA connector model. Metal parts were modeled

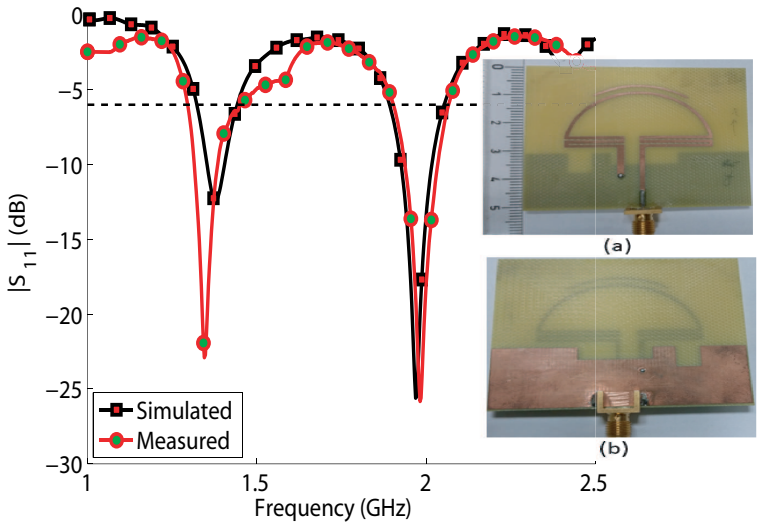

Fig. 4.31. Single element simulated and measured s-parameter curves (inset shows the fabricated prototype of the single element (a) top view (b) bottom view).

with copper material properties to have better match with the actual fabricated prototype (as compared to using PEC). The prototype was fabricated at the Antennas and Microwave Structure Design Laboratory (AMSDL-KFUPM) using a Protomat-S103 (LPKF) milling machine. An Agilent N9918A vector network analyzer (VNA) was used to measure the S-parameters. Fig. 4.31. shows the simulated and measured s-parameter curves, while the inset figure shows the fabricated prototype of the single element. It has a minimum return loss of 23 dB, measured -6 dB bandwidth of 190 MHz (1.29-1.48 GHz) in the lower band, and measured bandwidth of 196 MHz (1.904-2.1 GHz) in the upper band. A good agreement between the simulated and measured results is observed.

The antenna radiation characteristics were measured in a Satimo Star-Lab chamber at KAUST-KSA. Fig. 4.32 shows the single element measured and simulated gain and efficiency curves. The inset shows the measurement setup.

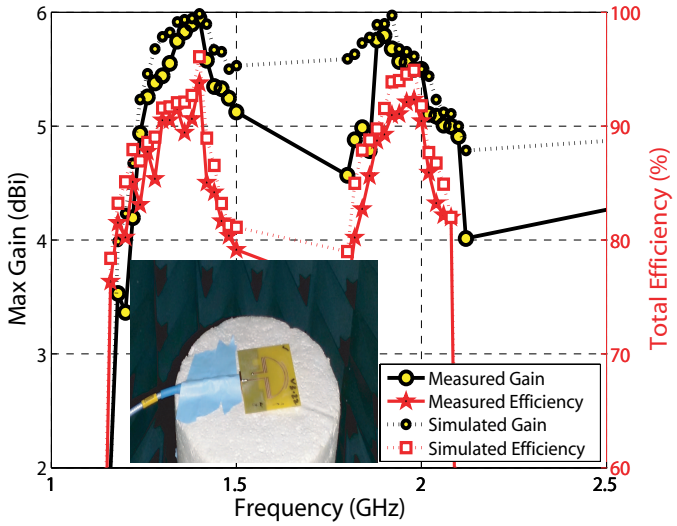

Fig. 4.32. Single element measured and simulated gain and efficiency curves (inset shows the measurement setup inside the chamber)

.

It can be seen that the maximum measured gain is more than 5 dBi in both bands, while the minimum measured total radiation efficiency is around 90%. A good agreement is found between the measured and simulated results with slight differences, which are attributed to the losses (cable and connector) and non-idealities of material properties.

Sensitivity analysis were performed on various design parameters and it was noticed that some of the parameters were very sensitive in determining good Yagi-Uda performance like gain, efficiency, and FBR. Table 4.6 summarizes the effect of the length and spacing of the director element from the driven loop element on the gain of the antenna. It can be seen that by increasing the length of the director until 25 mm, the gain significantly increases while it starts decreasing afterwards. Similarly, the gain of the antenna increases by increasing the spacing until 1.6 mm and starts decreasing afterwards. Therefore, the length of the director element is

Table 4.6. Effect of length and spacing of the director element from the driven element on gain of the antenna

Length (mm)	Gain (dBi)	Spacing (mm)	Gain (dBi)
18	3.4	0.3	2.34
20	4.38	0.6	2.97
22	4.98	0.9	4.2
24	5.23	1.2	4.678
25	5.98	1.5	5.4
27	4.68	1.6	5.97
30	2.91	1.9	3.43

tuned to 25 mm and its spacing is optimized to 1.6 mm.

Table 4.7 summarizes the effect of spacing between the driven loop element and GND plane (reflector), and spacing between the meandered arms of the loop element on the efficiency of the antenna. It can be observed that the efficiency of the antenna is very sensitive to these parameters. The efficiency increases with an increase in the spacing between the driven element and the GND plane until 1.9 mm, after that it starts decreasing. Moreover, the efficiency increases to 94% by increasing the spacing between the arms of the loop element until 0.5 mm and it is significantly decreased when the spacing is further increased.

Slit-2 (S-2) as shown in Fig. 4.26 is mainly responsible for the suppression of the back-lobe radiation after the pattern is shifted by 90^0 by slit-1 (S-1) towards the end-fire direction. Table 4.8 shows the effect of the width and depth of S-2 on the FBR. It can be observed that by increasing the width and depth of S-2 increases the FBR by around 18 dB and hence its values were set to 5.9 mm and

Table 4.7. Effect of the loop-GND spacing and spacing between the loop arms on the efficiency of the antenna

Loop-GND spacing (mm)	Efficiency (%)	Loop-Arms Spacing (mm)	Efficiency (%)
0.4	52	0.2	43
0.8	58.76	0.4	68
1.2	69.9	0.5	94
1.5	87.2	0.6	71.23
1.9	93.8	0.8	82
2	81	1	62.45
2.4	62	1.2	54.67

6.8 mm for the width and depth, respectively.

Fig. 4.33 (a) and (b) show the normalized measured 2D radiation patterns of the proposed single antenna element in both azimuth and elevation planes at 2 GHz. Fig. 4.33(a) shows the 2D pattern in azimuth plane (phi- cut) obtained at $\theta = 90^0$, while Fig. 4.33(b) shows the pattern in elevation plane (theta-cut) obtained at ϕ-max $= 6^0$. It can be seen from both azimuth and elevation planes that the proposed antenna has a minimum measured FBR of 18 dB which ensures very good Yagi performance.

Table 4.8. Effect of the width and depth of slit- 2 (S-2) on FBR

S-2 Width (mm)	FBR (dB)	S-2 depth (mm)	FBR (dB)
1.5	4	2	3.69
3	7.92	3	4.98
4	9	4	6.51
5.5	13.3	6	12.57
5.9	21	6.5	20.61
6.2	16	6.8	21
8	10	7.3	17

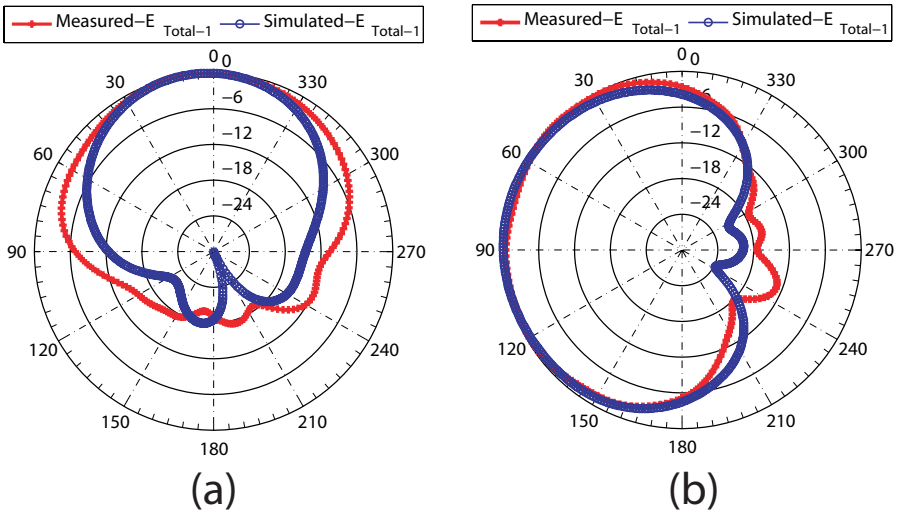

Fig. 4.33. Normalized simulated and measured radiation patterns for the single element, E_{Total} (in dB) at 2 GHz (a) *azimuth cut (at* $\theta = 90^0$*)* (b) *elevation cut (at* $\phi - max = 6^0$*).*

4.3.2.4 MIMO Antenna System Results

The simulated and measured s-parameter curves for the MIMO antenna system are shown in Fig. 4.34. The fabricated prototype of the MIMO antenna system is shown in the figure inset. It is observed that this MIMO antenna system has

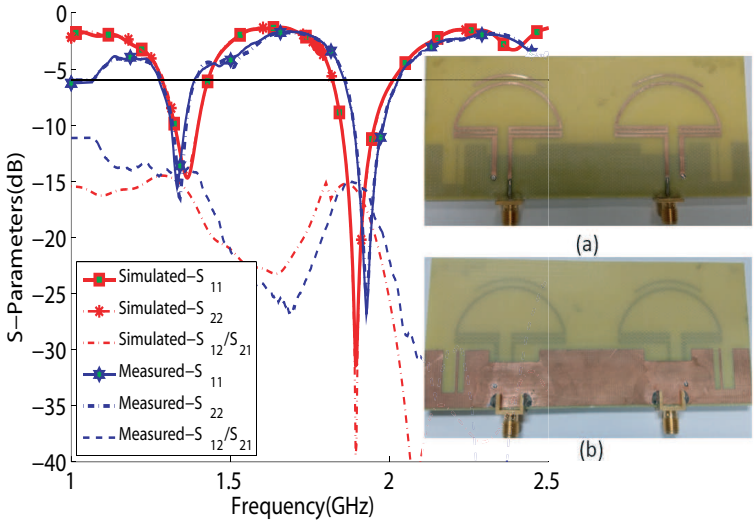

Fig. 4.34. Simulated and measured MIMO S-parameter curves (inset shows the fabricated prototypes of the MIMO antenna system (a) top view (b) bottom view).

a minimum measured -6 dB bandwidth of 160 MHz, from 1.27-1.43 GHz in the lower band, and minimum measured bandwidth of 333 MHz from 1.8-2.133 GHz in the upper band. The measured isolation is atleast 15 dB within both bands even by considering small inter-element spacing of $0.133\lambda_0$ which ensures good port efficiency performance. Good agreement is observed between the simulated and measured results.

Fig. 4.35 shows the simulated and measured maximum gain and total radiation efficiency of the MIMO antenna system. It can be observed that the gain is 4.6 dBi while the measured efficiency is around 78% in both bands. The figure inset shows the MIMO antenna setup inside the chamber. Simulated and measurement results are in good agreement.

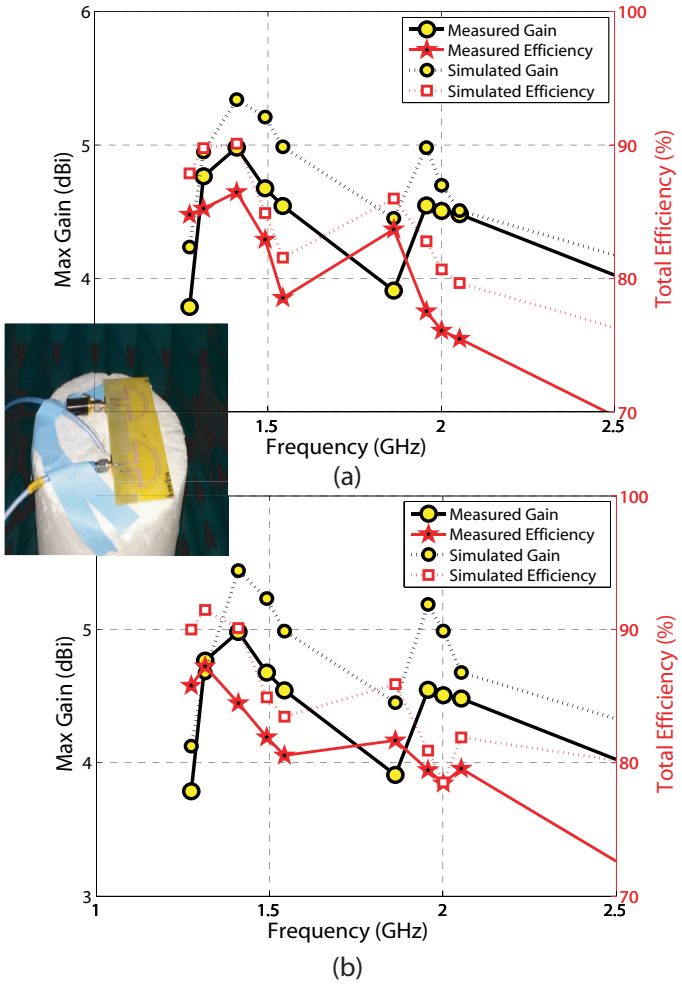

Fig. 4.35. Simulated and measured efficiency and gain curves (a) ant-1 (b) ant-2. (inset shows the antenna setup inside the chamber).

The normalized measured and simulated 2D radiation patterns of the MIMO antenna system in terms of E_{Total} at 1.35 GHz are shown by both ϕ and θ planes of Fig. 4.36. Fig. 4.36 (a) and (b) shows these patterns obtained at $\theta = 90^0$ (azimuth cut) for element 1 and 2, respectively. It can be observed that the field for element 1 and 2 is maximum at $\phi = 42^0$ and $\phi = 330^0$ respectively, and are apart from each other by 72^0. Fig. 4.36(c) and (d) shows the patterns obtained at $\phi_{max} = 42^0$ (elevation cut) and $\phi_{max} = 30^0$ for element 1 and 2, respectively.

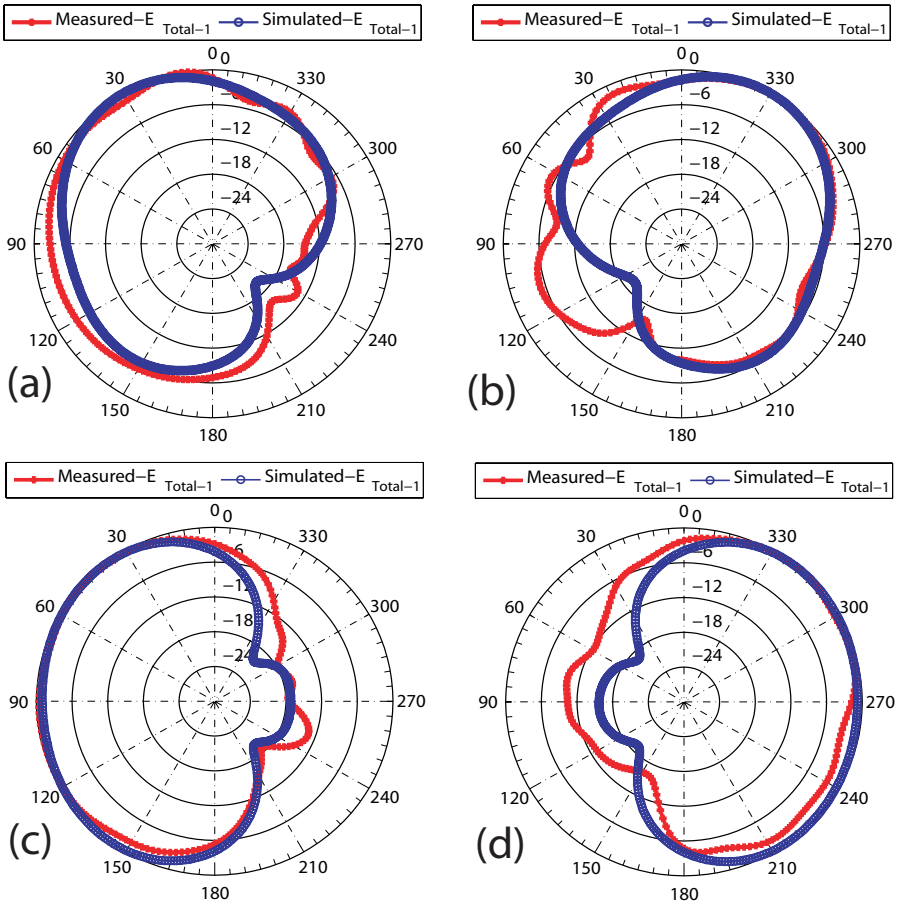

Fig. 4.36. Normalized measured and simulated 2D radiation patterns in terms of E_{Total} (in dB) at 1.35 GHz. (a) azimuth cut at $\theta = 90^0$, element 1 (b) azimuth cut at $\theta = 90^0$, element 2 (c) elevation cut at $\phi_{max} = 42^0$, element 1, (d) elevation cut at $\phi_{max} = 30^0$, element 2.

Similarly, Fig. 4.37 shows the normalized simulated and measured patterns at 2 GHz. Fig. 4.37 (a) and (b) shows the measured and simulated patterns obtained at $\theta = 90^0$ for element 1 and 2, respectively. It can be observed that the field for element 1 and 2 is maximum at $\phi = 43^0$ and $\phi = 328^0$ respectively, and are apart from each other by 75^0. Fig. 4.37(c) and (d) shows these patterns obtained at $\phi_{max} = 43^0$ and $\phi_{max} = 32^0$ for element 1 and 2, respectively. As evident from both figures, the patterns are completely tilted in both ϕ and θ planes which ensures

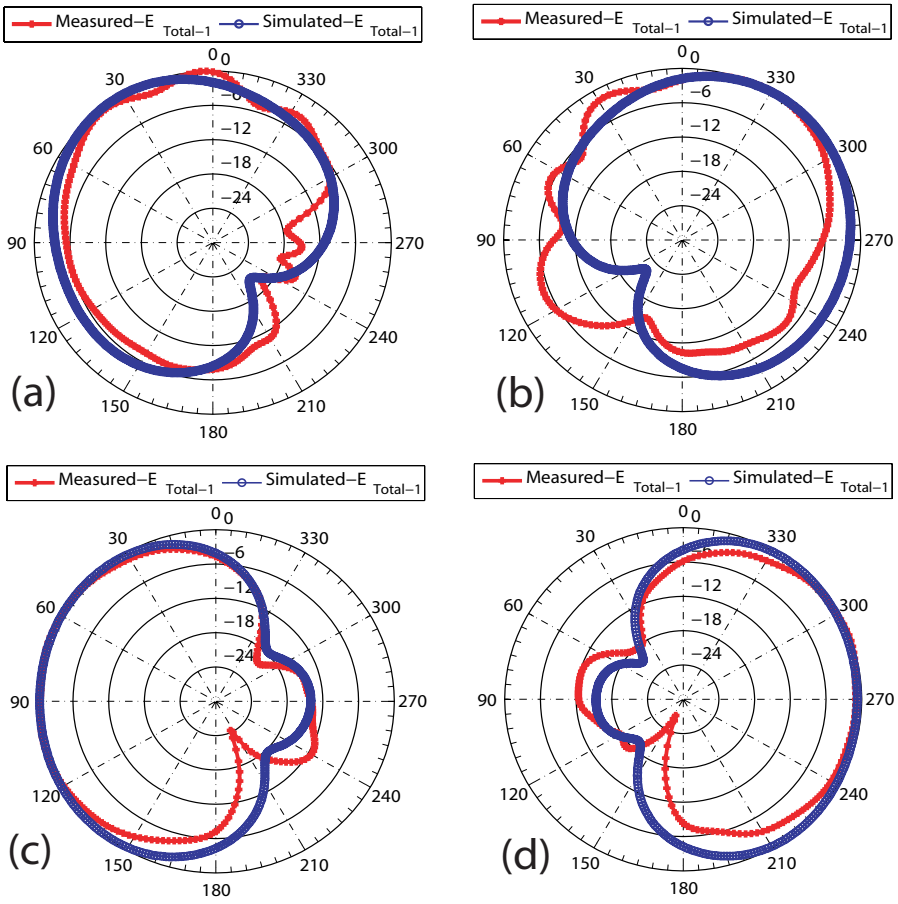

Fig. 4.37. Normalized measured and simulated 2D radiation patterns in terms of E_{Total} (in dB) at 2 GHz. (a) azimuth cut at $\theta = 90^0$, element 1 (b) azimuth cut at $\theta = 90^0$, element 2 (c) elevation cut at $\phi_{max} = 43^0$, element 1, (d) elevation cut at $\phi_{max} = 32^0$, element 2.

that the MIMO channels are highly uncorrelated. In both planes, simulation and measurement results are in close agreement. The obtained FBR in both planes (Fig. 4.36 and Fig. 4.37) is above 15 dB.

Table. 4.9 summarizes the comparison of different parameter results of both the single element and the MIMO antenna system of this work to other works in literature. It can be seen that the proposed single element as well as MIMO antenna systems use a loop as a driven element and is compact in size by covering

Table 4.9. Comparison of different antenna parameters to other Quasi-Yagi designs

Parameters	Single Element						MIMO				
	[177]	[178]	[39]	[60]	Design-1	Design-3	[Design-2]	[142]	[143]	Design-1	Design-3
Driven Element	Monopole	Dipole	Dipole	Dipole	Loop	Loop	Magnetic-Dipole	Dipole	Dipole	Loop	Loop
Freq (GHz)	2.4	0.431	2.5	2.4	2	1.4, 2	3.6	5.2	5.2	2	1.4, 2
Dielectric Constant (ϵ_r)	—	—	4	4.4	4	4	4	10	4	4	4
Size (mm^2)/(mm^3)	$65 \times 120 \times 130$	$214 \times 380 \times 203$	64×100	89×66	118×78	60×50	80×40	55×50	154×154	263×263	120×50
FBR (dB)	6-meas	16.7-sim	20-sim	13-sim	9.5-meas	18-meas	10-meas	——	——	13.8-meas	17-meas
Gain (dBi)	4-sim	5.7-sim	4-sim	——	5.98-meas	5-meas	4.3-meas	6-sim	5-sim	5.8-meas	5-meas
Efficiency (η%)	——	86-sim	—	—	65-meas	85-meas	73-meas	—	—	65-meas	78-meas

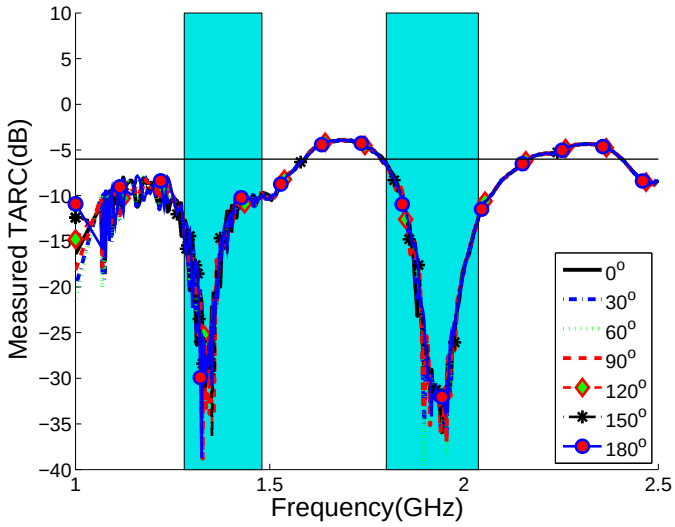

Fig. 4.38. TARC curves for MIMO antenna system.

dual low frequency bands with higher efficiency values. The proposed design also ensures good Yagi performance in terms of FBR and gain as compared to other works.

Using the measured S-parameters, TARC curves [1] are calculated as shown in Fig. 4.38. A stable response is observed irrespective of the phase variation between the two ports.

For diversity performance evaluation, the 3D radiation patterns are used to find the ECC values using (4.1). Simulated and measured ECC curves (evaluated

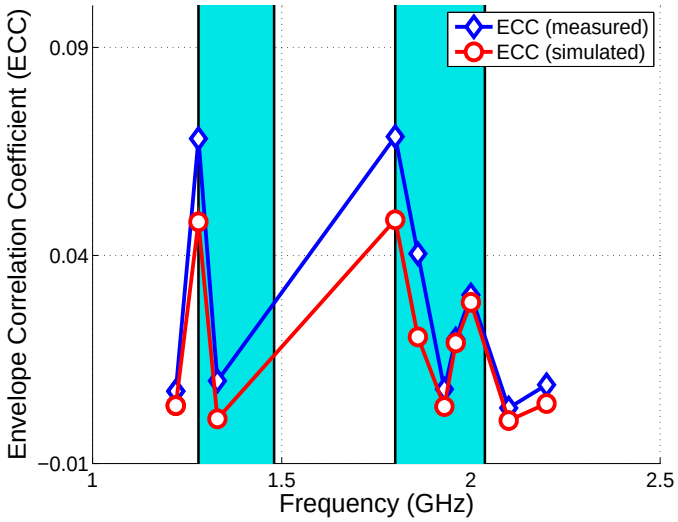

Fig. 4.39. Measured and simulated ECC curves for the proposed MIMO antenna system

at specific frequency points within the band) are shown in Fig. 4.39. It is observed that the measured ECC reaches to the maximum value of 0.0785 (in both bands), which indicates that the radiation patterns are not correlated (the tilts are obvious from Fig. 4.36 and 4.37). The average diversity gain (DG) computed from ECC values according to [20] is 9.6 dB which is very close to the maximum value of 10 dB. Thus good diversity performance can be obtained from this design. The multiplexing efficiency calculated from the measured ECC and total efficiencies of the individual antennas according to [171] is 75%. Hence, the proposed MIMO antenna system ensures good MIMO performance in terms of isolation, correlation, TARC, DG, and Multiplexing efficiency.

Table 4.10. Performance Comparison of the single element of design-3 with the dipole excited Quasi-Yagi antenna at 2 GHz

Parameters	Loop excited	Dipole Excited
Frequency (GHz)	2	2
Size (mm^2)	60×50	35×60
Bandwidth (MHz)	196	94
FBR (dB)	18	12
Gain (dBi)	5.6	4.2
Efficiency %	92	79

4.3.2.5 Performance Comparison of the single element of design-3 with traditional dipole based Quasi-Yagi antenna of [30]

For the purpose of comparison with the miniaturized loop excited antenna (i.e. design-3), the dipole excited Quasi-Yagi antenna presented in [30] was tuned to resonate at 2 GHz. Table 4.10 summarizes the performance comparison between the two antennas in terms of different parameters. It can be seen that the loop excited design has far better performance in terms of gain, bandwidth, FBR, and efficiency but at the cost of 43% greater size.

4.4 Conclusions

In this chapter, firstly, a dual wideband 4-element circular Quasi-Yagi MIMO antenna system with loop excitation is presented for potential use in wireless access points or vehicular applications. This antenna system shows very good percentage

bandwidth[4] of 55% and 24% at 2 and 4 GHz center frequency bands respectively. The radiation pattern of the antenna system is highly directional with FBR of 13.8 dB and directivity of 7 dB. The minimum measured gain is 5.8 dBi and minimum measured efficiency is 65%. The proposed antenna system shows good MIMO performance in terms of isolation and correlation. A minimum measured isolation of 18 dB is obtained. The concept of pattern orthogonality is used to get low correlation between the MIMO channels. A maximum measured envelope correlation value of 0.1589 is obtained in both bands.

We then discussed the second design based on a half wavelength semi-ring slot 2-element Yagi-like MIMO antenna system. The proposed single layer MIMO antenna system is compact having an overall size of $80 \times 40 \times 0.8\ mm^3$ and can be employed in number of wireless portable devices operating in WiMAX band. A minimum measured FBR of 10 dB is achieved by introducing a very simple and compact complementary slot reflector element having a size of $14 \times 9.5\ mm^2$ without using any complex back-lobe reduction technique, multiple reflectors or any additional reflector layers as found in literature. This antenna system shows the minimum measured total radiation efficiency greater than 73% over the entire band of operation. The proposed MIMO antenna system has minimum measured isolation of 12 dB across the band of operation and has a minimum measured realized gain of 4.3 dBi without using any additional metallic director layers. The measured envelope correlation coefficient (ECC) did not exceed 0.0385, hence it

[4] Antennas having percent bandwidth of greater than 20% are considered as wideband, while if the bandwidth is greater than 30%, such antennas are considered as ultra-wideband (UWB) [1].

ensures good MIMO performance.

A highly miniaturized dual wideband Quasi-Yagi based MIMO antenna system is then presented. A miniaturization of 68% is achieved by using semi-loop meandering and small GND plane structure. Both single element and MIMO antennas are compact in size as compared to other single or MIMO Quasi-Yagi designs. The proposed antenna system has a very high measured FBR of 17 dB at 2 GHz with a small GND plane width of 19.1 mm. The omnidirectional pattern is shifted by 90^0 towards the desired end-fire direction and the back-lobe radiation is reduced by using a very simple DGS, unlike complex back-lobe reduction techniques present in the literature. The proposed design has a maximum measured gain of more than 5 dBi and 4.6 dBi for the single element and MIMO antenna system, respectively. It has a measured total radiation efficiency of around 85% and 78% for both single and MIMO antennas. The proposed antenna system also ensures good MIMO performance in terms of isolation, ECC, TARC, DG, and multiplexing efficiency. Towards the end of the chapter, a comparison of performance between the miniaturized loop excited antenna and the dipole based Quasi-Yagi antenna of [30] was presented. It was shown that the loop based design has better performance except for the overall size.

CHAPTER 5

CONCLUSIONS AND FUTURE WORK

5.1 Conclusions

In this work, we present three Yagi based MIMO antenna designs with loop based excitation. The first design showed a percentage bandwidth of 55% and 24% at 2 and 4 GHz center frequency bands, respectively. The radiation pattern of the antenna system was highly directional with FBR of 13.8 dB and directivity of 7 dB. The minimum measured gain was 5.8 dBi and minimum measured efficiency was 65%. The proposed antenna system showed good MIMO performance in terms of isolation and correlation. A minimum measured isolation of 18 dB was obtained. The concept of pattern orthogonality was used to get low correlation between the MIMO channels. A maximum measured envelope correlation value of 0.1589 was obtained in both bands.

In the second design, we have introduced a compact single layer MIMO antenna system having an overall size of $80 \times 40 \times 0.8\ mm^3$ targeting WiMAX applications. A minimum measured FBR of 10 dB was achieved by introducing a very simple and compact complementary slot reflector element having a size of $14 \times 9.5\ mm^2$ without using any complex back-lobe reduction technique, multiple reflectors or any additional reflector layers as found in literature. The minimum measured isolation of the the proposed MIMO antenna system was 12 dB across the band of operation with a minimum measured realized gain of 4.3 dBi which was achieved without using any additional metallic director layers.

Lastly, we presented a highly miniaturized dual wideband Quasi-Yagi based MIMO antenna system where a miniaturization of 68% was achieved using semi-loop meandering and small GND plane structure. The minimum measured FBR was 17 dB at 2 GHz using a small GND plane having width of 19.1 mm. A directional radiation pattern with a high FBR was obtained by introducing a novel DGS unlike complex back-lobe reduction techniques presented in the literature. The total radiation efficiencies of the single and MIMO antenna system were 85% and 78%, respectively. All the three designs ensured good Yagi-Uda as well as MIMO performance. A very good agreement between the simulated and measured results was observed in all the results.

5.2 Future Work

- The work can be extended towards the design of a directional wideband Quasi-Yagi MIMO antenna systems based on frequency as well pattern reconfigurability, targeting the WLAN bands for mobile communication.

REFERENCES

[1] M. S. Sharawi, *Printed MIMO antenna engineering*, Artech House, Norwood, MA, 2014.

[2] D. Raychaudhuri and N. B. Mandayam, "Frontiers of wireless and mobile communications," *IEEE Proceedings*, vol. 100, no. 4, pp. 824-840, 2012.

[3] A. J. Paulraj, D. A. Gore, R. U. Nabar, and H. Bolcskei, "An overview of mimo communications-a key to gigabit wireless," *IEEE Proceedings*, vol. 92, no. 2, pp. 198-218, 2004.

[4] Q. Li, G. Li, W. Lee, M.-i. Lee, D. Mazzarese, B. Clerckx, and Z. Li, "Mimo techniques in wimax and lte: a feature overview," *IEEE Communications Magazine*, vol. 48, no. 5, pp. 86-92, 2010.

[5] V. Garg, *Wireless Communications and Networking*, San Francisco: Morgan Kaufmann, 2007.

[6] Y. S. Cho, Ed., *MIMO-OFDM wireless communications with MATLAB*, Reprinted. Singapore [u.a]: Wiley, 2011.

[7] Sagar Kumar Dhar, "*Active integrated MIMO antenna design*," MS Thesis, Electrical Engineering Department, KFUPM, 2015.

[8] K. S. Yngvesson, T. L. Korzeniowski, et al, "The tapered slot antenna-a new integrated element for millimeter-wave applications," *IEEE Transactions on Microwave Theory and Techniques*, vol. 37, no. 2, pp. 365-374, 1989.

[9] P. F. Goldsmith, C. T. Hsieh, et al, "Focal plane imaging systems for millimeter wavelengths," *IEEE Transactions on Microwave Theory and Techniques*, vol. 41, no. 10, pp. 1664-1675, 1993.

[10] Y. Qian, W.R. Deal, N. Kaneda, and T. Itoh, "Microstrip-fed quasi-yagi antenna with broadband characteristics," *Electronics Letters*, vol. 34, no. 23, pp. 2194-2196, Nov 1998.

[11] "Simulation of Mobile Phone Antenna Performance." [Online]. Available: https://www.cst.com/Applications/.

[12] C. A. Balanis, *Antenna theory: analysis and design*, John Wiley and Sons, 2012.

[13] S. H. Chae, S.k. Oh, and S.O. Park, "Analysis of mutual coupling, correlations, and tarc in wibro mimo array antenna," *IEEE Antennas and Wireless Propagation Letters*, vol. 6, pp. 122-125, 2007.

[14] M. Manteghi and Y. Rahmat-Samii, "Multiport characteristics of a wideband cavity backed annular patch antenna for multipolarization operations," *IEEE Transactions on Antennas and Propagation*, vol. 53, no. 1, pp. 466- 474, 2005.

[15] S. W. Su, C. T. Lee, and F. S. Chang, "Printed mimo-antenna system using neutralization-line technique for wireless usb-dongle applications," *IEEE Transactions on Antennas and Propagation*, vol. 60, no. 2, pp. 456-463,2012.

[16] M. S. Sharawi, "Printed multi-band mimo antenna systems and their performance metrics," *IEEE Antennas and Propagation Magazine*, no. 55, p. 218, 2013.

[17] T. Taga, "Analysis for mean effective gain of mobile antennas in land mobile radio environments," *IEEE Transactions on Vehicular Technology*, vol. 39, no. 2, pp. 117-131, 1990.

[18] A. Ando, T. Taga, A. Kondo, K. Kagoshima, and S. Kubota, "Mean Effective Gain of Mobile Antennas in Line-of-Sight Street Microcells With Low Base Station Antennas," *IEEE Transactions on Antennas and Propagation*, vol. 56, no. 11, pp. 3552-3565, Nov. 2008.

[19] A. A. Glazunov, A. F. Molisch, and F. Tufvesson, "Mean effective gain of antennas in a wireless channel," *IET Microwaves, Antennas and Propagation*, vol. 3, no. 2, pp. 214-227, March 2009.

[20] K. Rosengren and P.-S. Kildal, "Radiation efficiency, correlation, diversity gain, and capacity of a six-monopole antenna array for a mimo system: theory, simulation and measurement in reverberation chamber," *IET Microwaves, Antennas and Propagation* , vol. 152, no. 1, pp. 716, 2005

[21] S. Uda, "Wireless Beam of Short Electric Waves," *Journal of Institute of electrical engineers of Japan*, pp. 273-282, 1926.

[22] H. Yagi, "Beam Transmission of Ultra Short Waves," *IRE Proceedings*, vol. 16, pp. 715-740, 1928.

[23] H. Yagi, "Beam Transmission of Ultra Short Waves," *IEEE Proceedings*, Vol. 72, No. 5, pp. 634-645, May 1984.

[24] H. J. Song, M. E. Bialkowski, and P. Kabacik, "Parameter study of a broadband uniplanar quasi-Yagi antenna," *13th IEEE International Conference on Microwaves, Radar, and Wireless Communications-MIKON*, vol. 1, 2000.

[25] E. A. Navarro, A. S. Martnez , et al. "A lowcost compact uniplanar Quasi-Yagi printed antenna," *Microwave and Optical Technology Letters*, vol. 50, no. 3, pp. 731-735, 2008.

[26] X. Zhang, S. Lin, et al. "Research on broadband and high-gain Quasi-Yagi antenna and array," *IEEE International Conference on Control, Automation and Systems Engineering (CASE), Singapore*, pp. 1-4, 2011.

[27] E. A. Navarro, J. M. Blanes, et al, "Yagi-like printed antennas for wireless sensor networks," *IEEE International Conference on Sensor Technologies and Applications (SENSORCOMM), Valencia*, pp. 254-259, 2007.

[28] J. M. Floc'h, J. M. Denoual, and K. Sallem, "Design of printed dipole with reflector and multi directors," *IEEE conference on Antennas and Propagation, Loughborough*, pp. 421-424, 2009.

[29] W. Nannan, Q. Jinghui, et al. "Research on wide beamwidth and high gain Quasi-Yagi antenna," *IEEE 8th International Symposium on Antennas, Propagation and EM Theory, Kunming*, pp. 302-305, 2008.

[30] Y. Qian, W. R. Deal, N. Kaneda, and T. Itoh, "A uniplanar quasi-yagi antenna with wide bandwidth and low mutual coupling characteristics," *Antennas and Propagation Society International Symposium*, vol. 2, pp. 924-927, July 1999.

[31] D. Schaubert, E. Kollberg, et al, "Endfire tapered slot antennas on dielectric substrates," *IEEE Transactions on Antennas and Propagation*, vol. 33, no. 12, pp. 1392-1400, Dec 1985.

[32] P. F. Goldsmith, C. T. Hsieh, et al. "Focal plane imaging systems for millimeter wavelengths," *IEEE Transactions on Microwave Theory and Techniques*, vol. 41, no. 10, pp. 1664-1675, 1993.

[33] Y. Qian, W.R. Deal, N. Kaneda, and T. Itoh, "Microstrip-fed quasi-yagi antenna with broadband characteristics," *Electronics Letters*, vol. 34, no. 23, pp. 2194-2196, Nov 1998.

[34] O. Kramer, T. Djerafi, and K. Wu, "Vertically Multilayer-Stacked Yagi Antenna With Single and Dual Polarizations," *IEEE Transactions on Antennas and Propagation*, vol. 58, no. 4, pp. 1022-1030, April 2010.

[35] N. Kaneda, Y. Qian, and T. Itoh, "A broadband microstrip-to-waveguide transition using quasi-yagi antenna," *IEEE Transactions on Microwave Theory and Techniques*, vol. 4, pp. 1431-1434, June 1999.

[36] Y. Qian and T. Itoh, "A broadband uniplanar microstrip-to-cps transition," *Proceedings of the Asia-Pacific Microwave Conference*, vol. 2, pp. 609-612, Dec 1997.

[37] H. Cheunsoo, Y. Qian, and T. Itoh, "A modified quasi-Yagi planar antenna with wideband characteristics in C-band," *IEEE International Symposium on Antennas and Propagation Society, Boston, MA, USA*, vol. 3, pp. 154-157, 2001.

[38] G. Zheng, A. A. Kishk, et al, "Simplified feeding for a modified printed Yagi antenna," *IEEE International Symposium on Antennas and Propagation, Columbus, OH, USA*, vol. 3, pp. 934-937, 2003.

[39] E. A. Navarro, J. A. Carrasco, and C. Reig, "Design of Yagilike printed antennas for WLAN applications," *Microwave and optical technology letters*, vol. 49, no. 9, pp. 2174-2178, 2007.

[40] Y. Ding, Y. C. Jiao, P. Fei, et al. "Design of a multiband quasi-Yagi-type antenna with CPW-to-CPS transition," *IEEE Antennas and Wireless Propagation Letters*, vol. 10, pp. 1120-1123, 2011.

[41] C. D. Chang, B. C. Chang, et al, "Modified planar quasi-Yagi antenna for WLAN dualband operations," *Microwave and optical technology letters*, vol. 46, no. 5, pp. 443-446, 2005.

[42] S. J. Wu, C. H. Kang, K. H. Chen, and J. H. Tarng, "A multiband quasi-Yagi type antenna," *IEEE Transactions on Antennas and Propagation*, vol. 58, no. 2, pp. 593-596, 2010.

[43] H. C. Huang, H. Chu, J. Lu, and P. Hsu, "A Compact Dual-Band Printed Yagi-Uda Antenna for GNSS and CMMB Applications," *IEEE Transactions on Antennas and Propagation*, vol. 63, no. 5, pp. 2342-2348, 2015.

[44] D. M. Elsheakh, M. F. Iskander, "Circularly Polarized Triband Printed Quasi-Yagi Antenna for Millimeter-Wave Applications," *International Journal of Antennas and Propagation*, 2015.

[45] H. K. Kan, R. B. Waterhouse, et al, "A simple broadband planar Quasi-Yagi antenna," *10th IEEE Region Conference, TENCON, Hong Kong*, pp. 1-3, 2006.

[46] K. M. K. H. Leong, Yongxi Qian, and T. Itoh, "First demonstration of a conductor backed coplanar waveguide fed quasi-Yagi antenna," *IEEE International Symposium on Antennas and Propagation, Salt Lake City, UT, USA*, vol. 3, pp. 1432-1435, 2000.

[47] N. Kaneda, Y. Qian, and T.Itoh, "A broadband CPW-to-waveguide transition using quasi-Yagi antenna," *IEEE MTT S international microwave symposium digest*, vol. 2. pp. 617-620. 2000.

[48] Z. Zhang, K. Wu, and N. Yang, "Broadband millimeter-wave Quasi-Yagi antenna using substrate integrated waveguide technique," *IEEE Radio and Wireless Symposium*, pp. 671-674, 2008.

[49] N. Kaneda, Y. Qian, and T.Itoh, "A broad-band microstrip-to-waveguide transition using quasi-Yagi antenna," *IEEE Transactions on Microwave Theory and Techniques*, vol. 47, no. 12, pp. 2562-2567, 1999.

[50] K. Kim, J. Byun, and H. Y. Lee, "Substrate integrate waveguide quasi Yagi antenna using SIW-to-CPS transition for low mutual coupling," *IEEE International Symposium on Antennas and Propagation, Toronto, ON*, pp. 1-4, 2010.

[51] D. Woo, Y. Kim, et al, "A simplified design of quasi-Yagi antennas using the new microstrip-to-CPS transitions," *IEEE International Symposium on Antennas and Propagation, Honolulu, HI*, pp. 781-784, 2007.

[52] R. Hua, C. Wang, and T. Ma, "A planar quasi-Yagi antenna with a new microstrip-to-CPS balun by artificial transmission lines," *IEEE International Symposium on Antennas and Propagation, Honolulu, HI*, pp. 2305-2308,2007.

[53] T. G. Ma, C. W. Wang, et al, "A modified quasi-Yagi antenna with a new compact microstrip-to-coplanar strip transition using artificial transmission

lines," *IEEE Transactions on Antennas and Propagation*, vol. 57, no. 8, pp. 2469-2474, 2009.

[54] A. Abbosh, "Ultra-wideband quasi-Yagi antenna using dual-resonant driver and integrated balun of stepped impedance coupled structure," *IEEE Transactions on Antennas and Propagation*, vol. 61, no. 7, pp. 3885-3888, 2013.

[55] T. Wen-Hua, "Microstrip-coplanar stripline-fed Yagi-Uda antenna," *IEEE International Symposium on Antennas and Propagation, San Diego, CA*, pp. 1-4, 2008.

[56] T. Wen-Hua and K. Chang, "Wide-band microstrip-to-coplanar stripline/slotline transitions," *IEEE Transactions on Microwave Theory and Techniques*, vol. 54, no. 3, pp. 1084-1089, 2006.

[57] S. X. Ta, B. Kim, et al, "Wideband quasiyagi antenna fed by microstriptoslotline transition," *Microwave and Optical Technology Letters*, vol. 54, no. 1, pp. 150-153, 2012.

[58] S. X. Ta, B. Kim, et al, "Slot-line-fed quasi-Yagi antenna," *9th International Symposium on Antennas, Propagation and EM Theory (ISAPE)*, pp. 307-310, 2010.

[59] S. Trinh-Van, K. C. Hwang, Y. Yang, and K.-Y. Lee, "A printed quasi-Yagi antenna with a coupled slotline feed," *Journal of Electromagnetic Waves and Applications*, vol. 29, no. 3, pp. 402-409, 2015.

[60] C. Costa, G. Fontgalland, A. G. D'Assuncao, et al, "A new quasi-Yagi bowtie type integrated antenna," *IEEE International Telecommunications Symposium*, pp. 468-471, 2006.

[61] A. A. Eldek, A. Z. Elsherbeni, and C. E. Smith, "Wideband microstripfed printed bowtie antenna for phasedarray systems," *Microwave and optical technology letters*, vol. 43, no. 2 pp. 123-126, 2004.

[62] K. Jiang, Q. G. Guo, and K. M. Huang, "Design of a wideband quasi-Yagi microstrip antenna with bowtie active elements," *IEEE International Conference on Microwave and Millimeter Wave Technology (ICMMT)*, pp. 1122-1124, 2010.

[63] L. Mei, N. Zhang, and Y. Ma, "Design of a C-band 2 2 Quasi-Yagi antenna array," *General Assembly and Scientific Symposium (URSI GASS)*, pp.1-4, 2014.

[64] G. S. Shiroma and W. A. Shiroma, "A two-element L-band Quasi-Yagi antenna array with omnidirectional coverage," *IEEE Transactions on Antennas and Propagation*, vol. 55, no. 12, pp. 3713-3716, 2007.

[65] J. Sor, W. R. Deal, Y. Qian, and T. Itoh, "A broadband quasi-Yagi antenna array," *29th European Microwave Conference, Munich, Germany*, vol. 3, pp. 255-258, 1999.

[66] S. Jeon, Y. Wang, Y. Qian, and T. Itoh, "A novel planar array smart antenna system with hybrid analog-digital beamforming," *IEEE MTT-S International Microwave Symposium Digest, Phoenix, AZ, USA*, vol. 1, pp. 121-124, 2001.

[67] A. L. Amadjikpe, D. Choudhury, G. E. Ponchak, and J. Papapolymerou, "High gain quasi-Yagi planar antenna evaluation in platform material environment for 60 GHz wireless applications," *IEEE MTT-S International Microwave Symposium Digest, Boston, MA*, pp. 385-388, 2009.

[68] J. Wang, L. Sang, Z. Wang, et al, "A broadband quasiYagi array of rectangular loops on LTCC," *International Journal of RF and Microwave ComputerAided Engineering*, vol. 24, no. 2, pp. 196-203, 2014.

[69] X. C. Zhang, J. Liang, and J. W. Xie, "The quasi-Yagi antenna subarray fed by an orthogonal T junction," *Progress In Electromagnetics Research Letters*, vol. 4, pp. 109-112, 2008.

[70] T. Nishio, Y. Wang, Y. Qian, and T. Itoh, "High performance K-and Q-band quasi-Yagi linear arrays," *Internation Symposium on Antennas and Propagation,* , vol. 4, pp. 562-565, 2002.

[71] F. Weinmann, "Design, optimization, and validation of a planar nine-element Quasi-Yagi antenna array for X-band applications [Antenna designer's Notebook]," *IEEE Antennas and Propagation Magazine*, vol. 49, no. 2, pp. 89-96, 2007.

[72] W. Zhang, Q. Wang, X. He, Y. He, et al, "A broadband 16-element 2-D phased array based on quasi-Yagi antennas," *11th IEEE European Radar Conference (EuRAD), Rome*, pp. 325-328, 2014.

[73] T. Kouzaki, K. Kimoto, et al, "Quasi Yagi-Uda antenna array for detecting targets in a dielectric substrate," *IEEE International Conference on Ultra-Wideband, Vancouver, BC*, pp. 759-762, 2009.

[74] F. Weinmann, "Planar 9-element quasi-Yagi antenna array for X-band application," *IEEE European Conference on Wireless Technology*, pp. 539-542, 2005.

[75] D. Wu, Y. Fan, M. Zhao, and Y.-H. Zhang, "Millimeter wave omnidirectional quasi-Yagi array," *Progress In Electromagnetics Research Letters*, vol. 5, pp. 123-130, 2008.

[76] R. Bayderkhani and H. R. Hassani, "Wideband and low sidelobe linear series fed Yagi-like antenna array," *Progress In Electromagnetics Research*, vol. 17, pp. 153-167, 2009.

[77] N. Kaneda, Y.Qian, and T. Itoh, "A novel Yagi-Uda dipole array fed by a microstrip-to-CPS transition," *Proc. of Asia Pacific Microwave Conf. Japan*, pp. 1413-1416, 1998.

[78] W. R. Deal, N. Kaneda, J. Sor, Y. Qian, and T. Itoh, "A new quasi-Yagi antenna for planar active antenna arrays," *IEEE transactions on Microwave Theory and Techniques*, vol. 48, no. 6, pp. 910-918, 2000.

[79] N. bt. Ismail, M. T. Ali, et al, "Design and analysis of microstrip Yagi antenna for Wi-Fi application," *IEEE Asia-Pacific Conference on Applied Electromagnetics (APACE), Melaka*, pp. 283-286, 2012.

[80] L. C. Kretly, C. E. Capovilla, and S. E. Barbin, "A novel antenna array based on quasi-Yagi element for adaptive wireless system applications," *Proceedings of the SBMO/IEEE MTT-S International Microwave and Optoelectronics Conference, IMOC*, vol. 1, pp. 307-311 2003.

[81] M. S. Sharawi, A. B. Numan, and D. N. Aloi, "Design of an 8-element switched mode circular antenna array for vehicular direction finding," *12th Annual Conference on Wireless and Microwave Technology (WAMICON), Clearwater Beach, FL*, pp. 1-4, 2011.

[82] O. E. Vydalko and F. F. Dubrovka, "Matching and radiation characteristics of a phased array based on quasi-Yagi planar antennas with an additional screen," *Radioelectronics and Communications Systems*, vol. 58, no. 4 pp. 157-165, 2015.

[83] L. C. Kretly and C. E. Capovilla, "Patches driver on the quasi-Yagi antenna: analyses of bandwidth and radiation pattern," *Proceedings of the SBMO/IEEE MTT-S International Microwave and Optoelectronics Conference, IMOC*, vol. 1, pp. 313-316, 2003.

[84] L. C. Kretly and A. S. Ribeiro, "A novel tilted dipole quasi-Yagi antenna designed for 3G and Bluetooth applications," *Proceedings of the SBMO/IEEE*

MTT-S International Microwave and Optoelectronics Conference, IMOC, vol. 1, pp. 303-306, 2003.

[85] W. Anantapreecha, N. Duangkha, S. Pattichart, and D. Eungdamrong, "Novel e-shaped driver based on the quasi-yagi antenna," *9th International Conference on Advanced Communication Technology, Gangwon-Do*, vol. 2, pp. 894-896, 2007.

[86] K. M. K. H. Leong, Y. Qian, and T. Itoh, "Surface wave enhanced broadband planar antenna for wireless applications," *IEEE Microwave and Wireless Components Letters*, vol. 11, no. 2, pp. 62-64, 2001.

[87] J.-I. Lee and J. Yeo, "Modified broadband quasiYagi antenna with enhanced gain and bandwidth," *Microwave and Optical Technology Letters*, vol. 55, no, 2, pp. 406-409, 2013.

[88] S. E. Melais and T. M. Weller, "A Quasi Yagi antenna backed by a metal reflector," *IEEE Transactions on Antennas and Propagation*, vol. 56, no. 12, pp. 3868-3872 , 2008.

[89] Y. Qian, W. R. Deal, J. Sor, and T. Itoh, "A novel printed antenna with broadband circular polarization," *IEEE Asia Pacific Microwave Conference*, vol. 1, pp. 142-145, 1999.

[90] J. Wu, Z. Zhao, Z. Nie, and Q. H. Liu, "Bandwidth enhancement of a planar printed quasi-Yagi antenna with size reduction," *IEEE Transactions on Antennas and Propagation*, vol. 62, no. 1, pp. 463-467, 2014.

[91] M. Sironen, Y. Qian, and T. Itoh, "A 60 GHz conical horn antenna with polarizer fed by quasi-Yagi antenna," *International Symposium on Antennas and Propagation, Boston, MA, USA*, vol. 4. pp. 216-219, 2001.

[92] M. Sun and Y. P. Zhang, "100-GHz quasi-Yagi antenna in silicon technology," *IEEE Electron Device Letters*, vol. 28, no. 5, pp. 455-457, 2007.

[93] Y. P. Zhang, M. Sun, and L. H. Guo, "On-chip antennas for 60-GHz radios in silicon technology," *IEEE Transactions on Electron Devices*, vol. 52, no. 7 pp. 1664-1668, 2005.

[94] J. Lv, S.-X. Gong, F.-W. Wang, et al, "RCS Reduction of Quasi-Yagi Antenna," *Progress In Electromagnetics Research* , vol. 53, pp. 89-97, 2014.

[95] N. Nikolic and A. R. Weily, "Printed quasi-Yagi antenna with folded dipole driver," *International Symposium on Antennas and Propagation, Charleston, SC*, pp. 1-4, 2009.

[96] C. A. Balanis, *Antenna Theory: analysis and design*, New York, 1997, 2nd edition, p. 462.

[97] M. E. Bialkowski H. J. Song, "Investigations into a powercombining structure formed by trays of uniplanar quasiYagi antennas," *Microwave and Optical Technology Letters*, vol. 27, no.1, pp. 50-53, 2000.

[98] R. A. Alhalabi and G. M. Rebeiz, "High-gain Yagi-Uda antennas for millimeter-wave switched-beam systems," *IEEE Transactions on Antennas and Propagation*, vol. 57, no. 11, pp. 3672-3676, 2009.

[99] B. B. Adela, R. M. C. Mestrom, M. M. Paulides, and A. B. Smolders, "An MR-compatible printed Yagi-Uda antenna for a phased array hyperthemia applicator," *IEEE 7th European Conference on Antennas and Propagation (EuCAP), Gothenburg*, pp. 1142-1146, 2013.

[100] J. Y. Mao, Z. R. Li, Q.X. Guo, H. Zhang, et al, "A wideband Quasi-Yagi antenna with arrow-shaped dipoles for digital TV band applications," *Journal of Electromagnetic Waves and Applications*, vol. 26, no. 13, pp. 1716-1723, 2012.

[101] D. M. Elsheakh and E. A. Abdallah, "Ultra wide band planar printed quasiYagi antenna with size reduction for water detection in the Egyptian desert," *Microwave and Optical Technology Letters*, vol. 57, no. 1, pp. 226-233, 2015.

[102] S. Lin, G.-L. Huang, R.-N. Cai, and J.-X. Wang, "Novel printed Yagi-Uda antenna with highgain and broadband," *Progress In Electromagnetics Research Letters*, vol. 20 pp. 107-117, 2011.

[103] S. Chen and P. Hsu, "Broadband microstrip-fed modified quasi-Yagi antenna," *IEEE/ACES International Conference on Wireless Communications and Applied Computational Electromagnetics*, pp. 208-211, 2005.

[104] L. H. Truong, Y.-H. Baek, M.-K. Lee, et al "A highperformance 94 GHz planar QuasiYagi antenna on GaAs substrate," *Microwave and Optical Technology Letters*, vol. 51, no. 10, pp. 2396-2400, 2009.

[105] J. Huang and A. C. Densmore, "Microstrip yagi array antenna for mobile satellite vehicle application," *IEEE Transactions on Antennas and Propagation*, vol. 39, no. 7, pp. 1024-1030, Jul 1991.

[106] D. Gray, J. W. Lu, and D. V. Thiel, "Electronically steerable Yagi-Uda microstrip patch antenna array," *IEEE Transactions on Antennas and Propagation*, vol. 46, no. 5, 605-608, 1998.

[107] J. Huang, "L-band phased array antennas for mobile satellite communications," *37th IEEE Vehicular Technology Conference*, vol. 37, pp. 113117, June 1987.

[108] K. Uehara, K. Miyashita, et al, "Lens-coupled imaging arrays for the millimeter- and submillimeter-wave regions," *IEEE Transactions on Microwave Theory and Techniques*, vol. 40, no. 5, pp. 806-811, May 1992.

[109] G. R. DeJean, T. T. Thai, S. Nikolaou, and M. M. Tentzeris, "Design and analysis of microstrip Bi-Yagi and Quad-Yagi antenna arrays for WLAN applications," *IEEE Antennas and Wireless Propagation Letters*, vol. 6 , pp. 244-248, 2007.

[110] G. R. DeJean and M. M. Tentzeris, "A New High-Gain Microstrip Yagi Array Antenna With a High Front-to-Back (F/B) Ratio for WLAN and Millimeter-Wave Applications," *IEEE Transactions on Antennas and Propagation*, vol.55, no.2, pp.298-304, Feb. 2007.

[111] G. R. DeJean and M. M. Tentzeris, "A new high-gain microstrip Yagi array antenna with a high front-to-back (F/B) ratio for WLAN and millimeter-wave applications," *IEEE Transactions on Antennas and Propagation*, vol. 55, no. 2, pp. 298-304, 2007.

[112] N. B. Ismail, M. T. Ali, N. N. S. N. Dzulkefli, et al, "Design and analysis of microstrip yagi antenna for Wi-Fi application," *IEEE Asia-Pacific Conference on Applied Electromagnetics (APACE), Melaka*, pp. 283-286, Dec 2012.

[113] Z. Briqech and A. Sebak, "Low-cost 60 GHz printed yagi antenna array," *IEEE Antennas and Propagation Society International Symposium (APSURSI)*, pp. 12, July 2012.

[114] Z. Briqech, A. R. Sebak, and T. A. Denidni,, "High-Efficiency 60-GHz Printed Yagi Antenna Array," *Antennas and Wireless Propagation Letters*, vol. 12, pp. 1224-1227, 2013.

[115] G. DeJean and M. M. Tentzeris, "A printed microstrip Yagi antenna array for millimeter-wave multi-sector applications," *IEEE International Symposium on Antennas and Propagation*, vol. 2, pp. 529-532, 2005.

[116] M. Alsliety and D. Aloi, "A low profile microstrip Yagi dipole antenna for wireless communications in the 5 GHz band," *IEEE International Conference on Electro/information Technology*, pp. 525-528, 2006.

[117] M. Bemani and S. Nikmehr, "A novel wide-band microstrip Yagi-Uda array antenna for WLAN applications," *Progress In Electromagnetics Research*, vol. 16, pp. 389-406, 2009.

[118] P. R. Prajapati, A. Patnaik, M. V. Kartikeyan, "Design and characterization of an efficient multi-layered circularly polarized microstrip antenna," *International Journal of Microwave and Wireless Technologies*, pp. 1-9, 2015.

[119] O. Kramer,T. Djerafi, and K. Wu, "Very small footprint 60 GHz stacked Yagi antenna array," *IEEE Transactions on Antennas and Propagation*, vol. 59, no. 9, pp. 3204-3210, 2011.

[120] J. Zhao, L. Zheng, L. Zhao, Y. Fan, Y. Dou, and L. Xu. "Design and implementation of a printed yagi antenna working at the frequency of 2.4 GHz for monitoring physiological parameters," *IEEE 11th World Congress on Intelligent Control and Automation (WCICA), Shenyang*, pp. 543-548, 2014.

[121] Z. Liang, J. Liu, Y. Zhang, and Y. Long, "A Novel Microstrip Quasi Yagi Array Antenna With Annular Sector Directors," *IEEE Transactions on Antennas and Propagation*, vol. 63, no.10, pp. 4524-4529, Oct. 2015.

[122] D. C. Nascimento, R. Schildberg, and J. C. da S Lacava, "Low-cost Yagi-Uda monopole array," *International Symposium on Antennas and Propagation, AP-S*, pp. 1-4, 2008.

[123] Y. Yoon, B. Pan, J. Papapolymerou, M. M. Tentzeris, and M. G. Allen, "A vertical W-band surface-micromachined Yagi-Uda antenna," *International Symposium on Antennas and Propagation*, vol. 3, pp. 594-597, 2005.

[124] J. P. Gianvittorio and Y. Rahmat-Samii, "Fractal Yagi antennas: Design, simulation, and fabrication," *Microwave and optical technology letters*, vol. 41, no. 5, pp. 375-380, 2004.

[125] M. Farran, et al, "Microstrip-fed quasi-Yagi antennas for WLAN applications," *11th IEEE European Radar Conference (EuRAD), Rome, Italy*, pp. 384-387, 2014

[126] Y. Taguchi, Q. Chen, and K. Sawaya, "Broadband monopole YagiUda antenna," *Electronics and Communications in Japan (Part I: Communications)*, vol. 85, no. 1, pp. 49-57, 2002.

[127] S. Lim and H. Ling, "Design of a planar, closely spaced Yagi antenna," *International Symposium on Antennas and Propagation*, pp. 5997-6000, 2007.

[128] T. Maruyama, K. Uehara, and K. Kagoshima, "Design and analysis of small multisector antenna for wireless LANs based on monopole YagiUda elements," *Electronics and Communications in Japan (Part I: Communications)*, vol. 81, no. 12, pp. 80-90, 1998.

[129] O. M. Haraz, M. Abdel-Rehman et al, "Performance Investigations of Quasi-Yagi Loop and Dipole Antennas on Silicon Substrate for 94 GHz Applications," *International Journal of Antennas and Propagation*, 2014.

[130] W. Liang, Y. Qi, and Y. C. Jiao, "A novel small director array for slot loop antenna for LTE application," *IEEE Antennas and Wireless Propagation Letters*, vol. 12, pp. 1110-1113, 2013.

[131] Y. Ojiro and K. Hirasawa, "One-point-fed circularly polarized yagi-uda loop array," *International Symposium on Antennas and Propagation Society, AP-S*, vol. 4, pp. 1875-1878, 1995.

[132] P. J. Kajenski, "A circularly polarized mixed loop-dipole yagi antenna, " *Proceedings of the IEEE International Symposium on Antennas and Propagation*, 2012.

[133] R. A. Alhalabi and G. M. Rebeiz, "Differentially-fed millimeter-wave Yagi-Uda antennas with folded dipole feed," *IEEE Transactions on Antennas and Propagation*, vol. 58, no. 3, pp. 966-969, 2010.

[134] S. Lim and H. Ling, "Design of a closely spaced, folded Yagi antenna," *Antennas and Wireless Propagation Letters*, vol. 5, no. 1, pp. 302-305, 2006.

[135] W.L. Chang, "An integrated W-band high-performance Quasi-Yagi antenna array," *International Symposium on Antennas and Propagation (APSURSI)*, pp. 1-4, 2010.

[136] H. C. Huang, J. C. Lu, and P. Hsu, "A compact printed Yagi type antenna for GPS application," *Proceedings of IEEE Asia-Pacific Microwave Conference (APMC),Melbourne, VIC*, pp. 1698-1701, 2011.

[137] D. Z. Kim, S. Y. Park, W. S. Jeong, M. Q. Lee, and J. W. Yu, "A small and slim printed Yagi antenna for mobile applications," *Proceedings of IEEE Asia-Pacific Microwave Conference (APMC)*, pp. 1-4, 2008.

[138] S. X. Ta, H. Choo, and I. Park, "Wideband double-dipole Yagi-Uda antenna fed by a microstrip-slot coplanar stripline transition," *Progress In Electromagnetics Research*, vol. 44, pp. 71-87, 2012.

[139] M. Zinieris, R. Sloan and L. E. Davis, "A broadband microstrip-line-to-slotline transition," *Microwave and Optical Technology Letters*, vol. 18, No. 5, 339-342, Aug. 1998.

[140] K. Han, Y. Park, H. Choo, and I. Park, "Broadband CPS-fed Yagi-Uda antenna," *Electronics letters*, vol. 45, no. 24, pp. 1207-1209, 2009.

[141] E. Huang and T. Chiu, "Printed Yagi antenna with multiple reflectors," *Electronics Letters*, vol. 40, no. 19, pp. 1165-1166, 2004.

[142] A. D. Capobianco, F. M. Pigozzo, S. Boscolo, M. Midrio, et al, "A novel compact MIMO array based on planar Yagi antennas for multipath fading channels," *IEEE European conference on Wireless Technology (EuWIT),Paris*, 2010.

[143] H. R. Khaleel, H. M. Al-Rizzo, A. Abbosh, and S. Abushamleh,, "Printed Yagi-Uda array for MIMO systems," *2013 IEEE Antennas and Propagation Society International Symposium (APSURSI)*, pp. 1802-1803, Jul 2013.

[144] Y. Li, P. Yang, F. Yang, and S. He,, "A Method to Reduce the Back Radiation of the Folded PIFA Antenna with Finite Ground," *Journal of Applied Computational Electromagnetics Society*, vol. 28, No. 2, pp. 110-115. Feb.

[145] Y. Li, S. Sun, L. Jiang, P. Yang, and S. He, "Back radiation reduction of the folded shortedpatch antenna using finite ground strips with resistive loads," *Conference of Applied Computational Electromagnetics Society (ACES), Columbus*, Ohio, pp. 795-799, April 2012.

[146] L. Zhu and K. Li, "CPW-FED rectangular microstrip ring antenna for suppression of parasitic backside radiation," *Microwave and Optical Technology Letters*, vol. 36, pp. 65-67, Jan. 2003.

[147] T. J. Cho and H. M. Lee, "Front-to-back ratio improvement of a microstrip patch antenna by ground plane edge shaping," *Antennas and Propagation Society International Symposium (APSURSI)*, pp. 1-4, 2010.

[148] H-M. Lee and J-k. Kim, "Front-to-hack ratio improvement of a microstrip patch antenna using an isolated soft surface structure," *Proceedings of the European Microwave Conference, Rome, Italy*, pp. 385-388, Sep-Oct. 2009.

[149] E. Huang and T. Chiu. "Printed Yagi antenna with multiple reflectors," *Electronics Letters*, vol. 40, No. 19, pp. 1165-1166, 16 Sept. 2004.

[150] L. Ying, H. Liu, M. Wie, and S. Gong, "A Novel Slot Yagi-Like Multilayered Antenna With High Gain and Large Bandwidth," *IEEE Antennas and Wireless Propagation Letters*, vol. 13, pp. 790-793, 2014.

[151] C. Z. Li, C. M. Tong, and L. H. Qi, "Compact slot Yagi-Uda like antenna design with directional pattern," *IEEE International Conference on Communication Software and Networks (ICCSN),Chengdu*, pp. 147-150, 6-7 June 2015.

[152] W. Zhang, Y. Zhang, S. w. L, and T. Hong, "A Novel Design of Printed Yagi Antenna," *8th International Conference on Wireless Communications, Networking and Mobile Computing, Shanghai, China*, 2012.

[153] H. Lee and B. Cho, "CPW-Fed to CPS Dipole Antenna with an Inversed Triangular Loop Director," *International Conference on Computational Intelligence and Communication Networks, Bhopal*, 2014.

[154] B.-H. Sun, S.-G. Zhou, Y.-F. Wei, and Q.-Z. Liu, "Modified two-element Yagi-Uda antenna with tunable beams," *Progress In Electromagnetics Research*, vol. 100, pp. 175-187, 2010.

[155] N. Dashora, K. Venkatramana, and S. V. B. Rao, "Design and fabrication of crossed Yagi antennae for dual frequency satellite signal reception at ground," *Indian Journal of Radio & Space Physics*, vol. 43, pp. 124-129, 2014.

[156] B.-H. Sun, S.-G. Zhou, Y.-F. Wei, and Q.-Z. Liu, "Modified two-element Yagi-Uda antenna with tunable beams," *Progress In Electromagnetics Research*, vol. 100, pp. 175-187, 2010.

[157] S. S. Hsu, K. C. Wei, C. Y. Hsu, and H. Ru-Chuang, "A 60-GHz millimeter-wave CPW-fed Yagi antenna fabricated by using 0.18-CMOS technology," *Electron Device Letters, IEEE*, vol. 29, no. 6, pp. 625-627, 2008.

[158] Y. Huo, X. Dong, and J. Bornemann, "A wideband Artificial Magnetic Conductor Yagi antenna for 60-GHz standard 0.13-m CMOS applications," *12th IEEE International Conference on on Solid-State and Integrated Circuit Technology (ICSICT)*, 2014.

[159] S. Zhang, K. F. Chang, C. Jin, G. Katti, et al, "60GHz wideband Yagi-Uda antenna integrated on 2.5 D through silicon interposer," *IEEE 16th Electronics Packaging Technology Conference (EPTC), Singapore*, 2014.

[160] R. Willmot, D. Kim, and D. Peroulis, "A Yagi-Uda array of high-efficiency wire-bond antennas for on-chip radio applications," *IEEE Transactions on Microwave Theory and Techniques*, vol. 57, no. 12, pp. 3315-3321, 2009.

[161] P. V. Nikitin and K. V. S. Rao, "Compact Yagi antenna for handheld UHF RFID reader," *IEEE Antennas and Propagation Society International Symposium, Toronto, ON*, 2010.

[162] Y. X. Wu, L. Akhoondzadeh-Asl, and S. P. Hall, "Printed YagiUda array for onbody communication channels at 60 GHz," *Microwave and Optical Technology Letters*, vol. 53, no. 12, pp. 2728-2730, 2011.

[163] O. Kramer, T. Djerafi, and K. Wu, "Vertically multilayer-stacked Yagi antenna with single and dual polarizations," *IEEE Transactions on on Antennas and Propagation*, vol. 58, no. 4, pp. 1022-1030, 2010.

[164] X. Zou, C. M. Tong, J. S. Bao, and W. J. Pang. "SIW-Fed Yagi Antenna and Its Application on Monopulse Antenna," *IEEE Antennas and Wireless Propagation Letters*, vol. 13, pp. 1035-1038, 2014.

[165] S. Soltani, and R. D. Murch, " A compact planar printed MIMO antenna design," *IEEE Transactions on Antennas and Propagation*, vol. 63, no. 3, pp. 1140-1149, 2015.

[166] H. Wang, L. Liu, Z. Zhang, Y. Li, and Z. Feng, "A Wideband Compact WLAN/WiMAX MIMO Antenna Based on Dipole With V-shaped Ground Branch," *IEEE Transactions on Antennas and Propagation*, vol. 63, no. 5, pp. 2290-2295, 2015.

[167] C. Y. Chiu, and R. D. Murch, "Compact four-port antenna suitable for portable MIMO devices," *IEEE Antennas and Wireless Propagation Letters*, vol. 7, pp.142-144, 2015.

[168] K. L. Wong, Y. C. Chen, and W. Y. Li, "Four LTE low-band smartphone antennas and their MIMO performance with user's hand presence," *Microwave and Optical Technology Letters*, vol. 58, no. 9, pp. 2046-2052, 2016.

[169] R. Hussain, M S. Sharawi, "A cognitive radio reconfigurable MIMO and sensing antenna system," *IEEE Antennas and Wireless Propagation Letters*, vol. 14, pp. 257-260, 2015.

[170] Microwave Vision Group (MVG), Rome, Italy, Satimo-Star-Lab chamber, [online] http://www.satimo.com. August, 2016.

[171] R. Tian, B. K. Lau, and Z. Ying, "Multiplexing Efficiency of MIMO Antennas," *IEEE Antennas and Wireless Propagation Letters*, vol. 10, pp. 183-186, 2011.

[172] L. Ronglin, G. DeJean, et al, "Development and analysis of a folded shorted patch antenna with reduced size," *IEEE Transactions on Antennas and Propagation*, vol. 52, no. 2, pp. 555-562, 2004.

[173] J. Anguera, L. Boada, et al, "Stacked H-shaped microstrip patch an- tenna," *IEEE Transactions on Antennas and Propagation*, vol. 52, no. 4, pp. 983-993, 2004.

[174] S. F. Mahmoud, "A new miniaturized annular ring patch resonator par- tially loaded by a metamaterial ring with negative permeability and permittivity," *IEEE Antennas and Wireless Propagation Letters*, vol. 3, no. 1, pp. 19-22, 2004.

[175] D. Schaubert and K. Yngvesson, "Experimental study of a microstrip array on high permittivity substrate," *IEEE Transactions on Antennas and Propagation*, vol. 34, no. 1, pp. 92-97, 1986.

[176] J. S. Kuo and K. L. Wong, "A compact microstrip antenna with meandering slots in the ground plane,' *Microwave and Optical Technology Letters*, vol. 29, no. 2, pp. 95-97, 2001.

[177] G. C. Y. Chen, K. K. M. Chan, and K. Rambabu, "Miniaturized yagi class of antennas for GSM, WLAN, and WiMax applications," *IEEE Transactions on Consumer Electronics*, vol. 56, no. 3, pp. 1235-1240, Aug. 2010.

[178] H. B. Teisbaek and K. B. Jakobsen, "Koch-Fractal Yagi-Uda Antenna," *Journal of Electromagnetic Waves and Applications*, vol. 23, no. 2-3, pp. 149-160, 2009.

Vitae

- Name: Syed Shahan Jehangir
- Nationality: Pakistani
- Date of Birth: 20th Feb, 1989
- Email: *syedjehangir43@gmail.com; g201408480@kfupm.edu.sa*
- Permenant Address: Dist. Nowshera, Khyberpukhtonkhwa, Pakistan

- BS in Electrical Engineering (Major: Telecommunications), COMSATS Institute of Information Technology, Lahore, Pakistan.

PUBLICATIONS

Patents

1. M. S. Sharawi and Syed. S. Jehangir, A Compact Yagi-Like MIMO Antenna System, *Submitted to USPO*, June 16, 2016.

2. M. S. Sharawi and Syed. S. Jehangir, A Highly Miniaturized Semi-Loop Meandered Dual Wideband Quasi-Yagi MIMO Antenna System, *Submitted to USPO*, Dec, 2016.

Journal Papers

1. S. S. Jehangir and M. S. Sharawi, "A Single Layer Semi-Ring Slot Yagi-Like MIMO Antenna System with High Front-to-Back Ratio," *IEEE Transactions on Antennas and Propagation*, vol. 65, no. 2, pp. 937-942, Feb. 2016.

2. S. S. Jehangir and M. S. Sharawi, "A novel dual wideband circular quasi-yagi MIMO antenna system with loop excitation," *Microwave and Optical Technology Letters*, vol. 58, no. 11, pp. 2769-2774, 2016.

3. S. S. Jehangir and M. S. Sharawi, "A Highly Miniaturized Semi-Loop Meandered Dual Wideband Quasi-Yagi MIMO Antenna System," Submitted, *IEEE Transactions on Antennas and Propagation*, Dec, 2016.

4. S. S. Jehangir and M. S. Sharawi, " A Miniaturized UWB Bi-Planar Yagi-Like MIMO Antenna System," *Antennas and Wireless Propagation Letters*, To be submitted, March, 2017.

5. S. S. Jehangir and M. S. Sharawi, " A Miniaturized Multi-Wideband Quasi-Yagi MIMO Antenna System," *IET Microwaves, Antennas and Propagation*, To be submitted, March, 2017.

6. S. S. Jehangir and M. S. Sharawi, " A Miniaturized Dual-Wideband Quasi-Yagi MIMO Antenna System using DGS," *Microwave and Optical Technology Letters*, To be submitted, March, 2017.

Conference Papers

1. S. S. Jehangir, A. Hassan, and M. S. Sharawi, "A 4-element dual wideband circular Yagi MIMO antenna system with loop excitation," *IEEE International Symposium on Antennas and Propagation (APSURSI), Fajardo*, pp. 69-70, 2016.

2. S. S. Jehangir and M. S. Sharawi, "A Novel Compact Single Layer Semi-Ring Slot Yagi-Like Antenna with High Front-to-Back Ratio," Accepted, *IEEE 5th Asia-Pacific Conference on Antennas and Propagation (APCAP), Kaohsiung, Taiwan*, 2016.

3. S. S. Jehangir and M. S. Sharawi, "A comparison between two different excitations for Quasi-Yagi antennas," *IEEE Middle East Conference on Antennas and Propagation (MECAP), Beirut, Lebanon*, pp. 1-2, 2016.

4. S. S. Jehangir and M. S. Sharawi, "A miniaturized dual wide-band loop excited quasi-yagi antenna using a defected ground structure," *16th Mediterranean Microwave Symposium (MMS), Abu Dhabi, United Arab Emirates*,

pp. 1-3, 2016.

5. S. Jehangir and M. S. Sharawi, "A highly Miniaturized Quasi-Yagi Antenna with Loop Excitation," Accepted, *IEEE 11th European Conference on Antennas and Propagation (EUCAP), Paris, France*, 2017.

6. S. S. Jehangir and M. S. Sharawi, "A Miniaturized UWB Bi-Planar Yagi-Like Antenna," Submitted, *IEEE International Symposium on Antennas and Propagation (APSURSI), California, USA*, 2017.

7. S. S. Jehangir and M. S. Sharawi, "A Miniaturized Multi-Wideband Quasi-Yagi Antenna with Rectangular Loop Excitation," Submitted, *IEEE International Symposium on Antennas and Propagation (APSURSI), California, USA*, 2017.